Atomic Energy Control Board
P.O. Box 1046
Ottawa, Canada
K1P 5S9

Commission de contrôle de l'énergie atomique
C.P. 1046
Ottawa, Canada
K1P 5S9

INFO-0115

CONSEQUENCES OF PRESSURE TUBE RUPTURE ON IN-CORE COMPONENTS: PHASE 1 - TECHNOLOGY REVIEW

by

P.G. Hill, E.G. Hauptmann and V. Lee

A research report prepared for the
Atomic Energy Control Board
Ottawa, Canada

December 31, 1982

Canada

Research report

CONSEQUENCES OF PRESSURE TUBE RUPTURE ON IN-CORE COMPONENTS: PHASE I - TECHNOLOGY REVIEW

A report prepared by P.G. Hill, E.G. Hauptmann and V. Lee, University of British Columbia, under contract to the Atomic Energy Control Board.

ABSTRACT

An investigation has been made of the consequences of pressure tube rupture in calandria vessels of heavy water cooled and moderated reactors. The study included a review of previous experimental and analytical work, as well as supplementary investigations carried out to examine the validity of previous assumptions and findings.

The central questions considered were: the possibility of a propagating pressure tube failure; damage to the calandria vessel; and damage to the shut-off-rod guide tubes of the reactor shut-down system.

The results of the investigation do not indicate mechanisms of sufficient strength to cause propagating failure in a well-designed, well-operated reactor following a tube burst under normal operating conditions. However, not all the details of the physical processes involved in a tube burst have been revealed by existing experimental and analytical work.

Measured and calculated loads on the calandria vessel due to bursting of a single pressure tube appear to pose no hazard to the vessel considering both pressure loading and missile impacts.

Existing information on the crushing strength of shut-off-rod guide tubes or on the impulsive loading following one pressure tube burst is insufficient to provide a firm conclusion on the number of shut-off-rod guide tubes which could be damaged.

Further experimental work on the initial phase of the bursting process and on the integrity of the shut-off-rod guide tubes under impulsive loading is needed. There is a need for further computation of pressure transients in calandria vessels to provide improved estimates of impulsive loads on core components immediately adjacent to a tube burst.

RÉSUMÉ

On a mené une enquête afin de déterminer les conséquences qu'aurait la rupture d'un tube de force dans les calandres des réacteurs refroidis et modérés à l'eau lourde. Cette étude comprenait un examen des travaux expérimentaux et analytiques précédents, ainsi que des recherches supplémentares réalisées dans le but d'examiner la validité des hypothèses et des résultats antérieurs.

Les questions majeures à l'étude étaient les suivantes: la possibilité d'une propagation de la rupture aux autres tubes de force; les dommages occasionnés à la calandre; et les dommages aux tubes de guide des barres d'arrêt du système d'arrêt d'urgence du réacteur.

Les résultats de cette étude n'indiquent pas de mécanismes suffisamment puissants qui pourraient entraîner la propagation du phénomène de rupture dans un réacteur bien conçu et bien exploité, à la suite de l'éclatement d'un des tubes en conditions normales d'opération. Cependant, les travaux analytiques et expérimentaux actuels ne révèlent pas tous les détails des processus physiques en jeu lors de la rupture d'un tube.

Compte tenu des charges dues à la pression et de l'impact de projectiles, les charges mesurées et calculées qui s'exercent sur la calandre, lors de l'éclatement d'un seul tube, ne semblent poser aucun danger à la cuve.

L'information présentement disponible sur la résistance à l'écrasement des tubes de guide des barres d'arrêt, ou concernant la charge due à l'impulsion qui suit l'éclatement d'un tube de force, ne permet pas la formulation d'une conclusion sans équivoque quant au nombre de tubes de guide qui pourraient effectivement être endommagés.

Des travaux expérimentaux additionels sont requis afin de mieux comprendre la phase initiale du processus d'éclatement, et afin de déterminer la fiabilité des tubes de guide des barres d'arrêt lorsqu'ils sont soumis à une charge due à l'impulsion qui suit l'éclatement d'un tube. Il s'avère en outre nécessaire d'effectuer des calculs supplémentaires pour déterminer les pressions transitoires dans la calandre, afin d'obtenir une meilleure évaluation des charges dues à l'impulsion exercée sur les composants du coeur à proximité immédiate de l'éclatement d'un tube.

DISCLAIMER

The Atomic Energy Control Board is not responsible for the accuracy of the statements made or opinions expressed in this publication and neither the Board nor the authors assume liability with respect to any damage or loss incurred as a result of the use made of the information contained in this publication.

PREFACE

The authors are staff members at the University of British Columbia. The Scientific Authority during the initial stages of the work was Dr. F.R. Campbell; and for the latter stages, Dr. D.J. Martin.

TABLE OF CONTENTS

		Page
Abstract		i
Preface		iv
Table of Contents		v
List of Figures		x
1.0	**OVERVIEW**	1-1
1.1	INTRODUCTION	1-1
1.2	A TYPICAL PRESSURE TUBE REACTOR	1-3
1.3	POSSIBLE PROPAGATION OF PRESSURE TUBE FAILURE	1-8
1.3.1	Impulsive Pressure Loading	1-8
1.3.2	Missile Damage	1-10
1.3.3	Collapse of Large Vapour Pockets	1-10
1.3.4	Sustained Jet Impingement	1-11
1.3.5	Pipe Whip	1-12
1.4	POSSIBLE DAMAGE TO SHUT-OFF-ROD GUIDE TUBES	1-13
1.4.1	Pressure and Impact Loadings	1-13
1.4.2	Missile Damage	1-13
1.4.3	Collapse of Vapour Pockets	1-14
1.4.4	Sustained Jet Impingement	1-14
1.4.5	Pipe Whip	1-14
1.5	POSSIBLE DAMAGE TO CALANDRIA VESSEL	1-15
1.6	SCOPE OF THIS STUDY	1-16
1.6.1	Literature Review and Site Visits	1-16
1.6.2	Rupture Modes and Relevant Physical Processes	1-16
1.6.3	Computer Simulation of Pressure Tube Rupture	1-17
1.6.4	Experimental Simulation of Pressure Tube Rupture	1-17
1.6.5	Structure of this Report	1-17
2.0	**REVIEW OF EXPERIMENTAL WORK**	2-1
2.1	INTRODUCTION	2-1
2.2	PRESSURE TUBE RUPTURE IN POOLS	2-2
2.2.1	Burnup (1960)	2-2
2.2.2	Roberts and Swinhoe (1960)	2-4
2.2.3	Ross-Ross (1963) (1965) 1973)	2-5
2.2.4	Isles (1965)	2-9
2.2.5	Summary	2-14

			Page
2.3	PRESSURE TUBE RUPTURE IN CLOSED VESSELS		2-17
	2.3.1	Introduction	2-17
	2.3.2	Hareux, Roche, and Vrillon (1964)	2-19
	2.3.3	Holtbecker, Montagnani, and Verzeletti (1970)	2-21
	2.3.4	Tanaka (1971)	2-23
	2.3.5	Hayamizu, Tokomitsu, and Hayashi (1974)	2-24
	2.3.6	Famiglietti, Parmeggiani, Possa and Galbiati (1975)	2-24
	2.3.7	Dallavalle, Hotz, Possa (1977)	2-30
	2.3.8	Chevallard, Famiglietti, and Possa (1979)	2-33
	2.3.9	Summary	2-35
2.4	TUBE BURST PHENOMENA		2-37
	2.4.1	Introduction	2-37
	2.4.2	Modes of Tube Bursting	2-37
	2.4.3	Shock Waves	2-52
	2.4.4	Reactive forces and Pipe Whip	2-56
	2.4.5	Missile Damage	2-57
	2.4.6	Jet Impingement Forces	2-57
	2.4.7	Summary	2-58
2.5	CONCLUSIONS FROM EXPERIMENTAL WORK		2-60
	2.5.1	Introduction	2-60
	2.5.2	Possibility of Propagating Pressure Tube Failure	2-60
	2.5.3	Possible damage to Shut-off-rod Guide Tubes and Poison Injection System	2-62
	2.5.4	Possible Damage to Calandria Vessel	2-63
	2.5.5	Questions Unanswered by Experiments to Date	2-63
3.0	**REVIEW OF ANALYTICAL WORK**		
3.1	INTRODUCTION		3-1
3.2	OVERALL PROBLEM: PRESSURE TUBE RUPTURE IN CLOSED VESSELS		3-2
	3.2.1	The Pendergast Model	3-2
	3.2.2	The Kumar Model	3-4
	3.2.3	The Henry Models	3-6
	3.2.4	Computer Modelling	3-6
	3.2.5	Summary	3-7

			Page
3.3	MODELS OF SEPARATE MECHANISMS		3-10
	3.3.1	Rupture Mechanisms	3-10
	3.3.2	Shock Waves	3-10
	3.3.3	Bubble Dynamics	3-11
	3.3.4	Condensation and Collapse	3-14
	3.3.5	Slug Inertia Behavior	3-14
	3.3.6	Impulsive Loading on Adjacent Structures	3-15
	3.3.7	Calandria Stresses for the Calandria Vessel	3-18
	3.3.8	Discharge Flow	3-20
3.4	APPLICATIONS OF HENRY'S MODELLING TO HORIZONTAL-AXIS PRESSURE TUBE REACTORS WITH NO GAS CAP		3-21
	3.4.1	Bulk Pressurization	3-21
	3.4.2	Jet Reaction and Impingement Forces on Adjacent Tubes with Sustained Discharge	3-25
	3.4.3	Pipe Whip Damage	3-25
	3.4.4	Missile Damage	3-26
	3.4.5	Summary	3-26
3.5	COMPUTER MODELS		3-27
	3.5.1	Computer Code EURDYN	3-27
	3.5.2	Computer Code PISCES	3-28
	3.5.3	Summary	3-31
4.0	**SUPPLEMENTARY INVESTIGATIONS**		4-1
4.1	INTRODUCTION		4-1
4.2	EXPERIMENTAL SIMULATION OF PRESSURE TUBE RUPTURE		4-2
	4.2.1	Experimental Set-up and Procedure	4-2
	4.2.2	Variation of Experimental Conditions	4-2
	4.2.3	Results and Observations	4-4
	4.2.4	Discussion: Surrounding Fluid, Gas and Liquid Coolants, Liquid Coolant Temperature	4-9
4.3	COMPUTER SIMULATION OF PERIPHERAL PRESSURE TUBE RUPTURE		4-12
	4.3.1	Simulation Procedure and Boundary Conditions	4-12
	4.3.2	Hydrodynamic Transients Due to Peripheral Rupture	4-15
	4.3.3	Loading of Calandria Vessel Due to Peripheral Rupture	4-18
	4.3.4	Loading of Adjacent Tube Due to Peripheral Rupture	4-18

			Page
4.4	COMPUTER SIMULATION OF CENTRAL PRESSURE TUBE RUPTURE		4-23
	4.4.1	Hydrodynamic Transients Due to Central Rupture	4-23
	4.4.2	Loading of Calandria Vessel Due to Central Rupture	4-27
	4.4.3	Loading of Adjacent Tubes Due to Central Rupture	4-27
4.5	SUMMARY		4-31
	4.5.1	Qualitative Conclusions from Experimental Simulations	4-31
	4.5.2	Results from Computer Simulations and Observations	4-32
5.0	**CONCLUSIONS**		5-1
5.1	INTRODUCTION		5-1
5.2	MODES OF BURSTING		5-2
5.3	PRESSURE PULSE DEVELOPMENT		5-4
5.4	LOADING OF CALANDRIA-TUBE/PRESSURE-TUBE ASSEMBLIES		5-7
5.5	LOADING OF CALANDRIA VESSELS		5-8
5.6	LOADING OF SHUT-OFF-ROD GUIDE TUBES		5-9
5.7	POISON INJECTION PIPES		5-10
5.8	SUMMARY		5-11
	5.8.1	Propagating Pressure Tube Failure	5-11
	5.8.2	Calandria Vessel Failure	5-11
	5.8.3	Shut-down System Failure	5-12
6.0	**RECOMMENDATONS FOR FURTHER EXPERIMENTAL AND ANALYTICAL INVESTIGATIONS**		6-1
6.1	INTRODUCTION		6-1
6.2	EXPERIMENTAL INVESTIGATIONS		6-3
	6.2.1	Explosion Chamber	6-3
	6.2.2	Explosion Tube	6-3
	6.2.3	Pressure Tube and Shut-off-rod Guide Tube at Target	6-5
	6.2.4	Instrumentation and Data Acquisition	6-7

			Page
6.3	PARALLEL ANALYTICAL INVESTIGATIONS		6-8
	6.3.1	3-D Simulations	6-8
	6.3.2	Modelling of Tube Ruptures	6-9
	6.3.3	Computation Costs	6-9
6.4	CONCLUDING REMARKS		6-10
BIBLIOGRAPHY			B-1

LIST OF FIGURES

		Page
	Chapter 1	
Figure 1.1	Typical Pressure Tube Reactor	1-4
Figure 1.2	Power Channel Assembly	1-5
Figure 1.3	Typical Tube Lattice and Shut-off-rod Guide Tube	1-6
Figure 1.4	Schematic of Pressure Tube Reactor Core	1-7
	Chapter 2	
Figure 2.1	Test Rig of Ross-Ross (1963)	2-6
Figure 2.2	Test Rig of Isles (1965)	2-10
Figure 2.3	Pressure Decay with Radial Distance	2-15
Figure 2.4	Test Rig of Hareux, Roche and Vrillon (1964)	2-20
Figure 2.5	Typical Pressure Transient in Bettula Tests	2-26
Figure 2.6	The Bettula Pressure Vessel	2-26
Figure 2.7	Schematic of Bettula Pressure Vessel	2-27
Figure 2.8	Instrumentation on Target Tube	2-29
Figure 2.9	Characteristic Pressure Peaks in Pressure Vessel and Gas Plenum	2-29
Figure 2.10	Variations of Impulse with Height and Radial Distance - After Famiglietti, Parmeggiani, Possa and Galbiati	2-32
Figure 2.11	Peak Pressures on the Inner Vessel Wall, First Pressure Pulse - from Chevallard, Famiglietti and Possa	2-34
Figure 2.12	Pressure and Strain on Vessel during First Pressure Pulse - from Chevallard, Famiglietti and Possa	2-34
Figure 2.13	Idealized Modes of Tube Rupture	2-38
Figure 2.14	Peak Pressures and Rupture Lengths	2-40
Figure 2.15	Propagation of Crack Tips in Axial Split - from Baum	2-43
Figure 2.16	Idealized Choking Areas in Baum's Model	2-44

		Page
Figure 2.17	Comparison of Predicted and Measured Depressurization within the Breach at 12R from Centre of Defect (L = 2R, Po = 86 bar) - from Baum	2-45
Figure 2.18	Emery's Split Ring Model and Comparison with Experimental Results - from Emery	2-47
Figure 2.19	Decompression and Crack Extension of Air-filled Pipe and Hot-water-filled Pipe - from Emery	2-48
Figure 2.20	Pressure Undershoot during Decompression of Hot Water	2-50
Figure 2.21	Comparison of Predicted Quasi-static Recovery Pressure with Experimental Data - from Alamgir and Lienhard	2-51
Figure 2.22	Pressure Pulses from Shock and Bubble Expansion - from Cole	2-53
Figure 2.23	Shock Strength and Driving Pressure	2-55

Chapter 3

Figure 3.1	The Pendergast Model	3-3
Figure 3.2	Measured and Predicted Vessel Pressure and Bubble Radius (Pendergast)	3-5
Figure 3.3	Application of EURDYN to Explosion in Enclosed Vessel	3-8
Figure 3.4	Bubble Expansion in an Infinite Pool	3-12
Figure 3.5	Loading on Adjacent Tube - from Henry	3-17
Figure 3.6	Hoop Stress in the Calandria Vessel - from Henry	3-19
Figure 3.7	Longitudinal Stress in the Calandria Vessel - from Henry	3-19
Figure 3.8	Effect of Break Opening Time - from Henry	3-22
Figure 3.9	Pressure Transient within the Calandria Tank for a Very Long Rupture Length - from Henry	3-22
Figure 3.10	Pressure Transient within the Calandria Tank for a Postulated Guillotine Rupture of a Pressure Tube - from Henry	3-24
Figure 3.11	Total Impulse on Roof of Containment using EURDYN (see also Figure 3.3)	3-29
Figure 3.12	Simulated HCDA Transient Using PISCES	3-30

Page

Chapter 4

Figure 4.1	Simulation Loop Schematic	4-3
Figure 4.2	Ruptured Tubes from Experimental Simulation	4-6
Figure 4.3	Bubble Boundary Motions from High-speed Movie	4-7
Figure 4.4	Snapshots of Vapour Pockets	4-8
Figure 4.5	Saturation Pressures of Freon 114 and Water	4-11
Figure 4.6	Peripheral Pressure Tube Rupture Model	4-13
Figure 4.7	Moderator Grid for Peripheral Rupture	4-13
Figure 4.8	Velocity Vector Plots from Peripheral Rupture	4-14
Figure 4.9	Pressure Profiles along the Plane of Symmetry due to Peripheral Rupture	4-16
Figure 4.10	Pressure Histories due to Peripheral Rupture	4-17
Figure 4.11	Vessel Strain Histories from Peripheral Rupture	4-19
Figure 4.12	Forces on Adjacent Shut-off-rod Guide Tubes due to Peripheral Rupture	4-20
Figure 4.13	Impulses on Adjacent Shut-off-rod Guide Tubes due to Peripheral Rupture	4-21
Figure 4.14	Central Pressure Tube Rupture Model	4-24
Figure 4.15	Velocity Vector Plots from Central Rupture	4-25
Figure 4.16	Pressure Histories from Central Rupture	4-26
Figure 4.17	Vessel Strain Histories from Central Rupture	4-28
Figure 4.18	Force on Adjacent Pressure Tube due to Central Rupture	4-29
Figure 4.19	Impulse on Adjacent Pressure Tube due to Central Rupture	4-30

Chapter 6

Figure 6.1	Explosion Chamber	6-4
Figure 6.2	Pressure Tube as Target	6-6
Figure 6.3	Split Ring Model for Computer Simulation	6-6

1.0 OVERVIEW

1.1 INTRODUCTION

Pressure tube rupture implies discharge of high-pressure, high-temperature coolant and, possibly, of parts of the fuel bundles contained within the pressure tube of a pressure tube reactor. Could such a rupture lead to:

- rupture of a second pressure tube, i.e. to propagating failure in the tube array?
- damage of the shut-off rod guide tubes?
- damage of poison injection nozzles?
- damage of the calandria vessel? and/or
- penetration of the calandria vessel followed by damage to components outside of the vessel?

This study reviews the possible set of direct consequences of failure of a pressure tube. Consideration of all possible indirect consequences, and of the probability of such a failure has not been included in this study so that the results do not include estimates of risk. The "possible set of direct consequences" means those events which are not only conceivable, but may be shown (with existing knowledge of physical laws and the behavior of materials) to be causable directly by pressure tube failure. Each of these possible consequences could lead to others; the chain of causality is no doubt endless. Only the primary consequences delineated above are included in this review. The goal has been to identify and evaluate the phenomena (resulting from pressure tube failure) which can be shown by empirical reasoning to be capable of causing failure of other parts of the reactor.

For purposes of this study it is assumed that the reactor is designed and operated according to current best practice. Human operator error and terrorist intervention are not under consideration in this review though both could conceivably affect the results of a pressure tube failure.

Transient thermal-hydraulic-structural effects in nuclear power systems of various kinds is a subject of continuing activity (as indicated by the volume of work reported in SMIRT* conferences) and there is hope that techniques now being developed elsewhere may throw helpful light on the pressure tube safety problem. Thus the authors have not hesitated in this report to address matters which have been under careful scrutiny by experienced and able people for more than 25 years. Nor have they been deterred by the splendid operating record of pressure-tube reactors to date. Given that there are grounds for believing that pressure tube rupture in a well-designed, well-operated reactor is an event of very low probability, such an event is not impossible and serious re-examination of possible consequences (using in part methods which have not been employed heretofore) is not out of place.

Can we be sure that we have identified all physical mechanisms which could lead to these types of damage? No fundamental law is available to check the completeness of an analysis; thus the justification of any analysis rests solely on the failure of all attempts to detect logical or factual flaws, or missing elements. This suggests that in important safety problems, independent rational assessment, and effort to improve experimental or analytical techniques, are to be welcomed. Perhaps no analytical result will (or ought to) be considered the final definitive answer to an important safety problem in a continuing power system.

---

* Structural Mechanics In Reactor Technology

1.2 A TYPICAL PRESSURE TUBE REACTOR

Figure 1.1 shows a typical pressure tube reactor cooled and moderated by heavy water. Pressure tubes (approximately 400) containing the fuel and coolant are located in the calandria vessel. The calandria is surrounded by a shield tank and has integral end shields. The shut-off rods (approximately 30) penetrate the vessel from the top while liquid poison injection pipes (typically 4 or 8) run horizontally through the array. A typical pressure tube and its surrounding calandria tube are shown in Figure 1.2. Typical tube lattice geometry is given in Figure 1.3 as well as the relative size and location of one of the shut-off rod guide tubes. Coolant (D_2O) conditions inside the pressure tube are about 10 MPa and 310°C. The space between the calandria tube and the pressure tube is normally filled by nitrogen or cabon dioxide at about 0.1 MPa.

The pressure tube material is typically Zircaloy-2 or Zirconium-Niobium alloy, while the calandria tube is typically Zircaloy-2.

Figure 1.4 shows the schematic arrangement of shut-off rod guide tubes, and shut-off rods ready for insertion by gravity into the reactor core. It also shows typical locations of liquid poison injection pipes in the calandria vessel. Any one of these two systems acting alone is capable of shutting down the reactor. The calandria vessel and shield tank assembly shown in Figure 1.1 typically has a vessel of 38 mm thickness made of type 316 stainless steel, while the shield tank is typically the same thickness but made of carbon steel. The pressure tube support design allows for expansion of the pressure tube assembly with temperature and under irradiation. Figure 1.4 also shows the typical locations of the rupture discs, typically designed to burst at a moderator overpressure of about 0.14 MPa.

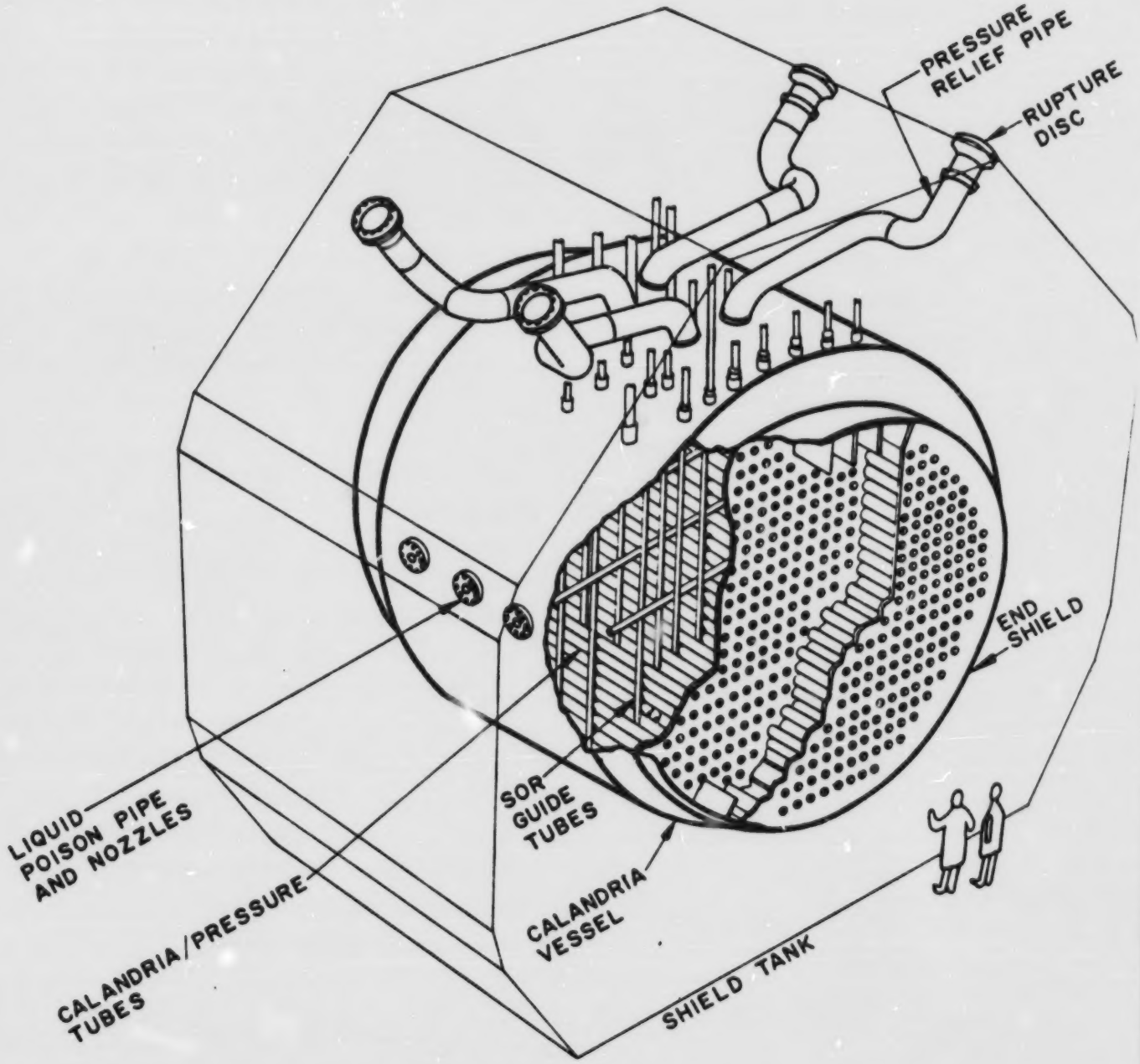

Figure 1.1 Typical Pressure Tube Reactor

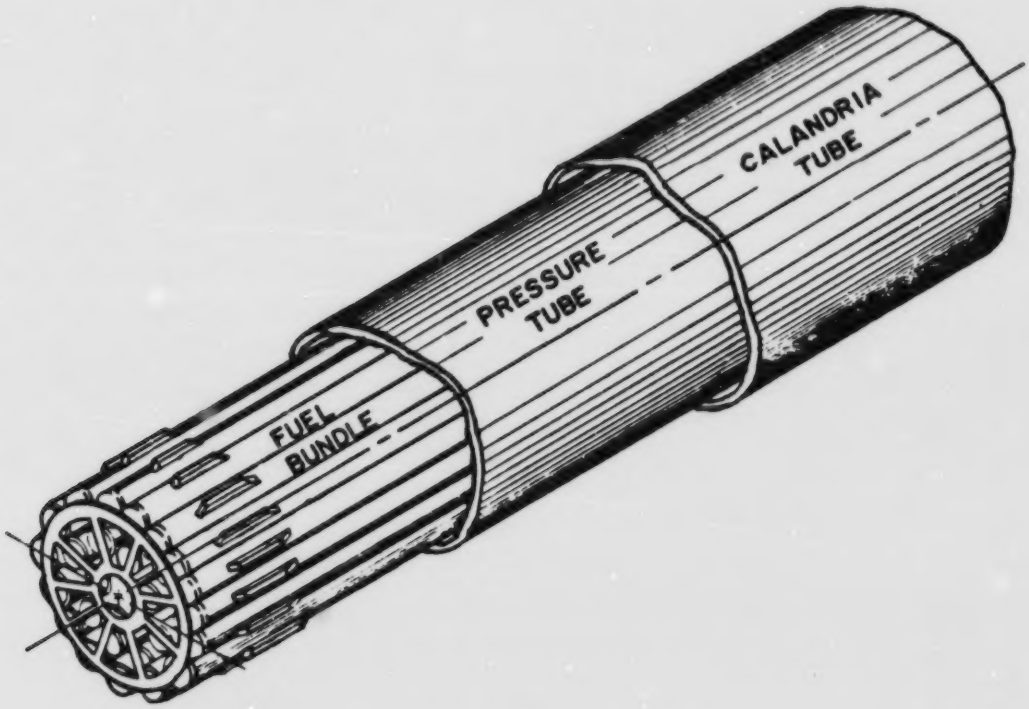

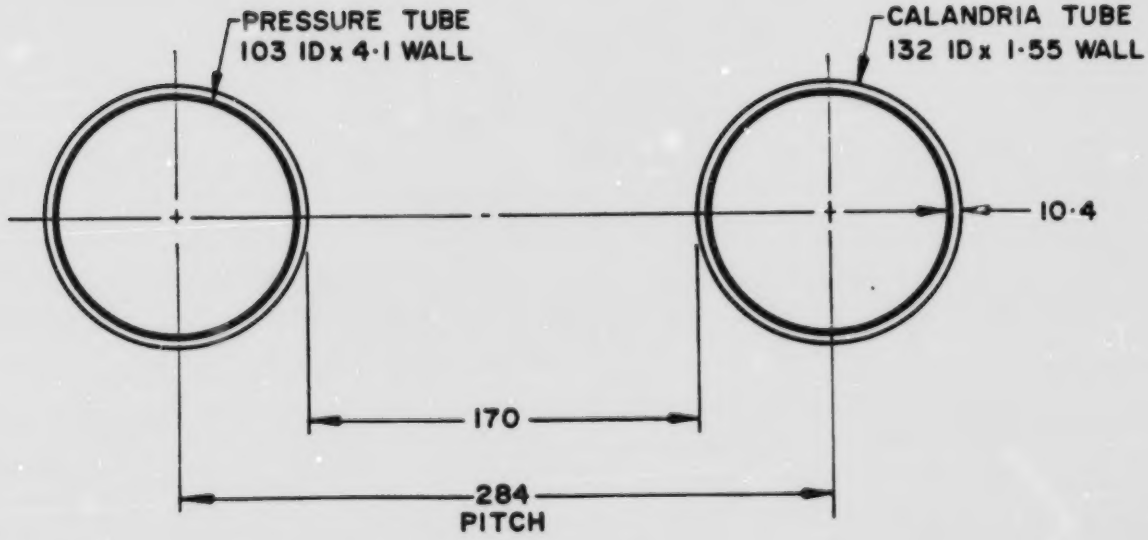

ALL DIMENSIONS IN mm

Figure 1.2 Power Channel Assembly

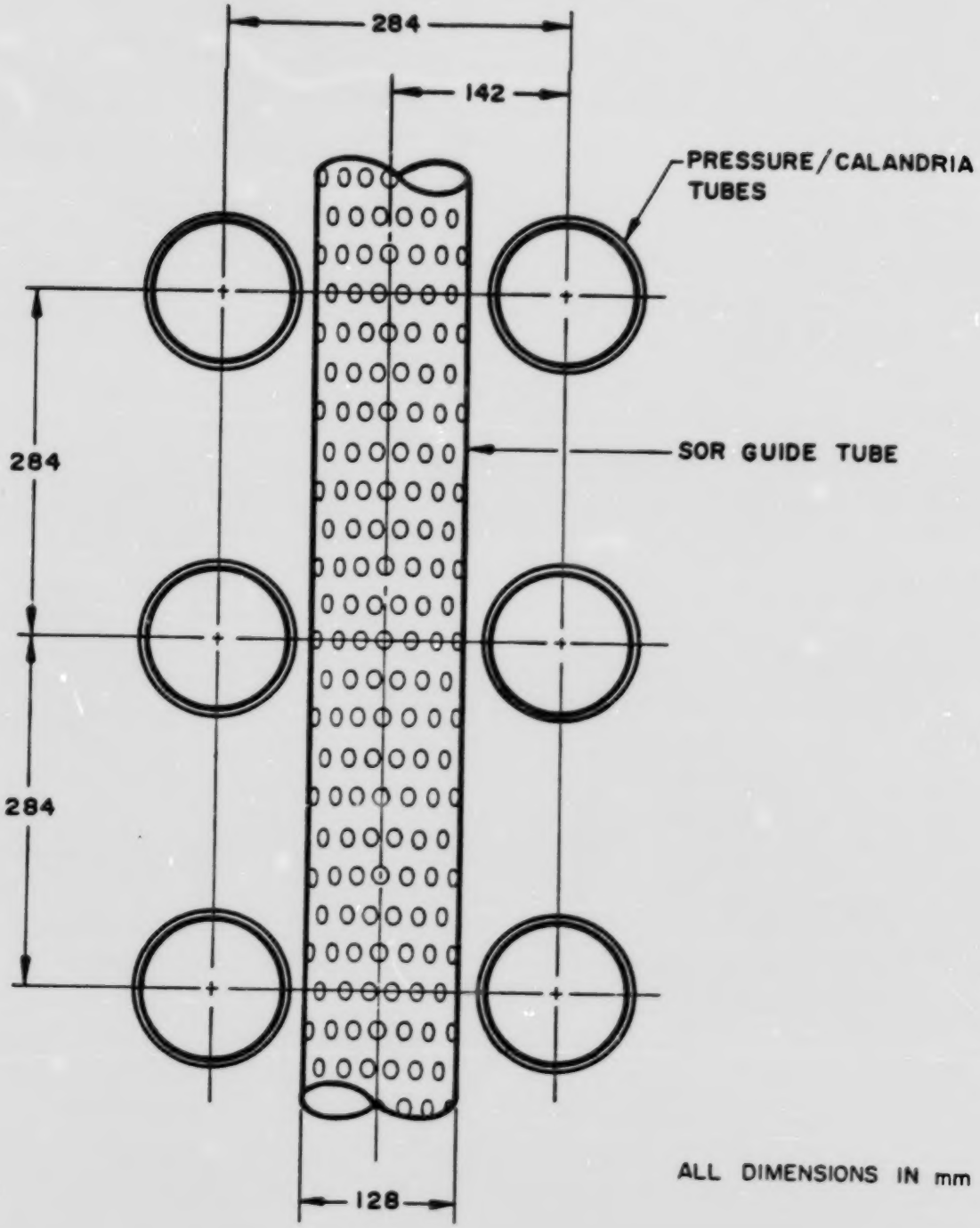

Figure 1.3 Typical Tube Lattice and Shut-of-rod Guide Tube

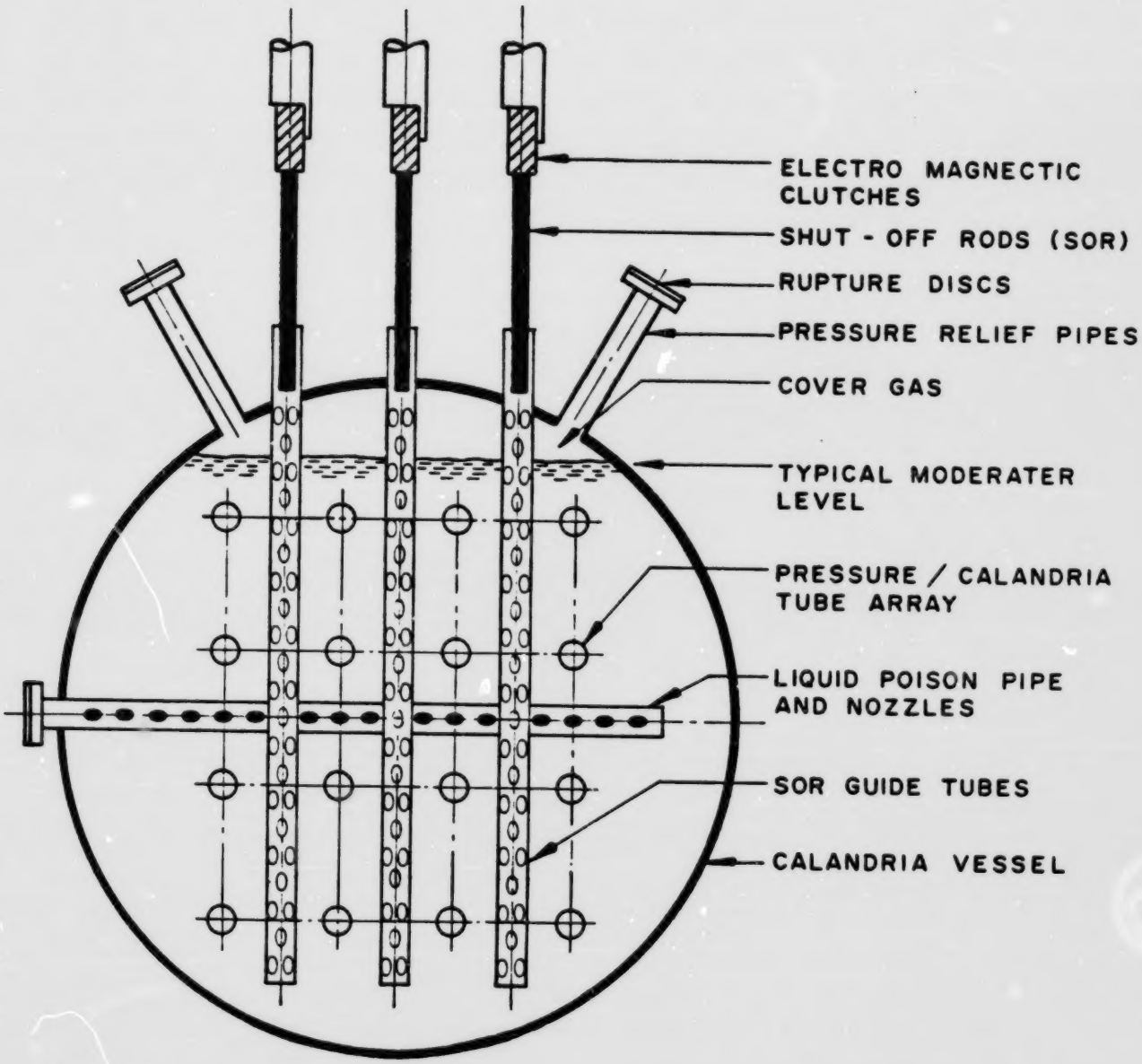

Figure 1.4 Schematic of Pressure Tube Reactor Core

1.3 POSSIBLE PROPAGATION OF PRESSURE TUBE FAILURE

If a pressure tube ruptures, its enclosing calandria tube might be able to contain the pressure of the steam-water mixture, but this possibility need not be allowed for in safety calculations. If the pressure tube bursts the conservative assumption is that the entire pressure-tube/calandria-tube assembly ruptures.

Discharge of high-temperature, high-pressure coolant from a bursting pressure tube can be expected to be violent and unsteady, with rapid tearing of the tube, large pressure transients in the moderator, vapour evolution and collapse and possible ejection of fuel bundle fragments. Rupture of an adjacent pressure tube as a result of the bursting must be considered, to see if it is a reasonable possibility.

Physical mechanisms which have been considered are described in the following sections.

1.3.1 Impulsive Pressure Loading

The deflection of a pressure-tube/calandria-tube assembly due to a pressure transient will depend on the amplitude and steepness of the pressure pulse and on its spatial distribution relative to the pressure tube array.

Inelastic collapse of the calandria tube onto its pressure tube has been observed experimentally in tests in which pressure tube bursting was simulated in various ways. While the collapse of the calandria tube may not lead directly to damage of the enclosed pressure tube it could lead to vapour evolution in the moderator due to enhanced heat transfer from the pressure tube, after the necessary time delay for conduction. Conceivably such vapour might contribute to damage via vapour collapse, but to date no evidence has been provided that this is a realistic possibility.

The amplitude of the impinging pressure wave will depend not only on the pressure difference between coolant and moderator but also on the rate of opening of burst area, the kind of rupture opening (e.g. axial or circumferential split), the rate of development of two-phase choked flow in the pressure tube upstream of the rupture opening, and on the effect of adjacent tubes on the wave form. Wave reflection effects could conceivably intensify the wave as it passes between two tubes, depending on the tube mass and flexibility. In general, however, one would expect most intense pressure wave loading to be on those tubes closest to the rupture opening.

Given the randomness associated with rupture of an inhomogeneous power channel and the randomness associated with two-phase flow, exact simulation of the pressure pulse is not a realistic possibility and the best that can be hoped for is a consideration of the maximum possible amplitude resulting from given coolant and moderator pressure, allowing for possible reflection effects.

The steepness of the pulse must be known if its impulse on the adjacent pressure tube-calandria tube assembly is to be estimated. Shock waves have been observed in underwater explosions, but even if a pressure tube could burst instantaneously the resultant shock wave would be of such low strength that its propagation speed would scarcely exceed the acoustic speed.

Damage of a pressure tube assembly due to a pressure transient will depend on its structural mass and rigidity and strongly on the shape of the wave front. Even in a long axial split of the bursting tube, time will be required for the split to propagate from some initial location. Assumption of instantaneous propagation of the split could produce a considerable overestimate of pressure pulse amplitude and steepness.

1.3.2 Missile Damage

Experiments simulating the effect of pressure tube burst have given examples of the forcible ejection of simulated fuel elements but no measurements of momentum or impact force appear to be available.

Plausible calculations have been made of the velocity which could be attained by solid fragments of various sizes, and of the retarding effect of the surrounding moderator as these fragments are projected toward the pressure tube or calandria vessel wall.

The impact loads depend strongly on the mode of pressure tube rupture, e.g. on whether a circumferential break (guillotine rupture), with subsequent rifle-like acceleration of a fuel bundle or part thereof, can be expected to take place.

1.3.3 Collapse of Large Vapour Pockets

If a large hot vapour pocket exists in a fluid, convection cooling of the liquid near the interface can lead to rapid collapse of the vapour zone and to large hydrodynamic forces being applied to structural surfaces. Experimental and theoretical work on the "chugging" phenomena associated with steam flow through the downcomers into the steam suppression zones of a Boiling Water Reactor (BWR) have confirmed the possibility of substantial structural damage.

In tests simulating vertical pressure tube reactors in which there is a substantial gas cap at the top of the moderator in the calandria vessel, large vapour zones have been observed to form as a result of pressure tube burst. The formation of this high pressure vapour region has led to considerable upward acceleration of a large "slug" of moderator which would compress the gas cap. The subsequent downward motion of this "slug", accompanied by cooling of the vapour interface, has been observed to lead to large impact pressures.

In other tests vapour evolution and collapse some distance from a bursting pressure tube may be inferred (from transient pressure signals) to have taken place.

Though the hydrodynamics of large vapour pocket collapse may not damage an adjacent pressure tube (other than causing partial collapse of the calandria tube) such forces might damage a shut-off-rod guide tube. Experimental data are not available on collapse of large vapour pockets in horizontal pressure tube reactors with essentially no gas cap. Also missing, however, are data or calculations which would rule out this possibility.

1.3.4 Sustained Jet Impingement

Jet impingement forces due to pipe break and consequent formation of a jet passing through air have been subject to considerable experimental study. Given the typical spacing of reactor pressure tubes (Figure 1.3) there are grounds for expecting that such impact forces would be somewhat attenuated by the intervening moderator liquid.

However, with a limited-size break it is possible that, given the inventory of coolant in a pressure tube reactor system, jet discharge could be sustained for times considerably larger than has been the case in which the coolant inventory has been limited essentially to that of the burst itself. It is also conceivable that the sustained two-phase jet could pass through vapour pockets (previously formed by the initial coolant discharge) before impacting adjacent tubes.

Experimental demonstration of this mode of damage is not available and simple estimates of the magnitudes of forces which could be realized need critical scrutiny.

1.3.5 Pipe Whip

Reactive forces on the burst tube provide substantial lateral displacement and impact on adjacent pressure-tube/calandria-tube assemblies. Experimental evidence is not available to demonstrate that this could lead to serious damage of an adjacent pressure tube, but calculations indicate that one or more shut-off-rod guide tubes could be damaged by pinching.

Approximate numerical calculations indicate that the surrounding moderator fluid would have a substantial damping effect on the pipe motion.

1.4 POSSIBLE DAMAGE TO SHUT-OFF-ROD GUIDE TUBES

Several mechanisms could lead to damage of shut-off-rod guide tubes, but these failures do not propagate and several such failures would be necessary before reactor shut-off by this system acting alone could be prevented.

1.4.1 Pressure and Impact Loadings

Shut-off-rod guide tubes being of relatively light construction appear to be considerably more susceptible (than adjacent pressure tubes) to failure by pressure loading. Thus pressure loading relatively far from the pipe burst location is of concern and several shut-off-rod guide tubes could be affected.

No experimental data on guide tube collapse due to pressure tube impact or pinching is available. The impulsive loading may be estimated from transient thermal hydrodynamic calculations, but such calculations and the crushing strength of guide tubes under impulsive loading need further attention.

1.4.2 Missile Damage

Some data is available on the loads required to collapse shut-of-rod tubes due to the three-point static loading. These data may be used to estimate the possibility of damage to single shut-off-rod guide tubes due to impact of a single missile.

A mechanism for missile damage to more than, say, two shut-off-rod guide tubes does not appear to be available.

1.4.3 Collapse of Vapour Pockets

Collapse of a large vapour pocket surrounding a shut-off-rod guide tube could cause substantial damage. However, there is no experimental evidence and, to date, no evidence from numerical simulation of thermal hydro-dynamic transients that vapour pocket collapse could crush several shut-off-rod guide tubes.

1.4.4 Sustained Jet Impingement

Again damage to two shut-off-rod guide tubes is possible but there does not appear to be a mechanism for damage of several shut-off-rod guide tubes from a single pressure tube burst.

1.4.5 Pipe Whip

The test data mentioned in Section 1.4.2 may also be used to estimate the possibility of damage to perhaps two shut-off-rod guide tubes due to pipe whip.

1.5 POSSIBLE DAMAGE TO CALANDRIA VESSEL

Propagating pressure tube failure could undoubtedly lead to overpressurization of the calandria vessel; damage to the vessel must therefore be of serious concern if it can be shown that propagation of pressure tube failure is a realistic possibility.

Bursting of a single pressure tube will lead to substantial pressure loading of the calandria vessel wall. Present experimental and analytical results indicate that though local stress from such a loading may be high, the expectation of substantial damage to the vessel cannot be quantitatively justified.

Even if the vessel walls were partially ruptured by pressure loading or by missile damage, the surrounding shield tank is of such construction as to be expected to contain the damage. At the top of the pressure tube reactor the calandria is contained by the concrete reactivity platform, which has at the bottom a 38 mm steel plate with stifferning ribs.

Impact on the calandria wall of pressure waves, missiles, sustained jets or vapour collapse due to a pressure tube bursting in the immediate vicinity of the wall would not lead to serious damage of the wall because of its considerable thickness (38 mm).

Numerical simulation methods are available for estimating deformation of calandria vessel due to pressure transference, generated by any configuration and location of pressure tube burst. In such calculations it is essential that structural material behavior as well as fluid properties and vessel configuration be represented in detail. Since the effect of the pressure tube array on wave propagation is neglected, accurate simulations have not been attempted. Simpler methods have been used to provide assurance that calandria vessel damage is unlikely.

1.6 SCOPE OF THIS STUDY

The possible damage mechanisms specified in Section 1.3 (Possible Propagation of Pressure Tube Failure), 1.4 (Possible Damage to Shut-off-rod Guide Tubes), and 1.5 (Possible Damage to Calandria Vessel) were the focus of attention in this study.

1.6.1 Literature Review and Site Visits

Besides published work, the literature review included unpublished reports and work on the underlying physics associated with behavior subsequent to pressure tube rupture. A complete list of these reports is in Appendix I.

Visits to reactors under construction, reactor component manufacturers and experimental facilities, as well as exchanges with investigators who have been active in associated fields were made to examine equipment and discuss safety issues. Literature review and exchanges with other investigators led to the conclusion that the rupture modes which have the most potential for violent explosion should be studied in order to establish a "worst possible" or "bounding" case of hypothetical pressure tube accident and to assess the potential damages of an accident.

1.6.2 Rupture Modes and Relevant Physical Processes

Experimental evidence indicated that credible pressure tube rupture modes include holes of limited size, circumferential breaks and axial splits. Among the three rupture modes, axial split appears the most probable and has greatest potential for damage due to pressure loading.

The physical processes associated with pressure tube rupture accidents include crack tip propagation, decompression of high enthalpy coolant through the crack opening, shock wave propagation, phase change of the fluid, bubble dynamics and fluid-structure interaction.

Although there have been a large number of experimental investigations into the various aspects of the physical processes due to pressure tube rupture, there are only three major existing analytical works which model physical processes relevant to the reactor of interest. However, due to the complexity of the physical processes, there exist differences in the assumptions made in the analytical model formulations.

1.6.3 Computer Simulation of Pressure Tube Rupture

To obtain an independent evaluation of the transient loadings due to pressure tube rupture, computer simulations were done with the computer code PISCES. Although computation models constructed are simple and conservative. the pressure and velocity fields in the moderator and the loadings of the calandria vessel so obtained do provide a basis for comparisons with existing analytical calculations.

1.6.4 Experimental Simulation of Pressure Tube Rupture

Using high speed photography, a simple visualization study was performed to gain qualitative insight into the physical processes that occur immediately after the initiation of tube rupture. Both liquid and gas were used as coolant in the experiment. The film obtained clearly illustrates the effect of coolant, moderator density, phase change and coolant temperature on crack propagation and vapour pocket pattern formations.

1.6.5 Structure of this Report

Damage mechanisms may be classified as short term or long term. Short term mechanisms include the pressure wave loadings which occur in the first tens of milliseconds after the initiation of rupture in the pressure tube. Long term mechanisms include impact damages from a sustained two-phase jet, pipe whip and missiles of ejected fuel elements from the ruptured tube. The emphasis of this report is on the potential damages to the adjacent pressure and shut-off-rod guide tubes and the calandria vessel due to the

short term mechanisms, since available data on long term mechanisms are exclusively those from tests done in air and objective assessment of damages in submerged environment cannot be based in such data.

In Section 2 of this report, previous experimental work is reviewed, the probability and damage potential of the rupture modes are compared, and the underlying physical processes are discussed. Previous analytical work is reviewed in Section 3, where the limitations and capabilities of simplified modelling and the detailed computer simulation are compared. Section 4 presents the results and findings of additional computer and experimental simulations performed in this study. Conclusions from previous and present experimental and analytical work are given in Section 5. Recommendations for future investigations are made in the final section.

2.0 REVIEW OF EXPERIMENTAL WORK

2.1 INTRODUCTION

This chapter reviews previous experimental work on pressure tube rupture in pools and closed vessels, and refers to related work on crack propagation in pressurized tubes and to data on submerged explosions. Although this past work is highly instructive, in no case does it provide exact simulation of pressure tube bursting which might occur in a typical pressure tube reactor.

No experimental data is available for spontaneous bursting; experiments generally employed weakened tubes (e.g. machined flats) or used explosive material (thermite) to initiate the burst. Thus these experiments did not provide information as to the kinds of burst opening geometry which would result from specific tube defects or modes of fuel overheating.

In general, non-irradiated materials were used in the experiments.

Several of the experiments used approximately full scale pressure tubes, but tube lattice geometry and the thermal-hydraulic-structural interactions between exploding coolant, moderator and pressure vessel were only approximately represented in few experiments.

Coolant conditions in the experiments generally fell somewhat short of the pressures and temperatures of pressure tube reactors, except for one experiment in which substantially higher pressures and temperatures produced considerable damage. In some experiments, gas or steam was used instead of hot water. In general, the coolant available to participate in the bursting process was limited to that contained within the tube itself; this precluded study of the possible effects of sustained discharge.

Despite these limitations, however, previous experimental work provides considerable insight into possible effects of pressure tube bursting: transient pressure loading of adjacent tubes and calandria vessel, expulsion of pressure tube contents as missiles which might damage tubes or structures in their paths, and pressure pulses generated by vapour collapse.

2.2 PRESSURE TUBE RUPTURE IN POOLS

Table 2.1 shows the main features of five experiments reported on pressure tube rupture in pools.

2.2.1 Burnup (1960)

Burnup's experiments were the first of a series of simulation tests performed to assess the potential consequences of pressure tube ruptrue in the NPD reactor. The rectangular tank housing a 3x3 tube array is the same tank that Ross-Ross leter used (see Figure 2.1). Both sealed small holes and machined flats were employed to initiate pressure tube rupture.

In the tests with sealed holes, the jet from a 3.175 mm hole in the pressure tube caused a 6.35 mm diameter indentation on the enclosing calandria tube. When a 6.35 mm hole was drilled in the enclosing calandria tube in line with the 3.175 mm pressure tube hole, the length of the coolant jet in the moderator oscillated rapidly between 50 and 100 mm, never reaching the nearest adjacent calandria tube.

In the tests performed with 76.2 mm and 150.2 mm machined flats, no damage to the enclosing calandria tube was observed, apart from marks where the lips of the pressure tube opening had touched. When 228.6 mm long machined flats were used, rupture of the enclosing calandria tubes occurred. In some cases, complete sections of the pressure-tube/calandria-tube assembly were torn out.

Describing the violent hydrodynamics in the moderator tank, Burnup further stated that

> "The tank had in this instance been lined with styrofoam, a foamed plastic with a crushing strength of about 30 psi. Much of this plastic was damaged, some were crushed while other pieces appeared to have been pulled from their mounting bolts by suction forces. However, the lack of reversal of the distorted frangible diaphragms (used to measure pressures in the moderator) indicates that a negative pressure wave would not have exceeded a third of the initial positive pressure."

Table 2.1 Pressure Tube Rupture in Pools

Investigators	Coolant	Materials, Press.Tube/ Cal. Tube	Explosion Tube and Lattice	Defect Type and Length	Pool	Main Concerns
Ross-Ross (1973)	Water -10MPa -280°C	Mild Steel/ Zr2	0.108 m tube 9 array	axial 0.15-0.20 m	H = 2.44 m W = 1.22 m L = 3.66 m	. PT/CT annulus pressurization vs annulus exhaust area
Ross-Ross (1963)	Water 7.9-13.3 MPa 250-270°C	Zr/Al	0.087 m tube 9 array	axial 0.13-0.30 m	H = 2.44 m W = 1.22 m L = 3.66 m	. PT/CT annulus pressurization . Probability of failure propagation . Damages by fuel element missiles
Isles (1965)	Water 22.06-26.89 MPa 340-375°C	Mild Steel/ Zr2	0.87 m tube 9 array	0.495 m thermite	H = 0.914 m W = 1.84 m L = 5.03 m	. Probability of failure propagation . Damage to adjacent tubes . Damage by fuel element missiles
Robert and Swinhoe (1960)	N_2 Gas - 6.9 MPa room temperature	Mild Steel/ Al	0.152 m tube 4 array	axial 0.05-0.23 m circumferential	H = 2.13 m W = 15.2 m L = 30.5 m	. Attenuation of pressure pulse with distance . Dependence of pressure transient on rupture modes
Burnup (1960)	Water 7.6-10.3 MPa 254-270°C	Mild Steel Al	0.102 m tube 9 array	axial 0.08-0.33 m small holes	H = 2.44 m W = 1.22 m L = 3.66 m	. Damage to enclosing and adjacent calandria tubes.

2.2.2 Roberts and Swinhoe (1960)

Low temperature nitrogen gas was used as simulated coolant at pressures of up to 8.6 MPa in a 152.4 mm diameter mild steel tube surrounded by an aluminum tube with an air gap of 6.35 mm. The test tube was located in a 4-tube array (spacing 254 mm) submerged in a pond.

Pressures were measured in the pond at various distances from the burst site.

Three types of tube weakening were employed:

- milled flats of 50.8 mm, 152.4 mm, and 228.6 mm axial length
- circumferential vee groove
- thin cylindrical section of 50.8 mm length.

The measurements of pressures near the array, due to pressure tube burst with and without calandria tube containment, showed that the aluminum calandria tube reduced the peak amplitude of the pressure pulse by an order of magnitude.

Much of the greatest pressure amplitudes and impulses were obtained from circumferential failures. The longest axial split was only half the circumference of the tube. As would be expected, the pressure amplitudes and impulses attenuated substantially with distance from the burst site.

Of the two effects - rate of fracture propagation and size of ruptured area, Roberts and Swinhoe concluded that the latter is the most important in determining the total impulse of the pressure wave.

These conclusions were drawn from experiments with high pressure gas as the bursting medium; subsequent work of others indicated that axial split produces higher pressure amplitudes than circumferential failure and that the rate of depressurization with hot water is quite different from gas.

2.2.3 Ross-Ross (1963) (1965) (1973)

The early work reported by Ross-Ross (1963) was concerned with the possibility of bursting an aluminum alloy NPD calandria tube subsequent to pressure tube burst. It was found that the calandria tube would burst when the pressure in the annulus had reached about 3.8 MPa.

In a subsequent experiment (1965) Ross-Ross found that with sudden pressurization of a short length of the same aluminum tube by a steam-water mixture at about the same temperature as in the earlier tests (but without the stress-concentrating effects of the discharge from the burst pressure tube), the burst pressure in the calandria tube was 4.5-4.8 MPa. In some cases, bursting occurred after the peak pressure, due apparently to stresses induced by heating. Initially the tube was in biaxial tension but heating was believed to have produced appreciable axial compression stresses. Heating appeared to take place within 0.2 s; accurate measurements of wall temperature were not feasible.

Ross-Ross (1963) reported the results of bursting a pressure tube in a 9-tube array representing (approximnately in full scale) a portion of the NPD calandria. The array was located in an open tank, 1219.2 mm wide and 2438.4 mm deep, as shown in Figure 2.1. The pressure tube was of Zircaloy-2 of 82.55 mm. internal diameter; it was enclosed by an aluminum calandria tube of 101.6 mm. internal diameter. Eleven simulated fuel bundles consisting of 7 steel rods were located inside the tube to be burst. The annular gap was filled with air.

The pressure tube to be burst was weakened by milling an axial flat and ruptured by over-pressurization. The light water in the pressure tube was heated to 277°C.

The tests showed that the calandria tube failed by axial splitting in the area over rupture site of the pressure tube.

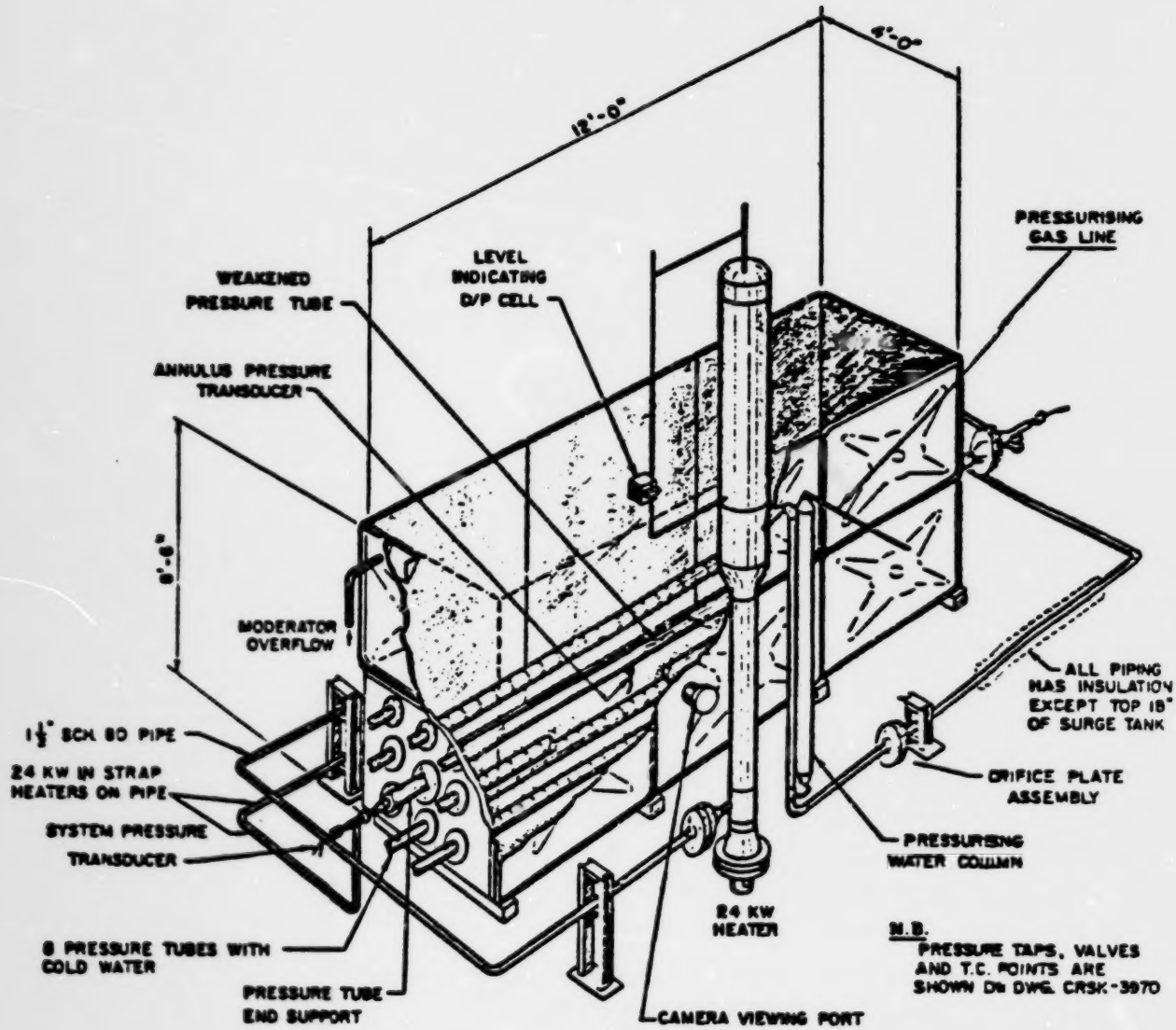

PICTORIAL VIEW OF TEST FACILITY

Figure 2.1 Test Rig of Ross-Ross (1963)

Ross-Ross reported that

> "When the calandria tube splits open, the pressure in the annulus drops quickly and the defect in the pressure tube which has begun to tear circumferentially is then able to continue tearing around completely, thus severing the tube. Once severed there are large impulsive end loads on the pressure tube end supports or end fittings. The reaction due to the discharge of steam either during this tearing around and severing and/or after bends the pressure tube at the suport; this allows the bundles to be fired out of the remaining halves of the pressure tube.
>
> The fuel bundle located at the rupture is bent or bowed outwards due to difference in pressure across the bundle. If the bowing is severe enough. the elements will break open. Indications are that the bundle is pretty well broken apart at this point. The ensuing discharge then distributes the elements of the bundle throughout the tank.
>
> The fuel bundles which are on either side, that is in the remaining halves. are fired out more or less axially with considerable force and are driven into the end of the tank (or calandria end wall) leaving in some cases dents in the 3/4 inch steel end plate. These bundles may also cause longitudinal scoring and cutting of the calandria tubes in adjacent positions, usually toward the ends of the tank. Imprints and marks on the end walls indicate that these bundles are more or less intact at impact.
>
> At impact the bundle elements suffer damage by axial buckling and usually some bending. The end plates of the bundles are broken and the elements may separate. Breaking of the elements may or may not occur and the individual elements may cause puncturing of the calandria tubes at the end wall; in most cases this results if there is piling up of the bundles. Some denting of the pressure tube beneath the punctured calandria tube has been found but there was no cutting, scoring or damage which could cause rupture of that tube.
>
> There is little evidence of damage from projectiles (fuel elements) to adjacent calandria tubes opposite or beside the burst position. Collapse deformation is found in those tubes directly opposite the burst, and partial collapse, i.e, becoming somewhat oval, is

found in the tubes further away. This damage results from the pressure wave propagated through the moderator, which accompanies the rupture of the calandria tube and the explosive decompression of the coolant.

The pressure wave, as well as collapsing the surrounding calandria tubes, presses the tube onto the garter spring spacer leaving the semicircular ridge or deformation around the tube on the side toward the rupture. This pressure wave also causes buckling or circumferential splitting of the calandria tubes at the end walls. Although a rolled joint similar to that in the NPD reactor was not used in these tests, undoubtedly the joint or material immediately adjacent would be damaged in some manner.

The pressure wave also produced significant bulging of the side walls and to a lesser extent of the end plates of the tank."

In general, these tests indicated that missiles and pressure waves could cause penetration and rupture of adjacent calandria tubes, though there was no evidence of failure of adjacent pressure tubes.

In later work Ross-Ross (1973) used Zircaloy-2 calandria tubes, surrounding a mild steel pressure tube weakened by machining and filled with fuel bundles. Light water flowed through the pressure tube, entering at 282°C and leaving at 272°C. Bursting pressures (inside the pressure tube) were as high as 11 MPa.

The pressure tube and calandria tube (3000 mm long) were separated by coil springs which were generally blown out of the annulus when the pressure tube burst. In all eight of these tests the pressure relief through the annulus was sufficiently rapid to prevent calandria tube failure. Ross-Ross observed surface boiling of the moderator took place before rupture. The steam bubbles "expanded, moved upwards around the outside of the tube, floated free and collapsed". Examination of the rupture pressure tube showed fuel elements pushed into the opening and against the calandria tube. In separate tests using the 1965 apparatus (for sudden pressurization of the

calandria tube without using pressure tube burst) Ross-Ross found that while the peak pressure inside the Zircaloy calandria tube would rise to 9.7 MPa, bursting would occur somewhat later when the internal pressure had fallen 6% to 9.2 MPa. Apparently about 0.5 s is required for the burst strength to drop about 20% due to thermal stress.

Ross-Ross found that irradiation of the Zircaloy calandria tube (to a level of $2x10^{24}$ n/m^2) increased the burst pressure by about 10% without mush loss in ductility. The irradiated tubes were not notch-sensitive ("the grooves cut into the test specimen did not reduce the burst strength in proportion to the local reduction in wall thickness".) Campbell (1979) points out that the radiation level cited above is only of the order of 1% of the typical lifetime level for a calandria tube so that firm conclusions cannot be drawn from the above as to irradiation effects.

Ross-Ross (1973) concluded that with suitable exhaust area from the annulus between pressure tube and calandria tube "the possibility of rupturing the calandria tube by overpressure following the rupture of a pressure tube is extremely small." In this sense the calandria tube could be considered an effective containment.

In current reactors, however, the spacers used in the pressure-tube/calandria-tube annuli are such that the annulus area cannot be considered open for flow. Given that the Zircaloy bursting pressures measured by Ross-Ross are close to the design operating pressure in the pressure tube (and disregarding pressure relief due to annulus flow and heat transfer to moderator) the design assumption must be that if the pressure tube fails the calandria tube will also fail.

2.2.4 Isles (1965)

Isles reported the results of bursting of a full size pressure (and calandria) tube in a 9-tube array in a pool longer than the array, 914.4 mm depth, and 1828.8 mm in width, as shown in Figure 2.2. Each of the 9 tubes was

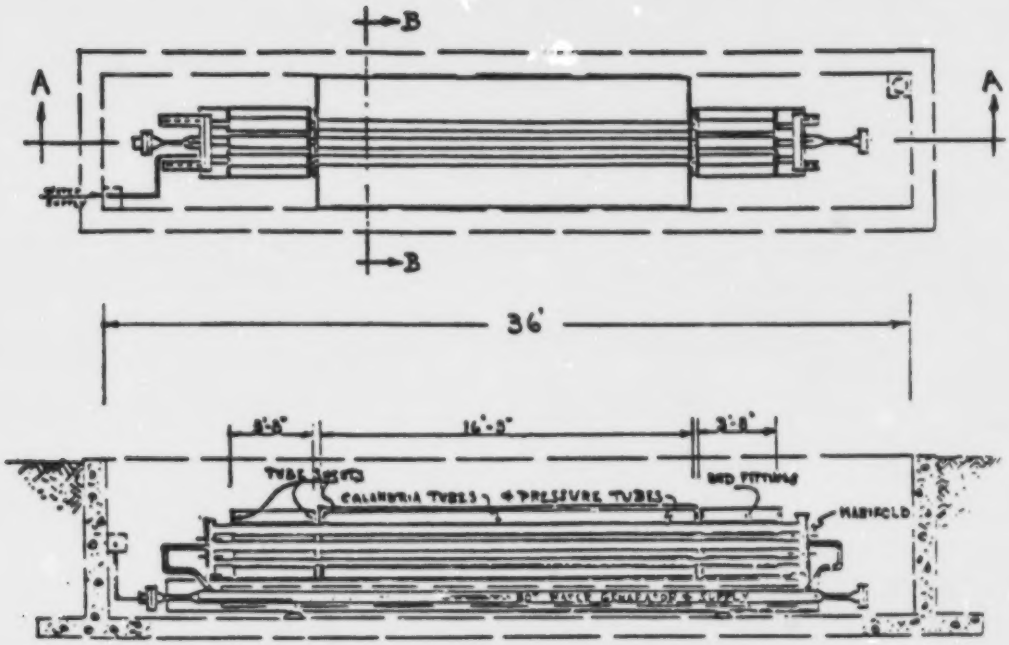

ELEVATION A/A

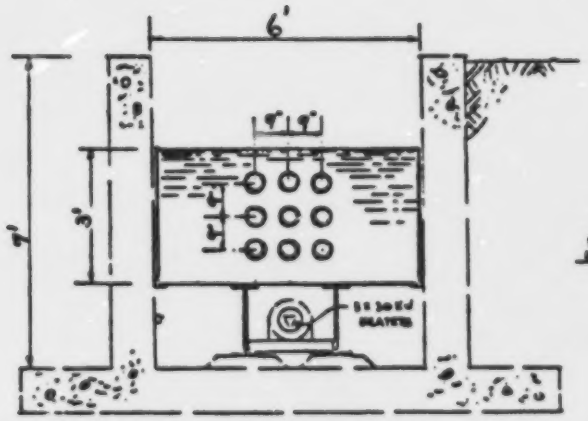

SECTION B/B
(DOUBLE SCALE)

LATTICE SITE
SHOCK TEST RIG

Figure 2.2 Test Rig of Isles (1965)

pressurized with hot water at the same pressure and temperature. The pressure tube and the calandria tube were made of mild steel (except in Test No. 8 and single channel calibration tests where Zircaloy-2 calandria tubes were used). The central pressure tube was loaded with carbon steel rods to simulate fuel elements.

Bursting was done with supercritical light water, typically at 24 MPa and 380°C in the pressure tube. Bursting was initiated by a thermite bomb which produced temperatures of around 2800°C and caused failure of the pressure tube by melting rather than by overpressurization.

Isles reported the results of Test No. 8 as follows:

"(1) None of the remaining eight pressure or calandria tubes were ruptured.

(2) No horizontal movement of the end fittings was detected and likewise the connecting feeder pipes remained undamaged.

(3) All calandria and pressure tubes were moved or distorted from their original position.

(4) All calandria tubes were collapsed against their respective pressure tubes at the mid section for approximately 5 feet.

(5) The distortion of the calandria tubes caused ribbing and fracture at the tube sheets. The calandria tube-to-tube sheet rolled joint, however, did not fail.

(6) A major portion of the 30,000 lbs. of moderator fluid was ejected during the blast and did not return to the tank.

(7) All fuel in the centre tube was ejected and badly damaged.

(8) No evidence was noted either during or after the test of a chemical fire in the zircaloy calandria tubes."

In a calibration test of a single burst channel (other array members missing), again with supercritical pressure and temperature in the pressure tube prior to burst, maximum pressures in the bottom half of the pool were measured at 4 positions, each 292.1 mm from the centre of the channel, as 4.1, 8.7, 3.1, and 8.8 MPa. At 635 mm from the centre line of the channel the maximum pressure measured was 1.5 MPa.

Isles reported that in Test No. 7 with the 9-tube array and coolant at 377°C and 24.1 MPa in the pressure tube before burst:

> "Lattice Position No. 1 also failed but at the north end of the rig only. In this case the area adjacent to a welded section of the pressure tube failed at the calandria wall. The calandria tube in this vicinity ruptured circumferentially."

He also reported that

> "All calandria tube rolled joints failed in varying amounts, from the No. 5 position where the tube was completely removed, to Position No. 7 where the calandria tube was shifted approximately 1/2 inch."

Also

> "The welded 19 element shell mock fuel bundles in the central location were projected from the pressure tube and "broken up" probably after impact with the surrounding enclosure, such as the walls of the tank. Several of the pencils or elements, however, were fired to distances of up to 100 feet from the rig."

Also

> "Puncture type holes were found in several calandria tubes due to flying missiles, such as fuel pencils, parts of the "hot" fuel bundle, etc."

Concerning the possibility of propagating failure, the one example demonstrated in the Isles test is puzzling. The No. 1 lattice tube, which was not directly above the explosion tube, evidently failed circumferentially

adjacent to the tube sheet from which it was completely removed. This failure was about 8 feet from the pressure tube burst site and its mechanism has not been explained. Campbell (1979) writes,

> "in an otherwise detailed report, the author's complete discussion and description of this event are severely limited; there are no detailed pictures. no post mortem examinations, no postulated failure mechanisms. With such an obscure reference it is not surprising that this instance of failure propagation seems to have been frequently overlooked."

It must be borne in mind that the maximum pressure prior to burst in the Isles experiment was about 2.3 times the maximum pressure typical of heavy water cooled and moderated pressure tube reactors. Also the supercritical temperature level would imply substantially greater "elasticity" in the fluid than at typical reactor coolant temperatures. Nevertheless it is clear that Isles experiments did demonstrate both missile damage and propagation failure.

Concerning the missile damage, Ross-Ross and Langford (1980) argue that the steel rods used to simulate the fuel elements in these experiments would be expected to be more damaging than "hot sheathed fuel elements which would have more mass and could be considered to behave like heavy lead slugs." Ross-Ross and Langford go on to conclude that

> "piecing of a pressure tube from lateral ejection of fuel elements seems remote. based on all the experimental data to date. Piercing would mean a loss of coolant through a small orifice and would be of less consequence than demonstrated in Japanese experiments."

(referring to a private communication from T. Kitihara of the Power Reactor and Nuclear Fuel Development Corporation of Japan). The "experimental data to date" referred to by Ross-Ross and Langford, would appear to include work of Ross-Ross (1963) in which he reported "extensive

damage when a calandria tube ruptured." the Isles report cited above. and the Japanese work, results of which were not available to us.

It is not clear to us how these three reports supply satisfactory evidence that flying fuel elements are unlikely to pierce adjacent pressure tubes. The converse is of course unproven from the Isles test in which the burst pressures and temperatures were exceptionally high and the dummy fuel elements. though designed to have about the same total mass as the real elements, could have been more likely to penetrate.

Peak pressures. measured as a function of distance from the burst site. are shown in Figure 2.3. which compares the data of Isles (Test No. 8e with coolant at 24.1 MPa and 371°C) and the data of Hayamizu. Tokumitsu and Hayashi who used steam at 7.1 MPa and 287°C.

2.2.5 Summary

If the pressure-tube/calandria-tube annulus were to offer no resistance to flow the pressure load on a calandria tube following a pressure tube burst would likely be well below its bursting pressure, due to annulus flow and cooling of the outer surface of the calandria tube by moderator. Current designs of pressure tube reactors include substantial flow blockage in the annular channel so that substantial pressure relief cannot be assumed. Rather. the prudent assumption is that if the pressure tube fails. the calandria tube does also. through the latter may well play a helpful role in attenuating the pressure pulse imparted to the moderator fluid.

Tests on pressure tubes in small arrays in pools have demonstrated substantial damage following pressure tube burst.

In the Isles test both missile damage to adjacent tubes and tube sheet. and circumferential failure of a second pressure tube (near the tube sheet and far from the burst site) were demonstrated. This failure has not been explained. It must be emphasized. of course. that the bursting pressure and

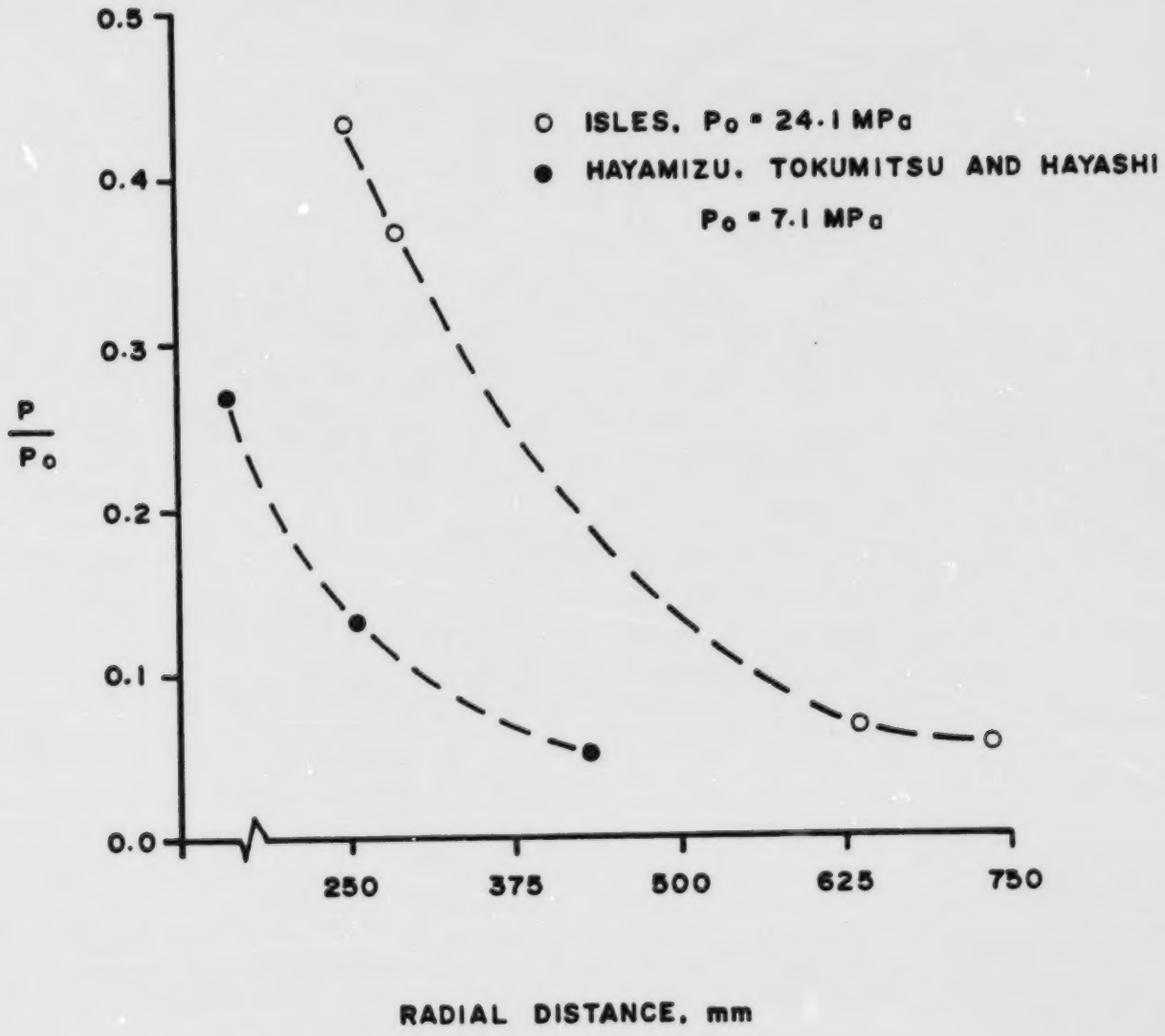

Figure 2.3 Pressure Decay with Radial Distance

temperature in these tests (24 MPa and 377°C) were much higher than the design values for pressure tube reactors. Thus. the Isles tests provide neither proof that propagative failure can take place following tube burst at design values of pressure and temperature. nor do they provide clear assurance that such an event cannot happen; the failure mode is unexplained. One reason for not ignoring such a failure mode is the discovery of cracks in the pressure tubes of Pickering 3 due to incorrect installation procedures (see Ross-Ross. Duncan Mitchell Towgood. and Hunter (1976)).

In the Isles and other tests there was considerable collapse of calandria tubes and denting of pressure tubes. These effects are not catastrophic

The question of possible missile damage is not conclusively settled by these tests. which supply evidence of some damage but not enough to cause propagating pressure tube failure. In the one case in which propagating failure occurred the caused failure. as noted earlier. has not been explained.

In the open pool tests. the typical expulsion of most of the liquid from the pool means that only the initial effects of the burst could be expected to simulate damage mechanisms inside a calandria vessel. Such tests cannot. however. represent the complex pressure gradient due to superimposed reflections from the wall of a closed vessel or due to the collapse of large vapour zones in the vicinity of an adjacent tube.

2.3 PRESSURE TUBE RUPTURE IN CLOSED VESSELS

2.3.1 Introduction

Experiments on pressure tube rupture in closed vessels invite attention to events external to the hypothetical ruptured pressure tube, i.e. the loading of adjacent tubes and the calandria vessel imparted by the pressure transients following explosion of the high temperature and high pressure coolant. Following the initial acoustic (or shock wave) the moderator is pressurized by expansion (or contraction) of the vapour pocket formed by the decompressed coolant. The transient pressure distributions are strongly influenced by the vessel flexibility, as well as the presence of vapour in the moderator. The vapour pocket is often referred to as a "bubble" and bubble dynamics is essential to the understanding of sequential events following the rupture of a pressure tube in a calandria vessel.

Table 2.2 summarizes tests in which pressure tube bursting took place in closed vessels. In one case the discharge (of gas following burst of a nitrogen-filled PVC tube) was recorded photographically; generally, the only evidence available is in the form of pressure transducer readings which show instantaneous pressure pulse amplitude at particular points in the pressure vessel. In two cases pressure loadings on an adjacent tube are indicated by the readings of transducers located on that tube. In another test strain gauges placed on the pressure vessel wall showed transient strains. Though the Bettula vertical calandria vessel tests (described in 2.3.2, .3, .4 below) provided much valuable information, their configuration is quite different to the horizontal-axis Canadian pressure tube reactor.

Table 2.2 Pressure Tube Experiments in Closed Vessels

Investigators	Coolant	Materials, Press.Tube/ Cal. Tube	Explosion Tube and Lattice	Defect Type and Length	Vessel	Main Concerns
Hareux et al Steel Model (1964)	N_2 Gas 293°C 6 MPa	PVC/-	D = 0.11 m 184 array	shattering of PVC tube 0.5 m	D = 0.50 m L = 0.50 m horizontal cylinder	. Maximum pressue and strain on vessel . Pressure transient . Visualization of explosion process with high speed photography
Holtbecker et al (1970)	Organic 0.6-4.2 MPa 400°C	SAP895/Al or SAP895/Zr2	D = 0.110 m 28 array	axial 0.3-1.5 m	D = 2.38 m H = 2.40 m vertical cylinder	. Hydraulic and thermal loading on adjacent tubes . 12 runs
Hayamizu et al (1974)	Steam 7.2 MPa 287°C	Steel/Al	D = 0.117 m 21 array	rectangular 90 x 50 mm	D = 1.70 m H = 4.50 m vertical cylinder	. Loading on adjacent tubes
Famiglietti et al (Bettula I) (1975)	N_2 Gas Water, Steam 4.1-5.4 MPa 247-268°C	Al/-	D = 0.118 m 51 array	axial 0.80 m	D = 2.38 m H = 2.40 m vertical cylinder	. Loadings of vessel and adjacent tubes . Influences of coolants and system parameters . Pressure transient
Dallavalle et al (Bettula II) (1977)	Steam-Water Mixture 4.60-6.32 MPa 274-281°C	Al/- Zr/-	D = 0.118 m 32 array	axial 0.237-3.000 m	D ~ 1.45 m H = 4.00 m vertical cylinder	. Influence of rupture lengths . Loading of adjacent tube and vessels
Chevallard et al (MARC) (1979)	N_2 Gas 3.0 MPa room temperature		D = 0.030 m 60 array	axial 0.445 m (long slot covered by 5 mm metal sheet)	D = 0.738 m H ~0.89 m vertical cylinder	. Loadings due to central and peripheral explosion . Loadings on structural member supporting vessel

2.3.2 Hareux, Roche, and Vrillon (1964)

This report describes tests of two model calandria vessels, both of diameter and lengh 0.5 m and filled with 113 small tubes to simulate fuel channels (see Figure 2.4). One vessel was made of a steel cylinder (2 mm thickness) mounted between rigid end plates. The other cylinder was made of plexiglass to permit photography of the bubble movement following explosion of high pressure gas contained in a tube.

High pressure gas was used since the experiments were to relate to a gas cooled (heavy-water moderated) pressure tube reactor.

The bursting pressure tube material was polyvinyl chloride, chosen because the material shattered along the whole tube length almost instantaneously, and thus provided rapid depressurization.

In their high speed photographic record of the gas bubble explosion and discharge of water through the relief pipe, one can clearly see cyclic expansions and contractions of the bubble due to vessel responses before discharge of water from the relief pipe occurs. Hareux et al stated that the maximum pressure on the vessel occurred before flow from the relief pipe started and wrote that

> "We must particularly insist on the fact that no result could show any influence from the outlet sections, from the water head in these outlets (we have examined a head exceeding the vessel 1.5 diameters) nor from the gas inlet section."

From these observations, they assumed a closed vessel would be satisfactory for calculation of maximum loading on the pressure vessel wall.

The recorded pressures showed several oscillations of rapidly declining peaks.

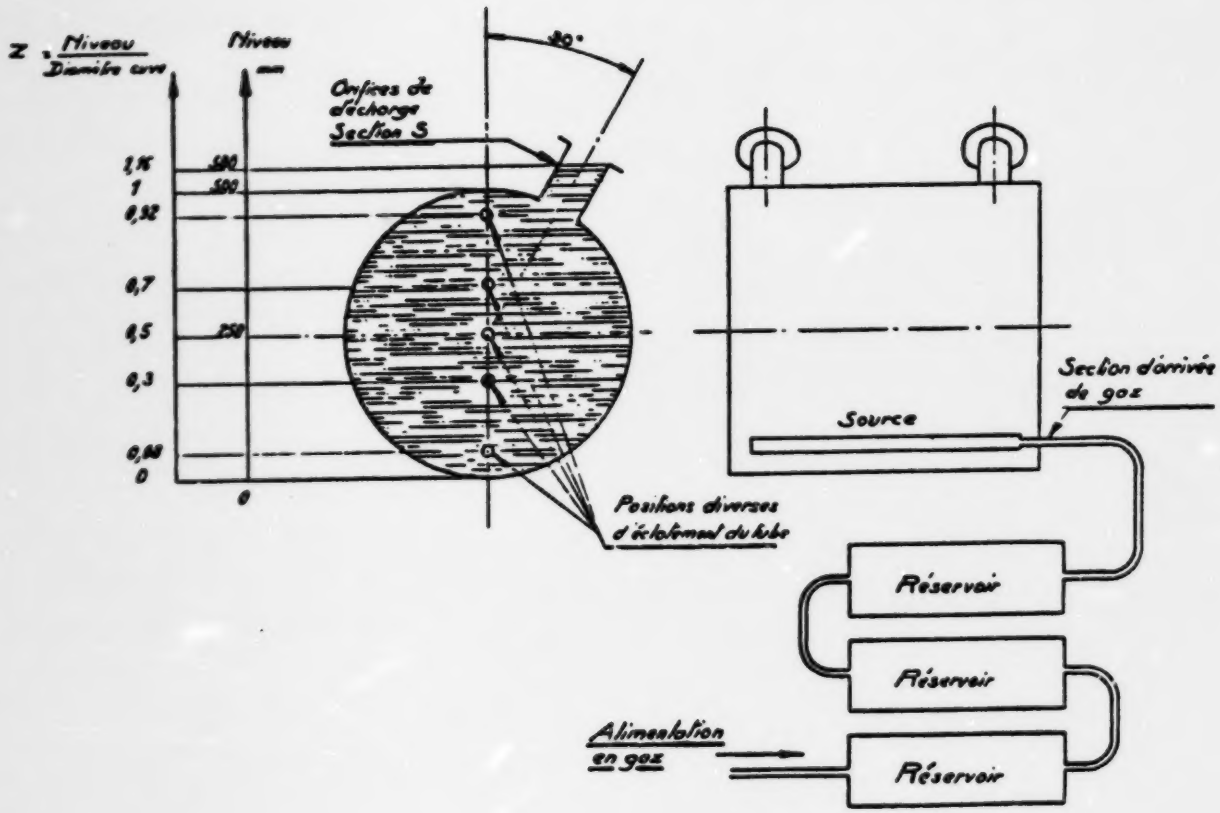

Schéma de la maquette.

Figure 2.4 Test Rig of Hareux, Roche and Vrillon (1964)

After testing the effects of many variables the authors concluded that the peak pressures in the vessel depended on

- the flexibility of the vessel $F = \left(\frac{\partial V}{\partial P}\right)_T$ in which V is vessel volume.
- the mass of air trapped in the vessel
- the nature of the gas.

All experiments were run with cold gas and mostly with nitrogen. for which the experimental results could be correlated by

$$\frac{P_{peak}}{P_o} = 1.111 \left(\frac{V_o}{FP_o}\right)^{0.44} ,$$

in which V_o is the initial volume of gas and P_o the initial gas pressure.

For the steel vessel $F = 30\ cm^3/bar$ and for the plexiglass vessel $F = 150\ cm^3/bar$.

2.3.3 Holtbecker, Montagnani, and Verzeletti (1970)

These tests were done on pressure tubes filled with simulated fuel elements and organic liquid at 400°C, pressurized to as high as 3.8 MPa before burst occurred. In their Experiment No. 4 the pressure tube material was designated SAP 895 (ID/OD 92/98 mm) and the calandria tube was Al 99.5 (ID/OD 112/115 mm). The calandria vessel (to be described in Section 2.3.6) was filled with about 10 m^3 of light water at 50°C prior to burst.

Both pressure tube and calandria tube were weakened with milled flats of about 1.5 m axial length and failed in long axial splits.

The maximum dynamic pressure experienced by the vessel (in Experiment No. 4) was 1.5 MPa.

The authors reported that

> "It was ascertained that the pressure waves in the water originate in the collapse of organic vapour and steam bubbles. The pressure wave that normally generates the greatest mechanical effects is the one recorded in the first instant after bursting of the channel.
>
> The locus of the collapse cannot be exactly pin-pointed though in most cases it was ascertained that the waves are generated at the rear of the channel struck by the jet and in any case at a certain distance from the bursting channel."

The pressure waves caused buckling collapse of two aluminum control rod tubes (not filled with water) in Experiment No. 4. Later the authors remarked that "The deformation of the channels and, in particular, the local collapse of the Al tube in Experiment 13* are due, as the tests showed, to the collapse of vapour bubbles." No quantitative observation or explanation of the extent or mechanism of vapour collapse and the consequent pressure pulse generation appear to be available.

The authors reported that the transmission of the pressure wave through the calandria vessel was markedly affected by the nature of the tubes in the vessel.

> "It was found that a wave can only be transmitted through water-filled channels and that empty channels prevent the wave from passing. This was one of the reasons why it was mainly in such tubes as the safety rods, which did not have to be filled with water, that buckling occurred during the tests. Of particular interest, likewise, are the experiments that were conducted to discover the variation in amplitude of pressure waves passing between 2 tubes. The measurements showed that the pressure readings behind the tubes can be higher by a factor of 1.45. It is thought that the reason may be that the 2 tubes act as a wave guide, turning the particles toward the gap between them."

*description not provided.

The tube spacing/diameter ratio in the experiments was not uniform and somewhat less than 2:1 in places.

2.3.4 Tanaka (1971)

Tanaka reported the results of 10 tests in which pressure tubes in a calandria vessel were burst by electric arc discharge from an electrode mounted "between the thin wall part of the tube and the calandria tube." Thinning of the pressure tube wall prior to burst provided a burst area approximately equal to the "discharge area in the pressure tube."

The calandria vessel axis was vertical and pressure tube bursting took place at three levels

(a) in the helium gas volume above the heavy water level

(b) at mid height

(c) at a lower level.

The coolant pressure and temperature was about 6 MPa and 275°C. The bursting gave maximum impact pressures of around 2 MPa on adjacent tubes and 0.2 MPa on the vessel wall. Even in case (a) above where an aluminum calandria tube spaced 225 mm from the break was "directly hit by a jet of high temperature and high pressure water," the tube showed no sign of deformation or damage.

Discharge from the burst tube was maintained over 30-40 minutes or more. building up calandria vessel pressure to around 0.2 MPa (at which level the vessel rupture discs burst) in about 10-40 minutes.

Tanaka concluded that the impact pressure following this burst of limited size does not cause deformation or damage to adjacent tubes.

2.3.5 Hayamizu, Takomitsu, and Hayashi (1974)

Tests reported by these authors were conducted in a 1.7 m diameter calandria vessel containing 21 carbon steel pressure tubes 4.5 m long and 139.8 mm in outside diameter and arranged in a square pitch of 225 mm spacing.

The central pressure tube was weakened by a machined flat and burst at a pressure of about 7.3 MPa when filled with light water at 287°C. This pressure tube had an aluminum calandria tube surrounding it.

Pressure measurements were made on six tubes facing the burst location. The highest pressure recorded was on the tube closest to the burst and had a peak value of 2.0 MPa.

The maximum reactive force on the burst tube was measured with a load cell and the authors concluded that it can be described by

$$F = 1.25\, A\, P_o$$

in which

A = the discharge area

P_o = the stagnation pressure

and the units of F and AP_o are the same.

2.3.6 Famiglietti, Parmeggiani, Possa and Galbiati (1975)

The Italian tests consisted of three major experiments as described in this and the next two sections. Two of these experiments used the Bettula facilities at ISPRA Euratom Research Center and one was done at the MARC facility at CISE.

The first of these three experiments is described in this section. The objectives were (1) to investigate the pressure transient field in the pressure vessel due to pressure tube rupture and (2) to investigate the influence of different fluid conditions in the explosion tube.

The diameter of the experimental pressure vessel (see Figure 2.6) was 2.38 m and its height was 2.4 m. The vessel accommodated as many as 51 tubes. The gas volume above the moderator inside the vessel was 2.8 m^3. The explosion tubes, located at the centre of the vessel, were made of aluminum alloy, with machined defects of 800 mm long and with a layer of foamed glass for thermal insulation. At rupture, pressure ranged from 4.1 to 5.4 MPa and temperature ranged from 247°C to 268°C in the explosion tubes.

Measurements indicated typical pressure transients with two characteristic peaks (see Figure 2.5). The explosion pushed the moderator rapidly upward, compressing the gas above. As the "bubble" of steam and water expanded, the first pressure peak was reached in 3-4 ms, then the pressure decreased to below initial value in 10-15 ms. Maximum gas pressure was reached in 30-40 ms, then moderator motion reversed and "bubble" volume decreased rapidly until collapse in 70-100 ms, producing the second pressure peak. Subsequent pressure pulses occurred with decreasing amplitudes.

The adjacent tube facing the explosion registered the highest pressure during the first pressure peak, whereas registered pressure increased with depth during the second pressure pulse. Random pressure spikes, with limited spatial correlation, were found near the explosion site and the lower part of the vessel during the second pressure peak when water was used as explosive.

In summary, the effects of the various fluid conditions in the explosion tube were as follows:

Liquid Coolant as Explosive: Maximum pressure measured in the vessel increased with temperature of liquid coolant.

Steam as Explosive: Pressure peaks showed faster rise time and shorter duration when compared to liquid discharge. Per unit mass, steam was more effective than water; per unit volume, slightly less effective.

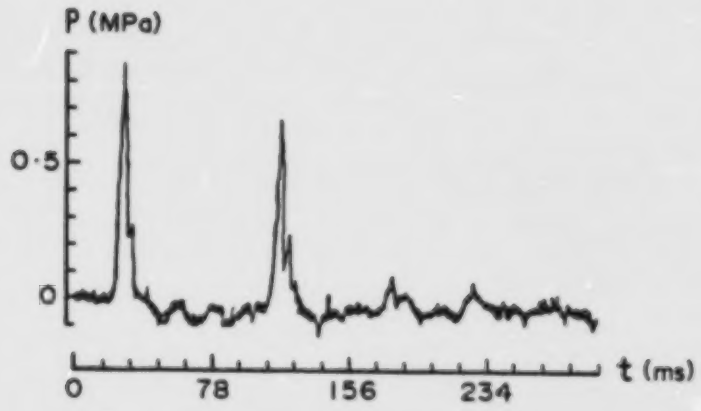

Figure 2.5 Typical Pressure Transient in Bettula Tests

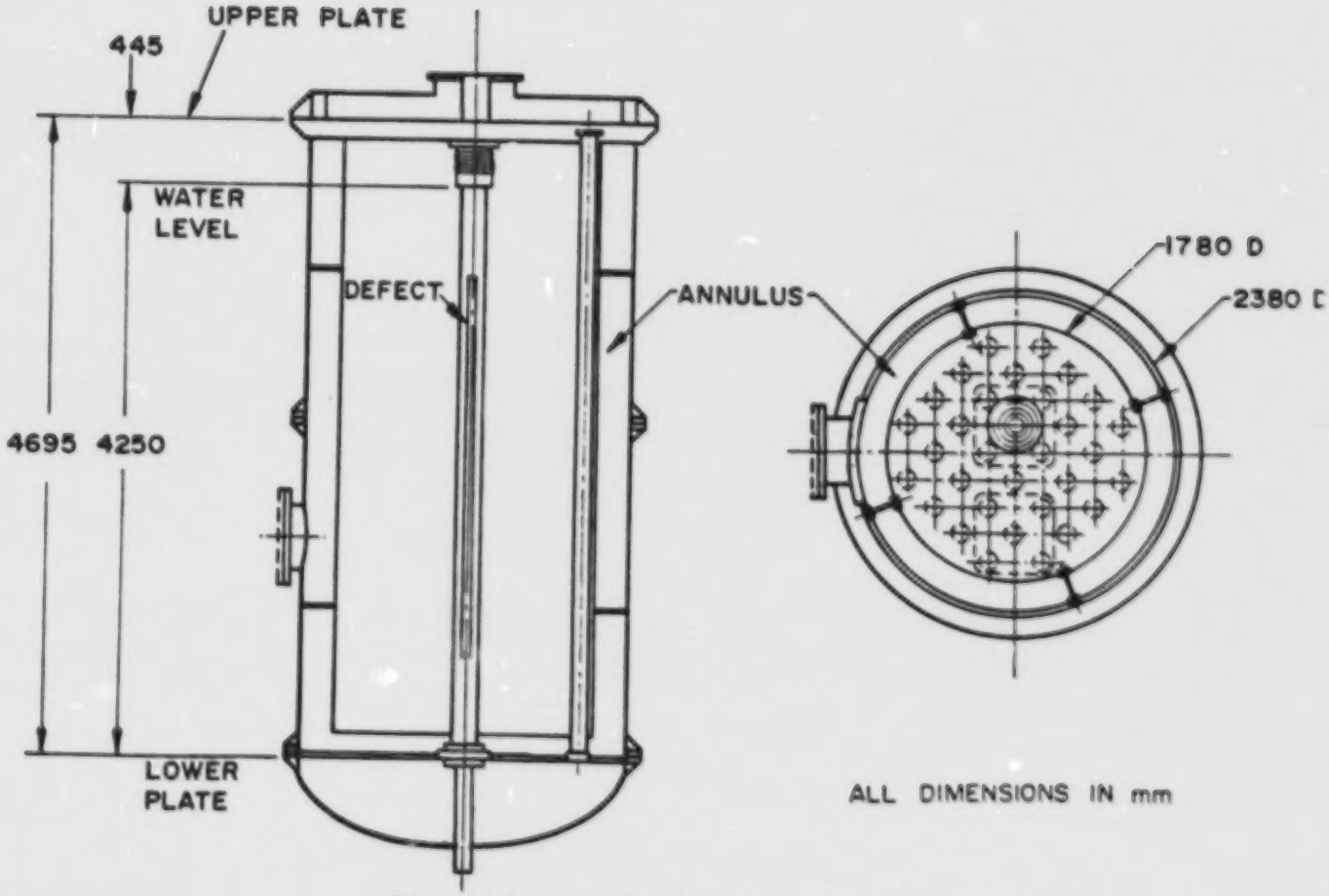

Figure 2.6 The Bettula Pressure Vessel

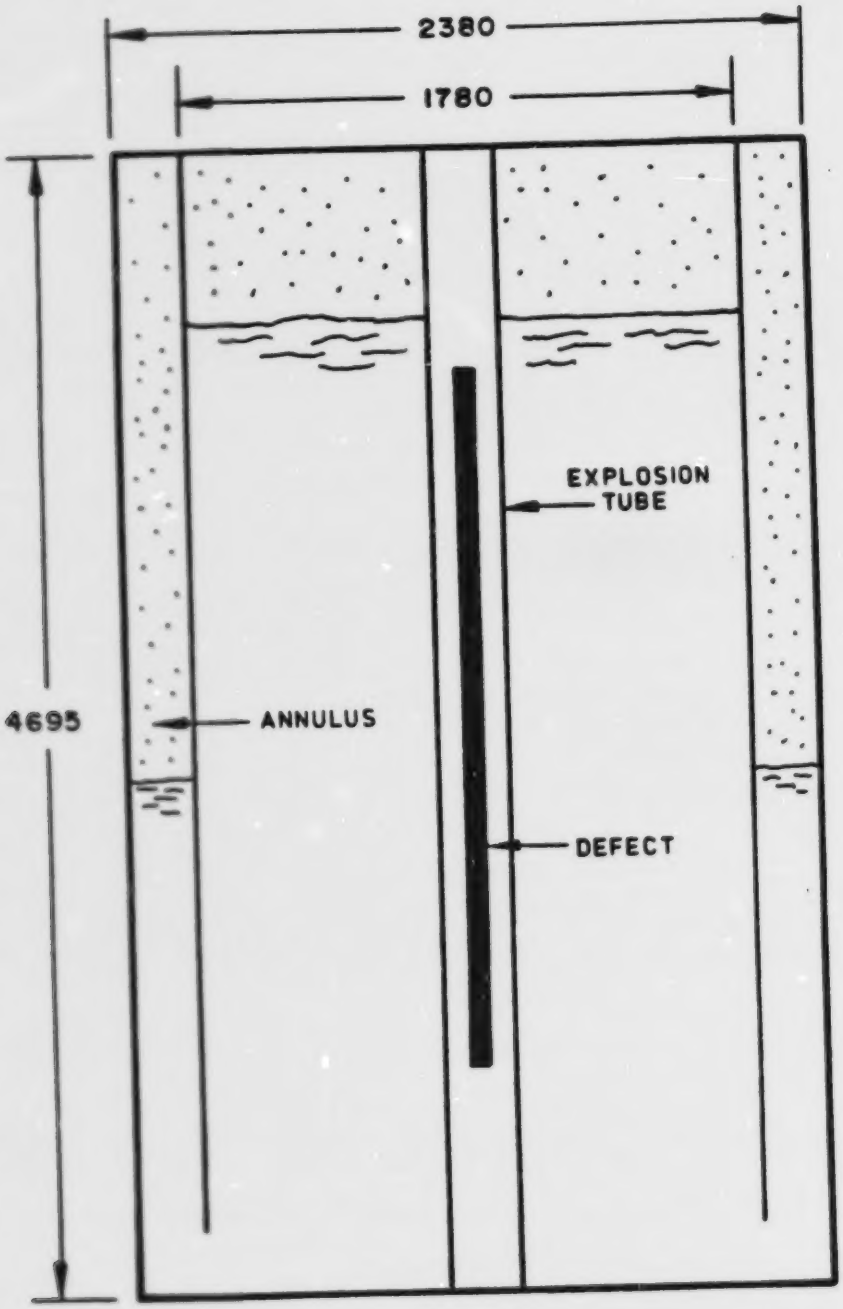

Figure 2.7 Schematic of Bettula Pressure Vessel

N_2 Gas as Explosive: The first pressure peak was similar to that of steam. The second pressure peak was lower and smoother, apparently due to the lack of bubble collapse.

Increased Fluid Volume in Explosion Tube: Only slight increase in maximum pressure was produced.

Flow Circulation in Explosion Tube: Lower pressure peaks than those of non-flow tests were recorded.

Gas Volume in Plenum: Reduced volume produced lower second pressure peak and high frequency of pressure oscillation.

These tests indicated that

- The dominant forces are inertial and thermal-hydrodynamic in nature; i.e. bubble expansion, vertical acceleration and deceleration of moderator slug and bubble collapse.

- Water and steam as explosives produce fundamentally different results from those by gas, mainly due to evaporation at rupture and bubble collapse.

- Factors leading to lower pressure peaks with flow in explosion tube need to be investigated. Small coolant inventory may not be the main factor.

- Dents on some adjacent calandria tubes indicated local water vapour bubble collapse, hence the spikes observed during the second pressure peak.

In one experiment pressure transducers were placed on a target tube, as illustrated in Figure 2.8. It was found, at the first pressure peak, maximum pressure registered by P_A is 1.34 times that of P_B and P_C. For subsequent

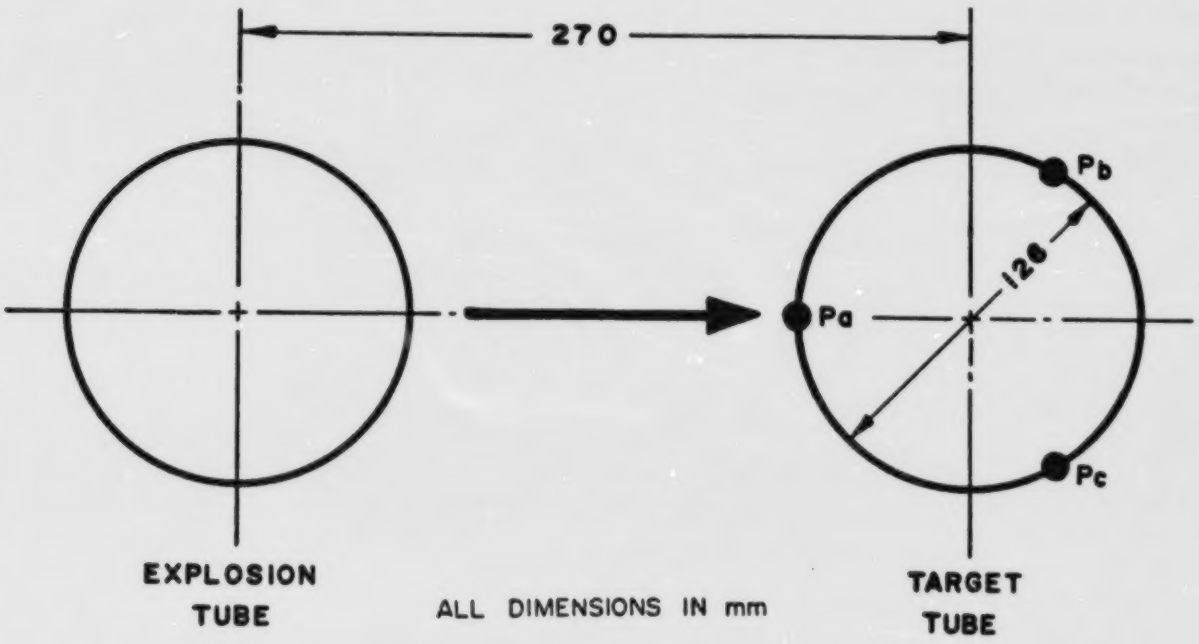

Figure 2.8 Instrumentation on Target Tube

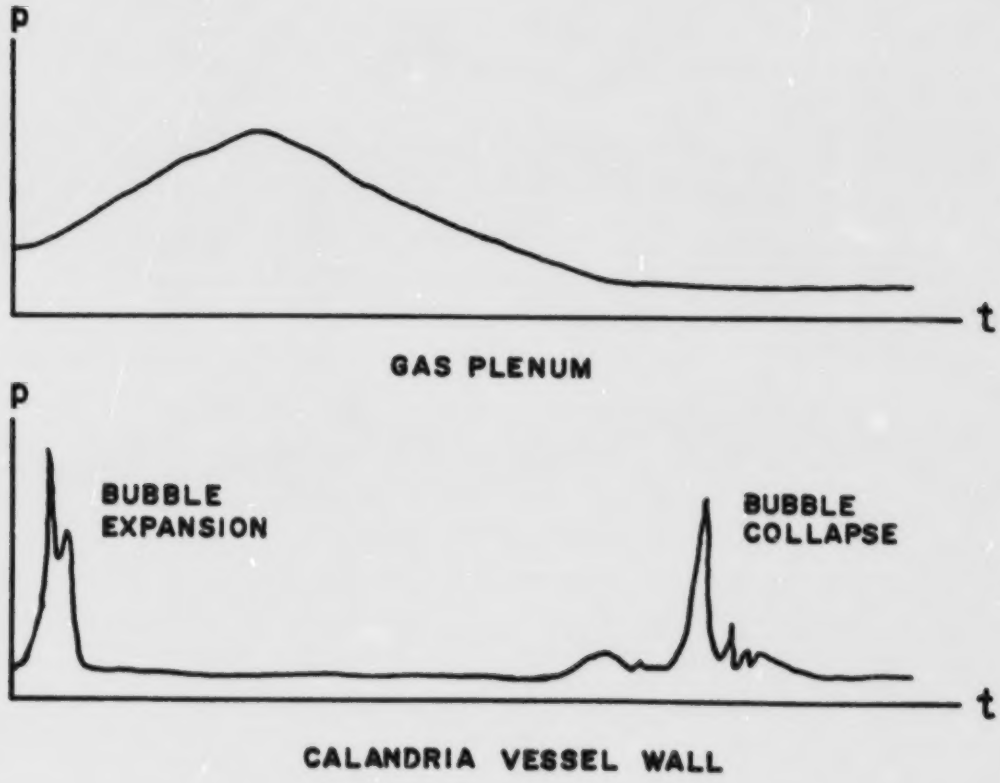

Figure 2.9 Characteristic Pressure Peaks in Pressure Vessel and Gas Plenum

pressure peaks, all three transducers registered equal pressures. The higher pressure at P_A reflected the directional discharge of coolant as the axial split developed.

2.3.7 Dallavalle, Hotz, Possa (1977)

Two major modifications were made to the Bettula facilities for the second major experiment. The height of the pressure vessel (Figure 2.6) was increased to that of the CIRENE reactor (4 m). An inner vessel was added. While reducing the number of tubes to 32, the inner vessel provided an additional gas plenum in the annulus to conform to the CIRENE reactor geometry. Both aluminum alloy and Zircalloy explosion tubes, with defect length of 273-3000 mm, were employed. Figure 2.7 shows schematically the defect length of the burst tube and its location in the modified calandria vessel.

The recorded pressure transients in this experiment clearly illustrate the expansion and collapse of the vapour bubble and the influence of the gas plenum above the moderator. The drop of pressure in the moderator to values below the initial pressure and the collapse of the bubble are due to the spring-like energy storage of the gas plenum and the inertia of the water slug, causing the presure drop in its upward movement and the bubble collapse in its reverse motion.

Figure 2.9 shows the two characteristic pressure peaks measured near the mid-height of the vessel and the pressure in the gas plenum at the top.

In this second investigation, a vertical target tube, instrumented with 24 pressure transducers at four different axial positions, was placed in front of the explosion tube to measure the resultant loading. The explosion tube had a premachined defect of 3000 mm to promote axial split. With the coolant at 5.69 MPa and 275°C, the pressure transducer readings indicated a peak force of 100 N/mm of tube length at about mid height; this peak lasted only a few milliseconds. The measured variation of impulse with

height and radial distance from explosion site are shown in the Figures 2.10 (a) and 2.10 (b). The investigators concluded that for the CIRENE reactor "no rupture propagation from one power channel to an adjacent one can occur" and that the pressure peak from the first bubble expansion has the most potential for damage.

The maximum recorded pressures on the vessel wall increased with defect length. For nominally the same pressure at rupture, a 3000 mm defect produced a maximum pressure of 2.2 MPa; 1000 mm, 0.89 MPa; 237 mm, 0.42 MPa.

When a CIRENE channel was used as a target tube, the calandria tube collapsed onto the pressure tube, while the pressure tube itself suffered no structural damage.

When all the adjacent pressure tubes were enclosed with calandria tubes, lower pressure pulses were recorded on the target tubes and vessel wall.

These experiments showed

- how "area free for coolant discharge" developed at rupture determines the subsequent pressure transient; the larger the area, the greater the explosive force.

- that the explosion resulting from the long axial defect is apparently the worst case possible.

- that the thrust from the first pressure peak is the most damaging.

- that calandria tube collapse reduced pressure amplitudes of pressure pulses resulting from pressure tube rupture.

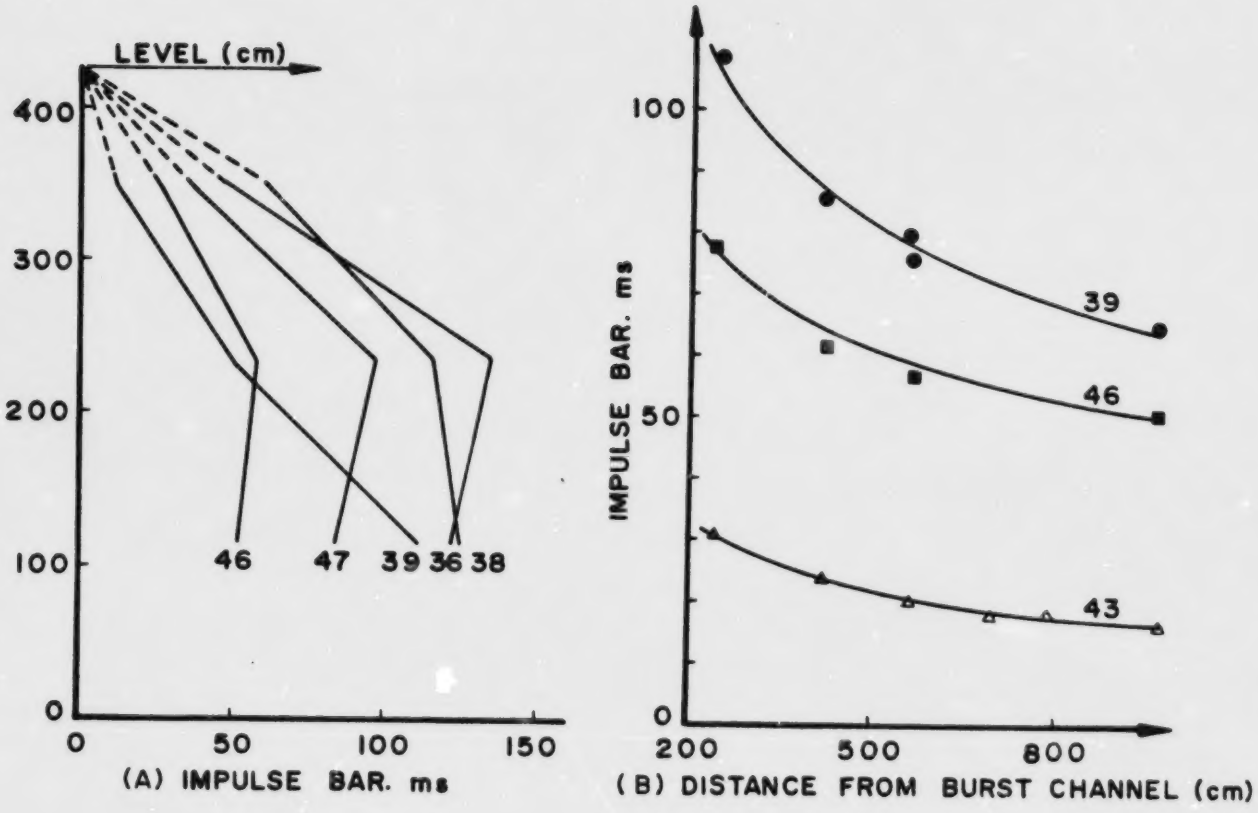

Figure 2.10 Variatons of Impulse with Height and Radial Distance - After Famiglietti, Parmeggianni, Possa and Galbatti

2.3.8 Chevallard, Famiglietti, and Possa (1979)

The MARC facilities were a 1/5 scale simulation of the CIRENE reactor. Primary objectives of the experiment were to measure the loadings on the structure supporting the pressure vessel and the vessel walls due to pressure tube rupture occurring in a central location or near the vessel wall. N_2 gas was used as an explosive.

A central explosion produced uniform loadings on the vessel wall, whereas the wall pressure in positions directly impacted by the explosion in the near-wall burst was found to be up to 2-3 times higher than the average values.

The loading on the tank wall due to pressure tube rupture is shown in Figure 2.11, which indicates the variation of pressure as a function of angular position from the explosion site. Continuous lines denote central explosions and dashes denote peripheral explosions. N_2 gas at 3 MPa was used as an explosive.

Tube burst near the wall also produced higher strain in the members supporting the pressure vessel. For both the vessel wall and supporting members, strains measured were well within the elastic limits of the materials.

Figure 2.12 shows the pressure and strain on the vessel during the expansion phase of the bubble. The vessel internal diameter was 738 mm and vessel thickness was 4 mm.

The first pressure peak was of oscillating shape, composed of several pressure pulses. The strain pulses in the vessel wall were in synchronization with the pressure pulses in the first pressure peak. Peak pressure was reached in about 5 ms.

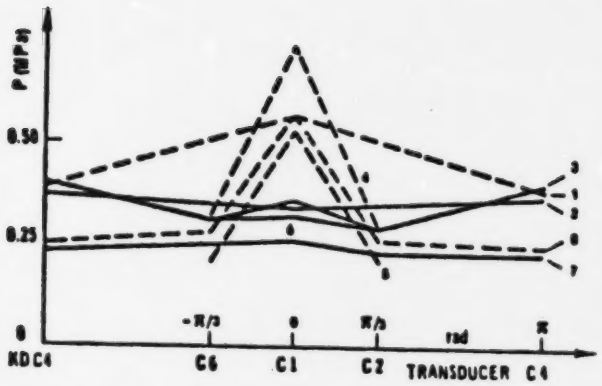

Peak pressures on the inner vessel wall (first pressure pulse).

Figure 2.11 Peak Pressures on the Inner Vessel Wall, First Pressure Pulse - from Chevallard, Famiglietti and Possa

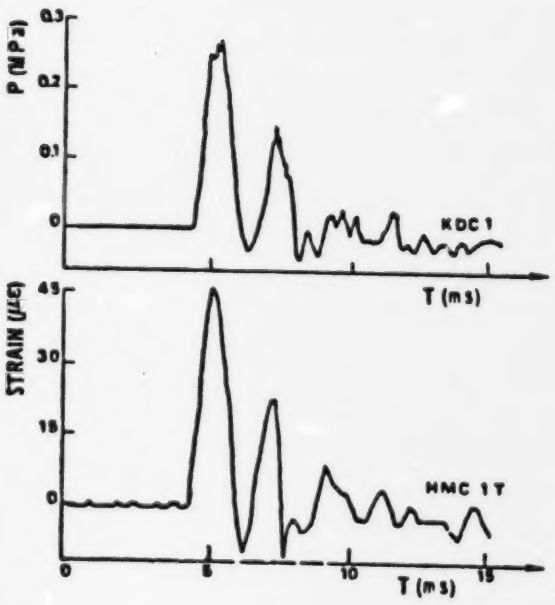

First pressure peak in the water tank.

Figure 2.12 Pressure and Strain on Vessel during First Pressure Pulse - from Chevallard, Famiglietti and Possa

In these experiments, pressure pulses due to shock waves were not observed. possibly due to the limited sensitivity of the instruments used. The speed of sound in the liquid was about 1200 m/s and the diameter of the vessel is 0.738 m. Thus the shock wave would reach the wall in about 0.3 ms after a central explosion; no such wave was registered.

2.3.9 Summary

Tests of pressure tube bursting in closed vessels indicate that;

- the amplitude of the pressure pulse produced by tube burst decays rapidly with distance. Pressure waves are strongly attenuated by collapse of neighbouring calandria tubes on pressure tubes. Bursting of a pressure tube near the wall of the vessel can produce much higher local pressure loading on the calandria vessel than bursting of a central tube.

- the pressure loading of surrounding tubes depends strongly on the length of the rupture opening (for a pressure tube weakened by milling a flat which is long in the axial direction).

- pressure amplitudes and durations depend on the nature of the coolant (gas, steam or high enthalpy liquid) and calandria vessel configuration.

There are indications (but only fragmentary evidence and for organic coolant in the pressure tube) of pressure pulses generated in the calandria vessel due to collapse of large vapour zones.

In general, pressure amplitudes measured in closed vessels were too small to cause damage to the vessel or to surrounding pressure tubes, except for collapse of calandria tubes onto their respective pressure tubes.

These experiments reveal little about the early stages of the discharge from a tube burst, including the initial shock wave. They also show little about the pattern of development and collapse of vapour resulting from the two-phase jet.

Missile damage and collapse of simulated shut-off-rod guide tubes were demonstrated in only one experiment (Holtbecker et al).

The pronounced expansion and collapse of the vapour bubble in the Italian experiments were due to the spring-like gas plenum above the moderator. which allowed rapid vertical acceleration and deceleration of the moderator slug. In the horizontal axis calandria vessels with no upper gas plenum a secondary spike would not be expected to occur for this reason.

2.4 TUBE BURST PHENOMENA

2.4.1 Introduction

The earlier sections of this chapter deal with experiments designed specifically to illuminate the consequences of failure of a pressure tube in a pressure tube reactor. In this section experimental information from other sources is discussed to the extent that it sheds light on the manner and consequences of tube bursting.

2.4.2 Modes of Tube Bursting

The shape of the burst opening resulting from a random crack or other flaw in a pressure tube will, of course, be complex and indeterminate. In the following discussion we simplify matters by discussing the results of axial or circumferential bursts (see Figure 2.13). One reason for doing this is that essentially all of the experimental information available to us comes from tubes weakened to fail in one of these two modes.

Circumferential Breaks:

Extensive local overheating due to a LOCA is a possible cause for a circumferential break in a reactor; various experiments have been done to simulate circumferential breaks.

A sudden circumferential break of a tube, at an appreciable angle to the plane perpendicular to the tube axis, will have sufficient reactive force for rapid lateral displacement and rapid discharge of both flashing liquid and fuel elements. Fuel bundles accelerating under pressure gradients in the tube can be considered missiles which can impact adjacent calandria tubes (probably at a glancing angle) and the calandria tube sheets.

In the event of a circumferential break, impact loadings on adjacent tubes from missiles and from pipe whip are potential damage mechanisms.

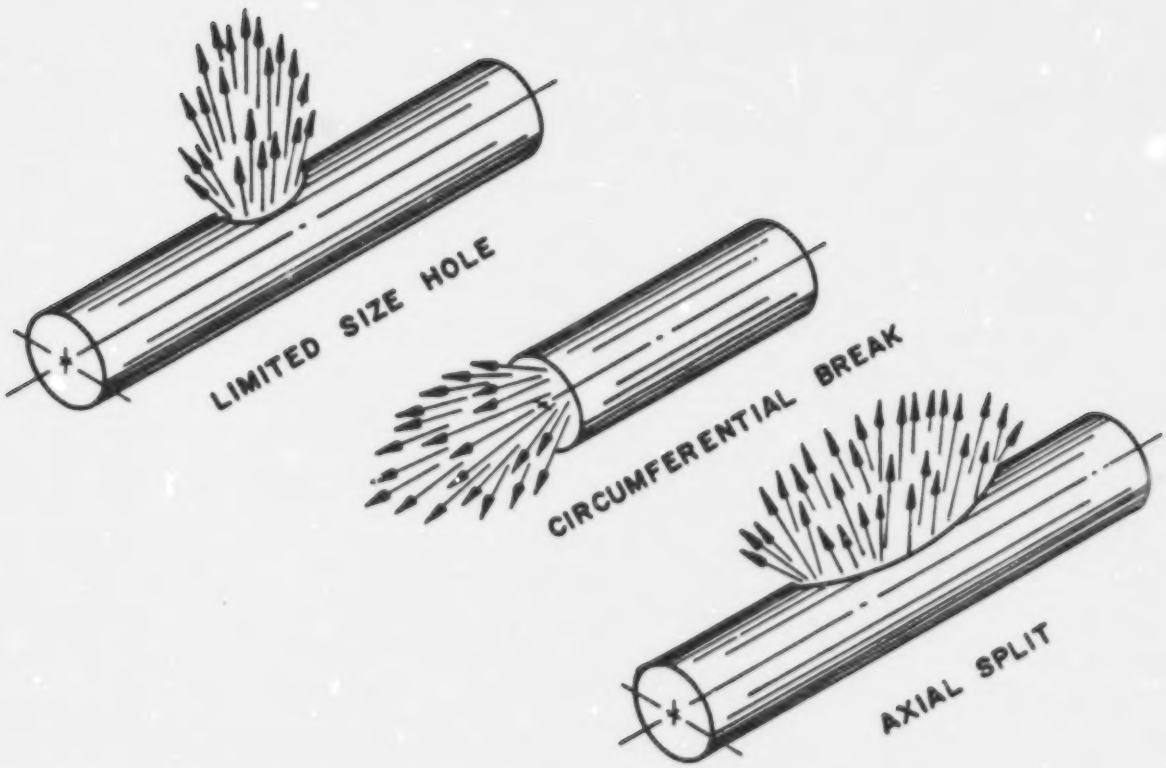

Figure 12.13 Idealized Modes of Tube Rupture

Damage from missiles was demonstrated in tests done by Ross-Ross (1963) and Isles (1965). Both investigators used long, open rectangular tanks and Isles used exceptionally high bursting pressure and temperature. Both investigators reported denting of the tank wall and calandria tube at the ends of the tank and Isles reported damage of an adjacent pressure tube (in one test only). While circumferential breaks give the missiles high velocities, the angles of strike on the adjacent tubes are small. Furthermore, it should be pointed out that because of the open tank in the Isles tests, the water was almost completely expelled during the explosion and the missiles were essentially projected through steam, rather than the liquid moderator of a calandria vessel. The drag forces on projectiles, would be 2 to 3 orders of magnitude higher in liquid.

Axial Split:

Axial split is the most thoroughly investigated pressure tube rupture mode, although no such rupture has actually been reported in a reactor.

Among the various investigations into consequences of axial split rupture, the Italian series are the most comprehensive and realistic in simulation of the reactor environment. The Italian investigators believe that this is the worst rupture mode possible. The "area free of cooling discharge" during the rupture determines the explosiveness of the rupture and also the first pressure peak after the explosion is the most damaging. They carried out tests with defects from 273 - 3000 mm long. For nominally the same pressure and temperature (approximately 6 MPa and 280^{o}C), Figure 2.14 shows how the maximum pressure measured on the vessel wall varies with the length of the rupture.

Ross-Ross and Langford (1980) concluded that "end-to-end propagation of a crack is generally recognized as the worst failure mode of a pressure tube."

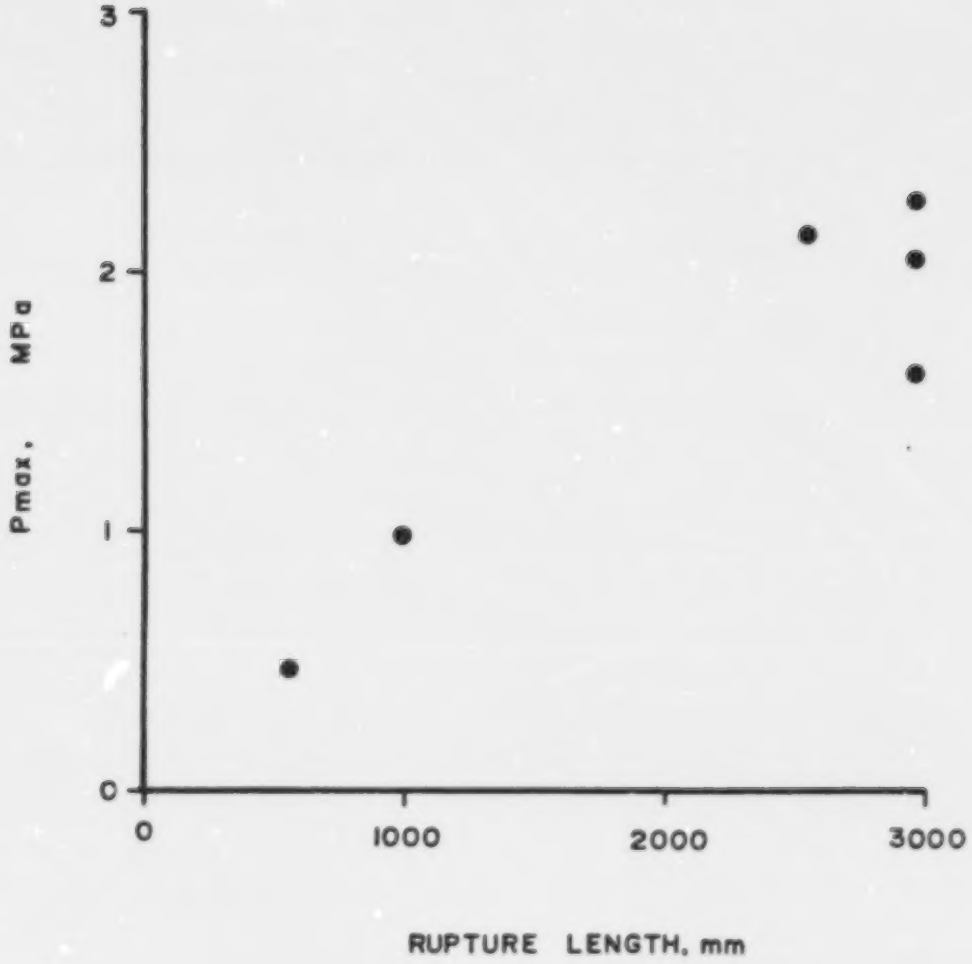

Figure 2.14 Peak Pressures and Rupture Lengths

Roberts and Swinhoe (1960) reported that their tests indicated circumferential breaks are more violent than an axial split. Several aspects of their experimental conditions should be noted: their axial defects were only 73.66 mm long; tube thicknesses were reduced to 0.254 mm in axial defects (those for circumferential defects were 0.508 mm); their explosion tubes were rather short when compared to that of a pressure tube.

The main damage mechanism of an axial split rupture is the pressure wave loading on an adjacent pressure tube and the calandria vessel. When high pressure and high temperature coolant is suddenly released into the moderator through large "areas free for coolant discharge" created by the very fast axial propagation of a crack, a rapidly expanding vapour bubble is formed with resultant calandria loading.

In his elastic-plastic analysis of crack instability in primary pipes in reactors, Ayes (1977) concluded that for one particular pipe (an SA516 Gr70 steel pipe of ID 762 mm and wall thickness 63.5 mm) cracks must be greater than one half diameter long in the axial direction or a half circumference in the circumferential direction before instability can occur under normal reactor conditions. The ratio of critical crack lengths between axial and circumferential propagation is 1 to . For pressure tube reactors, the critical axial crack length was estimated to be 15 times wall thickness; i.e. 73.66 mm. This indicates that a much higher pressure is required for circumferential break than for axial rupture if the initial crack lengths are the same.

The pressure tube is essentially a pressurized thin-wall vessel with circumferential stresses twice as high as the axial stress, thus favouring axial propagation of a crack. Ross-Ross and Langford (1980) stated that following the establishment of a critical flaw, crack propagation almost always extends axially regardless of the orientation of the original defect due to the directing influence of the principal (hoop) stress.

Pickles observed that in his tests (where slits 177.8 mm long and 80% reduction of the pressure tube thickness were used) all the pressure tubes

used as explosion tubes split axially end-to-end. It appears that axial split is more probable and more damaging than circumferential breaks.

Baum (1982) investigated propagation characteristics of axial splits in pressure tubes pressurized by gas. He recorded the crack tip movement with high speed photography (see Figure 2.15) and local pressures with pressure transducers inside a 102 mm ID and 1.6 mm wall steel pipe. The speed of propagation of the crack was about 230 m/s, considerably smaller than the acoustic speed in the gas which was about 345 m/s.

Baum observed that when the distance between the two crack tips, propagating in opposite directions, reached 6 radii of the tube, the split became "fully open", i.e. the open area of the split equalled or exceeded twice the tube cross-sectional area.

Baum also observed that at a point away from the initial rupture zone, prior to the arrival of the propagating crack tip there is a relatively low velocity axial flow within the pipe, and the arrival of the crack tip exposes the flow to additional transverse acceleration and increased decompression. Based on these observations, he proposed a model which considers the choking plane one-dimensional and propagating axially with the crack tips when the split length (l) is less than 6R. When l 6R, the process is idealized by transverse plane waves emanating from a time varying gap. Figure 2.16 shows the idealized choking planes for earlier and later stages of the burst process. Figure 2.17 shows calculated and measured pressures at a given point inside the tube, varying with time before and after arrival of the crack tip. The predicted pressure drop, as the crack tip travels past a fixed point on the tube, compares well with experimentally measured values. It must of course be borne in mind that Figure 2.17 is for decompression of gas. For hot water discharge the depressurization could be quite different because of much higher speed of sound in the water.

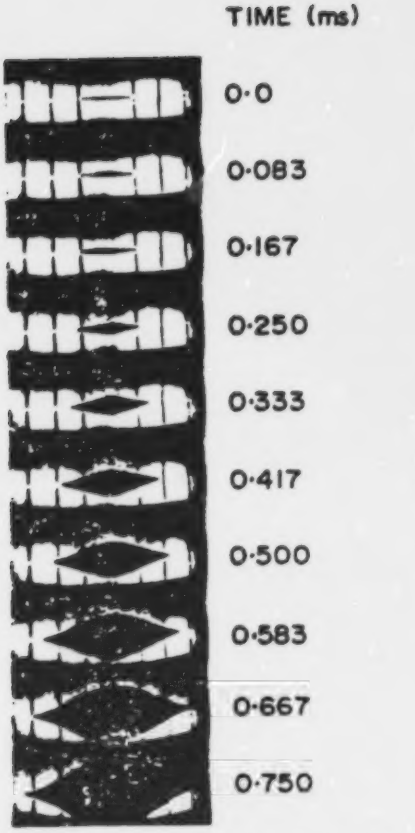

High-speed film of case P_o = 88 bar and L = 2R (12,000 pictures per s)

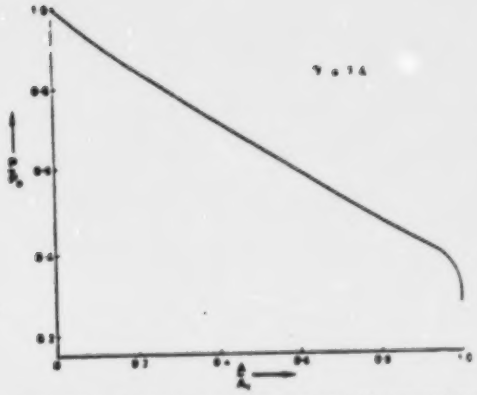

The relationship between pressure just upstream of the breach and the breach area

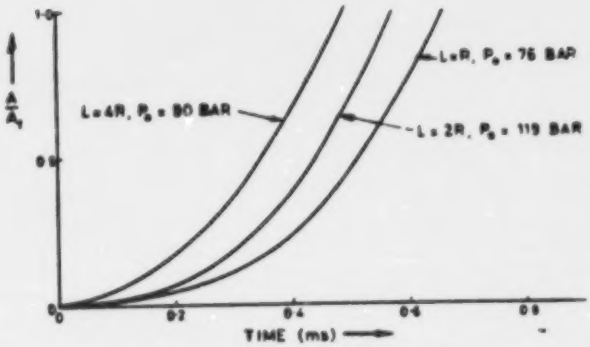

Breach growth to "fully open"

Figure 2.15 Propagation of Crack Tips in Axial Split - from Baum

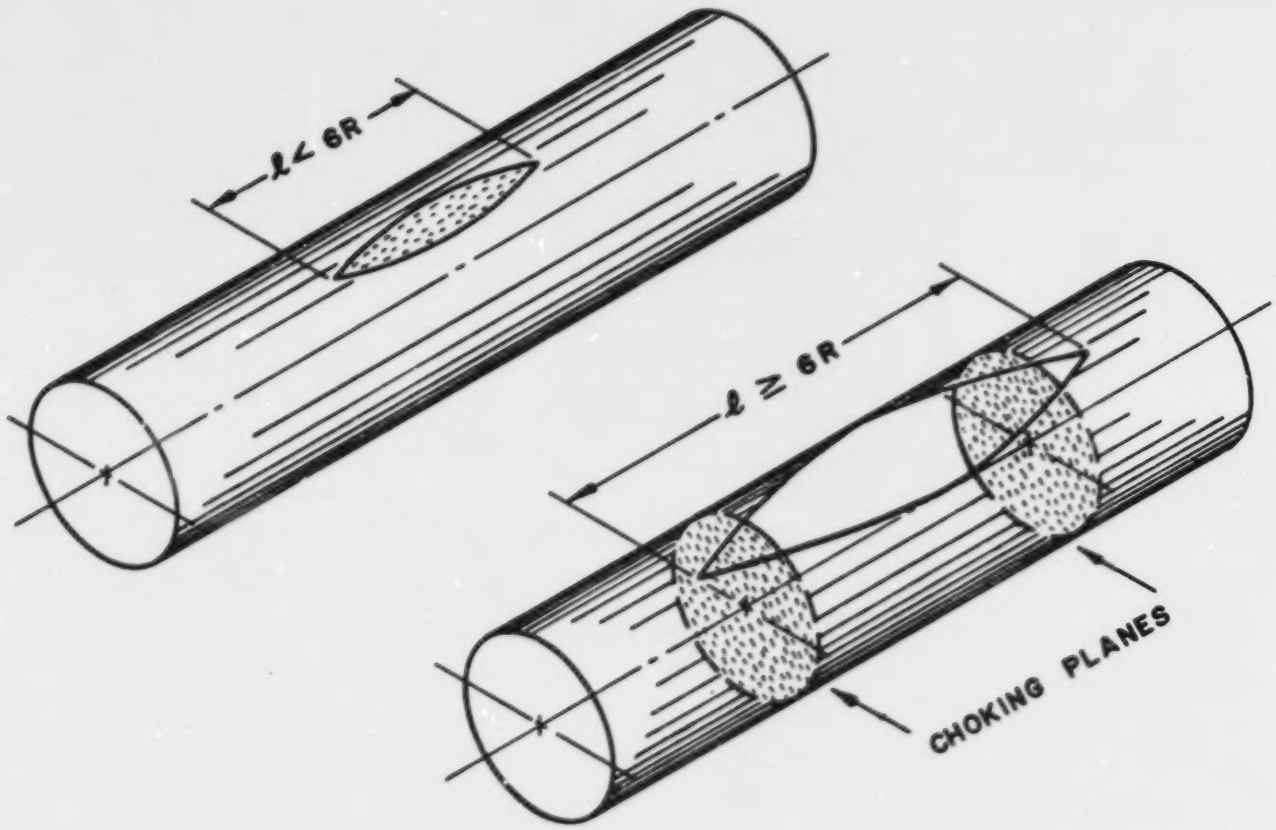

Figure 2.16 Idealized Choking Areas in Baum's Model

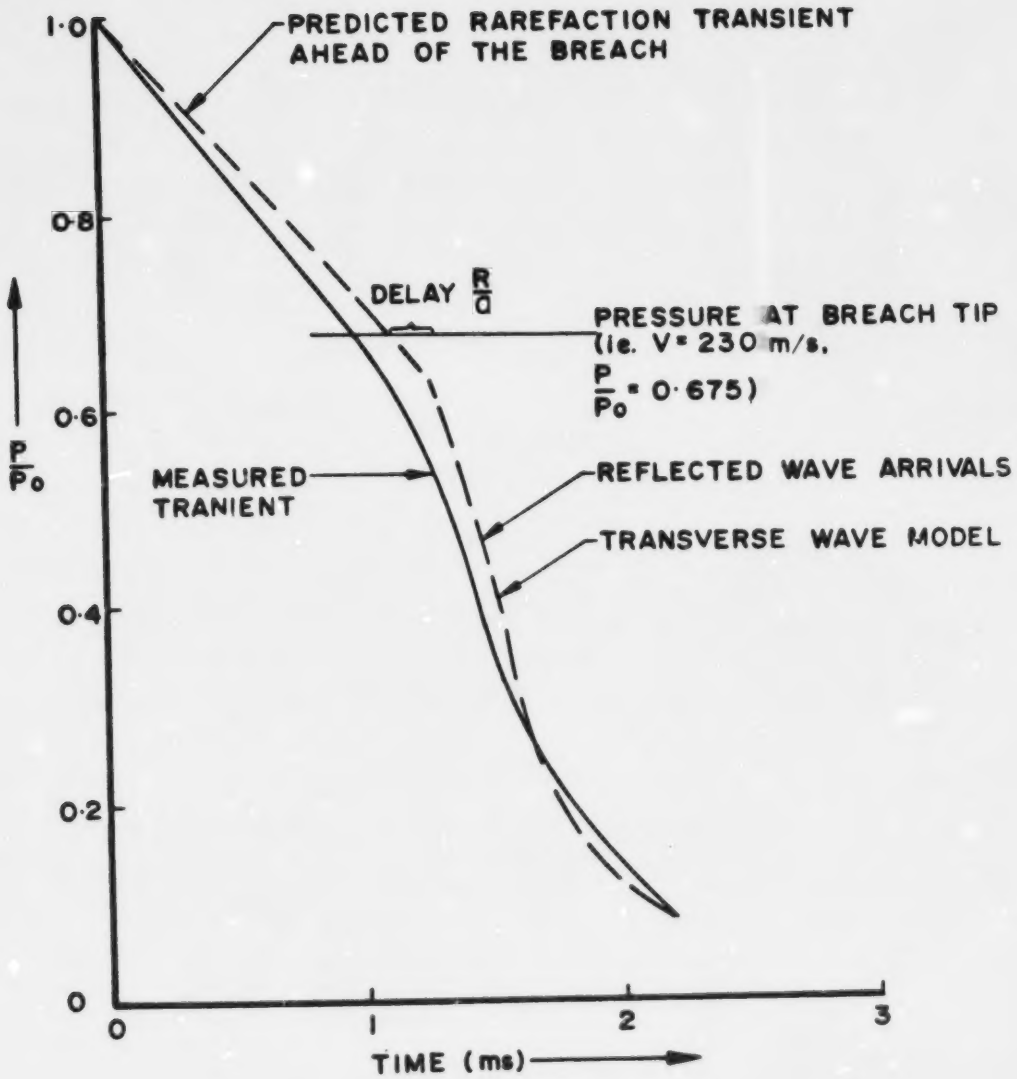

Figure 2.17 Comparison of Predicted and Measured Depressurization within the Breach at 12R from Center of Defect (L = 2R, Po = 86 bar) - from Baum

Emery, Pearl, Kobayashi, and Love (1981) analyzed the earlier data of Baum. They noted that the crack tip velocity became constant after it had extended 1.5 radii and remained so until a reflected depressurization wave arrested the advance of the crack tip.

On the assumption that circumferential shear stresses are small during crack opening, they modelled the pipe as a series of disconnected rings. They assumed that the opening motion of a ring is governed by its inertia, and once the ring opening reached a critical opening angle (θ) the crack tip advances to the next ring. Coupled with a one-dimensional fluid flow program, they calculated the instantaneous fluid pressure and velocity at every point in the pipe. Figure 2.18(A) shows the model employed in the calculation process. Figure 2.18(B) indicates both Baum's observations of crack tip displacement, and the calculated values of the opening width and crack tip position as function of time.

Emery and his colleagues found the pressure transient in the pipe pressurized by hot water very different from that if the pipe is pressurized by air. For air-pressurized pipes, the speed of sound in the air (345 m/s) is close to the crack speed in the burst tube and the crack tip is always in a zone of high pressure. In hot-water-filled pipes, because of higher sound speed (1100 m/s), higher density and vapour formation, decompression produced a high mass outflow and very strong depresurization wave, so that pressure at the crack tip quickly falls to saturation pressure. This means that the crack grows less rapidly, smaller pressure difference being available to accelerate the lateral opening of the tube. It also means that the rate of crack opening may approach zero as in Figure 2.19. Thus, where acoustic speed is much greater than maximum crack propagation speed (i.e. the crack propagation speed which would result from maximum pressure difference available to accelerate crack opening) the crack propagation rate may drop to zero. In this case the assumption of a long axial slit (in a non-weakened tube) would represent a very unlikely event.

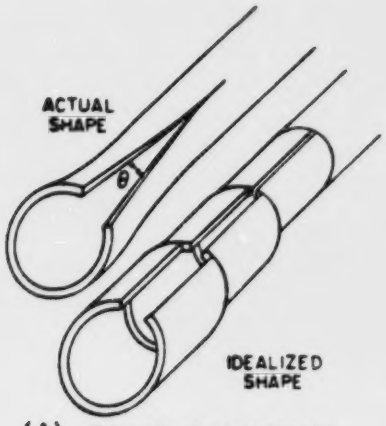

(A) Schematic of a fracturing pipe

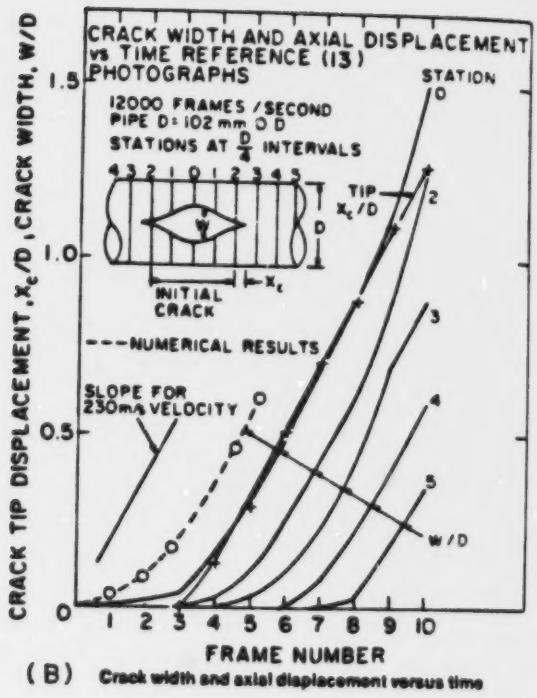

(B) Crack width and axial displacement versus time

Figure 2.18 Emery's Split Ring Model and Comparison with Experimental Results — from Emery

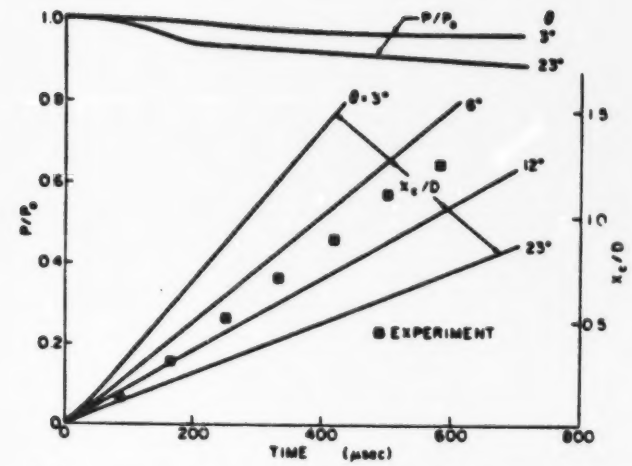

(A) Fluid pressure and crack extension history as a function of CTOA for an air-filled pipe

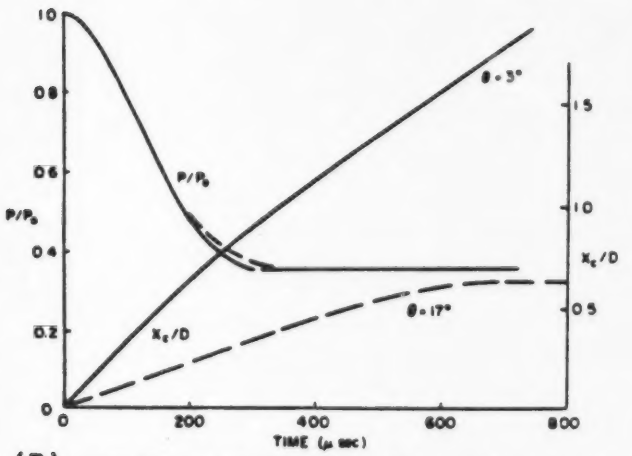

(B) Fluid pressure and crack extension history as a function of CTOA for a hot water-filled pipe

Figure 2.19 Decompression and Crack Extension of Air-filled Pipe and Hot-water-filled Pipe - from Emery

If, however, the crack propagation speed remains high a long axial split is quite possible.

A typical pressure tube reactor has a 6 m long pressure tube; assuming a crack speed of 300 m/s, a crack would take about 10 ms to propagate from mid-section to the end. The feeder pipe to the header is about 12 m long; it would take the first decompression wave about 24 ms to reach the header and be reflected to the pressure tube inlet. This long transmission time indicates that by the time the high pressure from the header reaches the calandria vessel, the whole pressure tube could have split end-to-end.

The decompression process is the driving force which determines the development of the ensuing events of bubble growth, moderator transients and fluid-structure interactions.

To gain an understanding of the decompression process, Edward and O'Brien (1976) and Alamgir and Lienhard (1980) and Alamgir, Kan and Lienhard (1980) carried out extensive experiments and analysis of pressurized hot water issuing from a pipe. They used quick opening devices and rupture discs to create circumferential types of pipe rupture. During depressurization, the water passes from a subcooled state to a superheated state by falling to a pressure below the saturation pressure at the initial temperature while flashing into vapour, as shown in Figure 2.20. The pressure then recovers to a quasi-steady pressure which is less than the saturation pressure. Alamquir found that the more rapid the decompression rate ($\Delta p/\Delta T$), the greater the undershoot, and greater will be the violence with which flashing occurs. They correlated the quasi-steady pressure (P_{qs})with the initial temperature (T_i) and fluid properties as follows:

$$T_{qs} = T_i - 1.26 \frac{\rho_g h_{fg}}{\rho_f C_{pf}} \quad .$$

Here T_{qs} is the quasi-steady saturation temperature corresponding to the quasi-steady pressure (knowing T_{qs}, P_{qs} may be estimated). For a coolant at 10 MPa and 280°C, one would expect a P_{qs} of 5 MPa (see Figure 2.21).

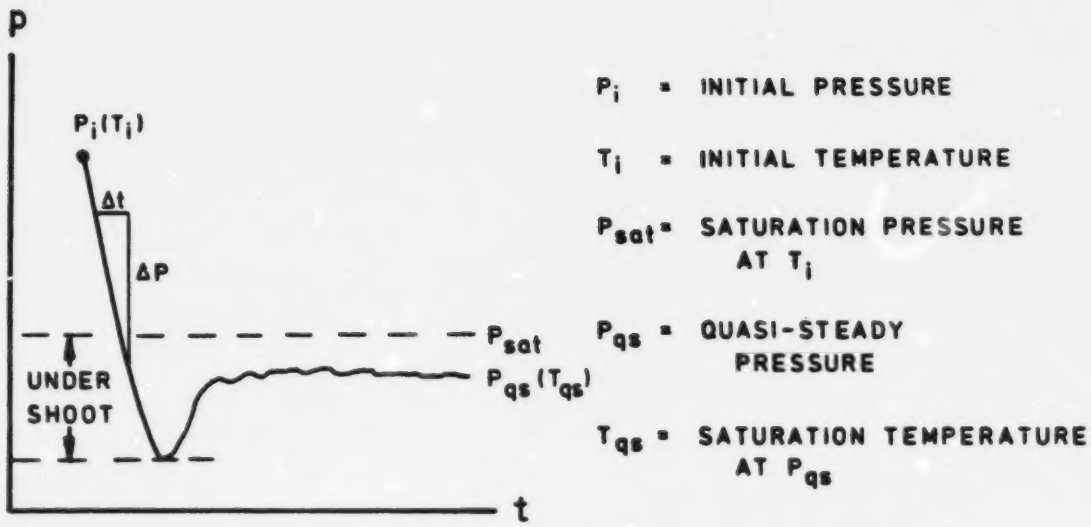

Figure 2.20 Pressure Undershoot during Decompression of Hot Water

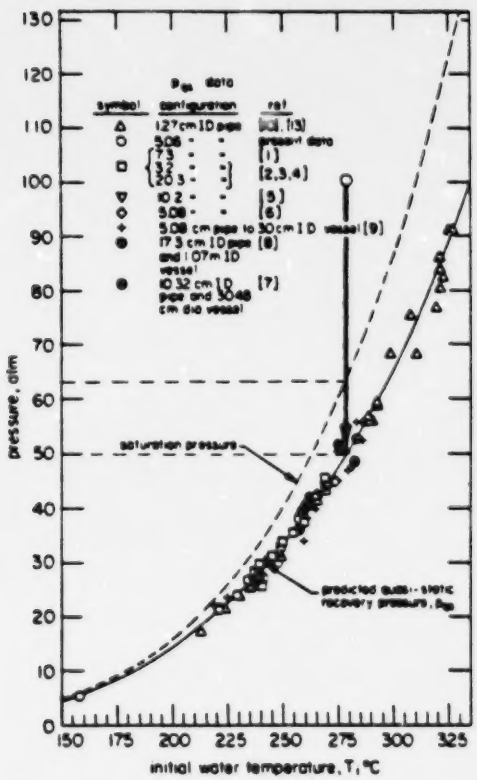

Figure 2.21 Comparison of Predicted Quasi-static Recovery Pressure with Experimental Data - from Alamgir and Lienhard

Although the above experiments were performed with the water discharging into the atmosphere, they do provide an insight into the decompression process of a tube rupture in a water moderator.

Alamgir and his colleagues measured decompression wave speeds of 1191 m/sec for 252°C water. Edward and O'Brien found comparable wave speeds of 997m/sec for 284°C water. They further reported that the pressure at the end of the pipe dipped to much lower undershoot as the decompression wave reflected from the closed end of the pipe. Ross-Ross observed similar pressure undershoot in the inlet to the pressure tube in his experiments, dropping from a burst pressure of 9.7 MPa to 6.2 MPa. In the first Bettula tests, pressures in the burst tube dropped from 5 MPa to 2.4 MPa.

2.4.3 Shock Waves

Despite arguments presented in Section 2.4 that instantaneous tube bursting is inconsistent with calculations of inertial forces in the fluid and in the opening sections of the tube wall, we consider in this section the nature of the pressure waves that would result from nearly instantaneous opening.

"Underwater Explosions" by Cole (1948) is an extensive treatment of submerged explosions, dealing mainly with high power explosives such as TNT. It characterizes the explosion process as composed of a shock wave expansion and an expanding-contracting gas sphere, i.e. a "bubble". These are the two main damage producing mechanisms.

As illustrated in Figure 2.22 (taken from Cole) two distinct pressure pulses may be measured following a high energy explosion. The first has large amplitude and short duration - the rapidly travelling shock wave. The pressure due to this shock wave is much higher than that due to the subsequent bubble motion, but the areas under the curve (impulses) are comparable. As to which mechanism will produce the most damage to an

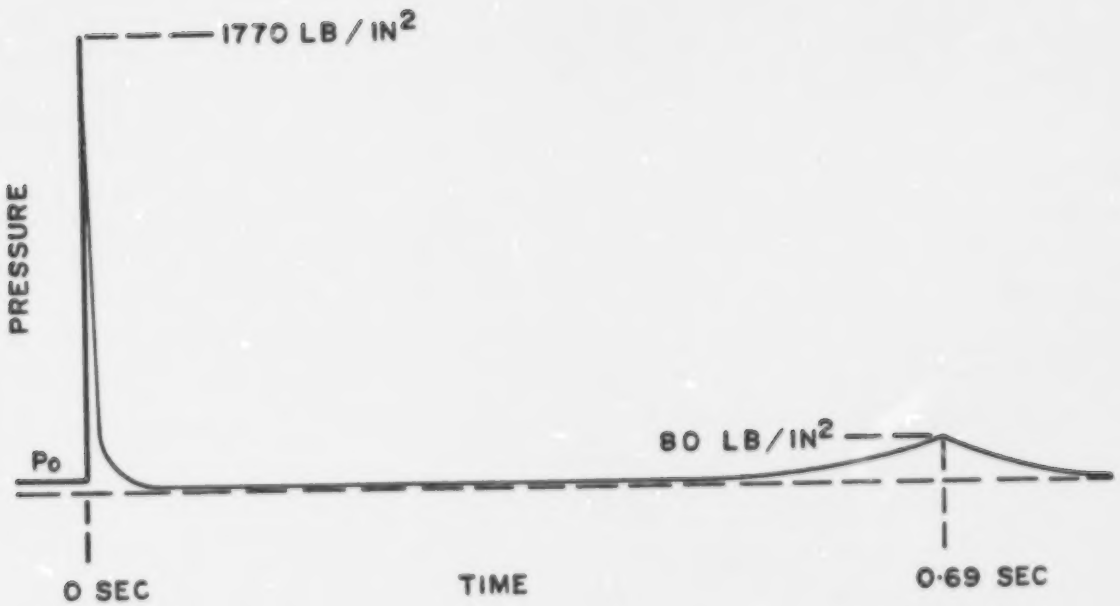

Figure 2.22 Pressure Pulses from Shock and Bubble Expansion - from Cole

obstacle, it depends on the pressure produced by the explosion at detonation. hence the strength of the shock wave.

Shock Wave Propagation:

The pressure of the expanding spherical shock wave falls off more rapidly with distance than the inverse first power law predicted for the small amplitude "acoustic" wave. The following table shows a case where, due to spherical dissipation, the pressure due to a TNT underwater explosion at five charge radii away falls off to one-tenth the initial valve.

Table 2.3 Pressure Decay in the Spherical Shock Wave from TNT

Distance (charge radii)	Peak Pressure (lbs/in.^{2}) Calculated	Measured
1	460,000	
2	167,000	
3	91,400	
5	42,800	
7	26,600	
10	16,400	16,250
15	9,670	9,640
20	6,720	6,720
25	1,090	1,090

The Mach number of the shock wave is determined by the pressure generated by the explosion. Figure 2.23, plotted with data from Cole (1948), demonstrates the functional relationship between shock wave strength and pressure.

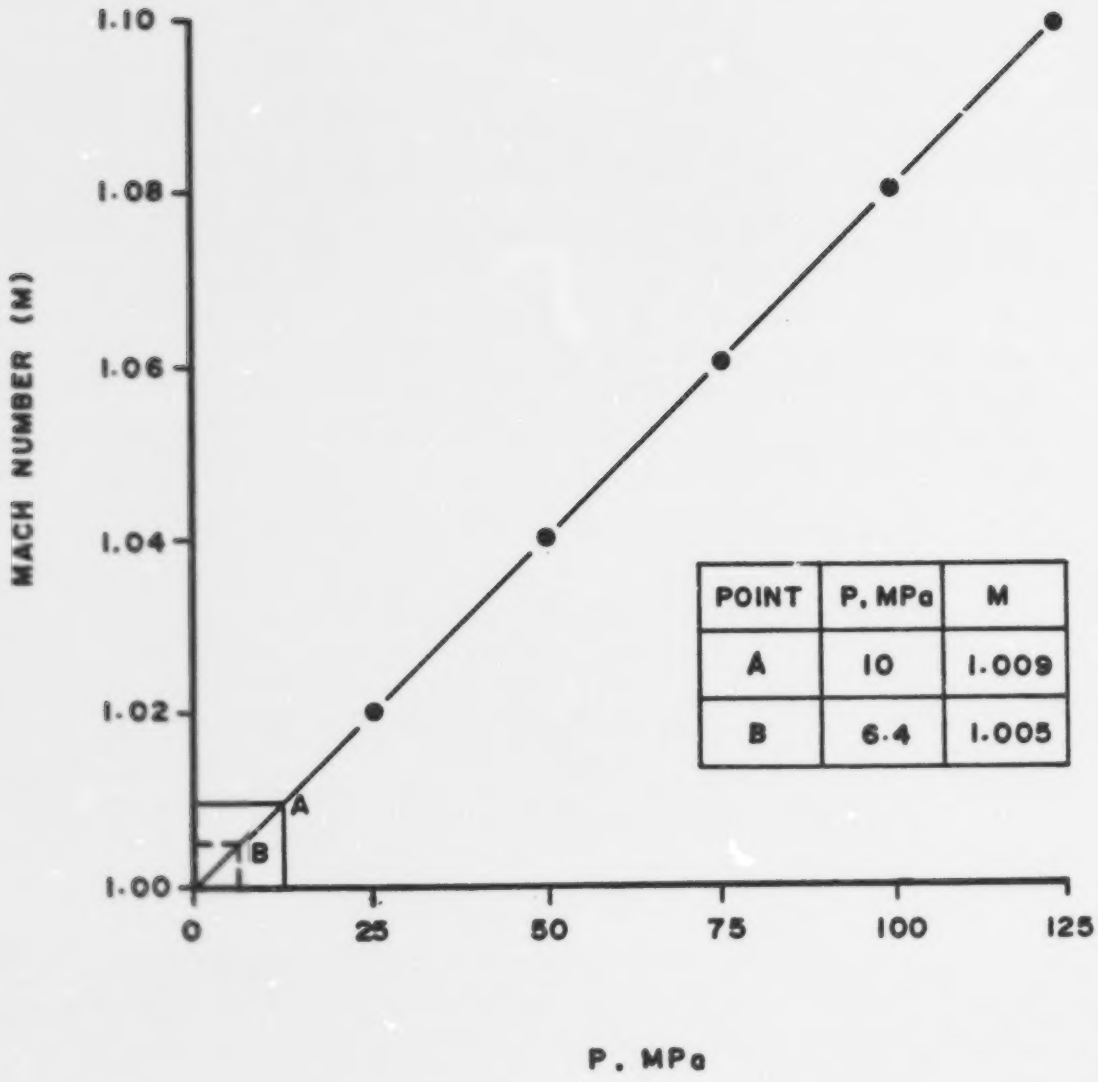

Figure 2.23 Shock Strength and Driving Pressure

In Canadian pressure tube reactors, the coolant is typically at 10 MPa and 310°C. If a section of the pressure and calandria tube disappears suddenly, one would expect a shock wave with Mach number about 1.009. Thus, even with instantaneous opening of the complete pressure tube, the resultant shock wave would have to be considered weak.

2.4.4 Reactive Forces and Pipe Whip

No experimental work has been done on submerged pipe whip under operating reactor conditions, although a large number of experiments have been conducted on pipe whip in air. In these experiments, the pipe is usually restrained with steel cables to gather restraint design data for primary piping external to the reactor core. However, these studies do provide data on the reactive force on the ruptured pipe.

Kitade, Nakatogawa, Nishikawa, Kawanishi and Tsuruto (1977) experimentally studied the reactive forces of hot water jets. The saturation pressure of the water was 4.3 MPa to 11.2 MPa and the diameters of the discharge nozzle were 10.7 mm to 40.8 mm. They were able to correlate the data with a modified Moody's blowdown thrust equation,

$$T = K A_e P_{sat},$$

in which A_e is the discharge area, P_{sat} is the saturation pressure of the water and K is the thrust coefficient, having a value of 1.2.

For discharge from a pressure tube of 100 mm diameter and coolant at 10 MPa and 280°C, this equation predicts a reaction force of about 60,000 N.

There are limited data on the angular motion of pipes whipping in air, recorded by high speed photography. The motion of a submerged whipping pipe in the complex pressure fields of the moderator created by the coolant explosion and fluid-structure interactions would be very different from that of pipe whip in air.

2.4.5 Missile Damage

Ohte, Yoshizawa, Chiba and Shida (1981) conducted tests in which carbon steel plates in air were subjected to missile impacts. The stainless steel missiles had three different nose shapes: cylindrical, semi-spherical and conical. The conical shape missiles have nose angles of 90°, 40° and 20°C. The mass of the missiles ranged from 5 kg to 50 kg and the target plate thickness ranged from 7 mm to 38 mm. The authors evaluated the critical fracture energy E_f(J) required for through-penetration of the target plate by the expression

$$E_f = 2.9\, T^{1.5}\, D_e{}^{1.5},$$

where T is the target thickness (mm) and D_e(mm) is the equivalent missile diameter. For a cylindrical missile, D_e equals the actual diameter.

Assuming a fuel bundle with a 90 mm diameter and a mass of 25 kg. an impact velocity of 190 m/s is needed before it has enough energy to fracture a calandria end plate of 32 mm thickness. The drag of the moderator makes such a high velocity unlikely.

2.4.6 Jet Impingement Forces

As in the case of pipe whip, no direct experimental data have been found on the submerged impingement force of a high temperature and high pressure water jet. Experimental investigations on jet impingement in air indicated that (for small discharge distance to nozzle diameter ratio) the impingement force on a target plate is about the same as the reactive force on the issuing pipe itself. This estimate would be the upper limit for submerged jet impingement forces. In the submerged environment of a calandria vessel. the depressurization of the two-phase jet with distance would certainly be a more rapid than that in air due to condensation, entrainment of the moderator and turbulence created by the high velocity discharge.

Hayamizu, Tokumitsu and Hayashi (1974) measured a maximum impact pressure of 2 MPa on an adjacent calandria tube when it was subjected to a coolant jet which was initially at 7.25 MPa and 287°C and discharging through a 90 x 50 mm hole in a pressure tube. This maximum impact pressure was reached 2 ms after rupture of a pressure tube and it decayed to a quasi-steady value of about 0.3 MPa in 4 ms. The impacted calandria tube suffered no deformation. Tanaka (1971) obtained a maximum impact pressure of the same magnitude with coolant at 6 MPa and 275°C discharging through a 95 x 55 mm hole in a pressure tube and impacting on an adjacent calandria tube at the same lattice distance as that used by Hayamizu and colleagues.

2.4.7 Summary

Although in the Bettula tests it was found that a given volume of pressurized hot water in an explosion tube produced only slightly higher pressure impulses than the same volume of equally pressurized gas, it must be remembered that these bursts resulted from long axial splits of artificially weakened tubes and that the moderator motion is significantly influenced by the gas plenum.

In a non-weakened tube the inertial forces required to accelerate the lateral opening of the tube may mean quite different propagation speeds (and ultimate opening lengths) for gas and hot water pressurization. The rate of crack propagation and the rate of opening of the burst area may also depend considerably on whether vapour or liquid surrounds the bursting tube.

If the acoustic speed of the fluid is much higher than the maximum crack opening speed (obtained with maximum pressure difference across the opening sides of the tube) the crack propagation speed may drop quickly to zero. In this case, a long axial split is unlikely and little of the fluid contained in the tube may participate in the immediate discharge which sets up the initial pressure pulse in the moderator.

The absence of data on submerged bursting of non-weakened tubes with hot-water pressurization means that we do not have reliable evidence on which to estimate the magnitude of the initial pulse, following tube burst.

Consideration of the mechanics of crack opening, the large initial forces encountered on rapid opening and the rapid decompression of the coolant indicates that the assumption of instantaneous end-to-end axial split of the pressure tube is highly conservative.

2.5 CONCLUSIONS FROM EXPERIMENTAL WORK

2.5.1 Introduction

The loading of the calandria vessel and its internals due to a pressure-tube burst are caused mainly by pressure pulses resulting from two-phase flashing discharge and possible subsequent vapour pocket collapse on mixing with relatively cool moderator liquid. This pressurization depends strongly on the flexibility of the calandria vessel and its array of pressure tubes. It is also affected by the yielding of calandria tubes collapsing onto their internal pressure tubes under large local pressure-gradient transients.

Evidence on the time required for the burst area to open, and the lack of direct pressure or strain impulses due to shock waves suggests that shock waves play a minor role following tube burst.

Peripheral pressure tube rupture produces greater loading on the nearby calandria vessel wall than central rupture. Experimental work indicates that stress in the calandria wall, caused by a single pressure tube rupture, is below the elastic limit of the material.

2.5.2 Possibility of Propagating Pressure Tube Failure

Tests on pressure tubes bursting in pools (or calandria vessels) have failed to supply evidence of propagating tube failure, except in one case where the pressure and temperature of the coolant inside the tube greatly exceeded the normal operating values in modern heavy-water cooled-and-moderated pressure tube reactors.

There is abundant evidence of collapse of calandria tubes, but not in such a way that would lead to subsequent failure of the enclosed pressure tubes.

Most of the experiments have used unirradiated tubing. However. Langford (1970) reports that "reactor service increases biaxial burst strength accompanied by a change in deformation mode that leads to reduced ductility after irradiation. Crack tolerance of the tubing is virtually unaffected by reactor service."

Vapour collapse, followed by damaging pressure pulses, does not seem to be a serious threat in a calandria vessel with little or no gas cap. There would appear to be little opportunity for a substantial vapour zone to form in such a case. Holtbecker alludes to such damage in an organic-fluid-cooled and water-moderated vessel test, but there is little or no detailed evidence provided.

Experimental evidence on the effects of vapour zone collapse appears largely to be missing. Numerical simulation of vapour collapse modes suggests possibilities worthy of experimental exploration.

Shock waves have not been directly detected by pressure transducers (which may not have been of sufficiently high frequency response to register the effect of a narrow wave, even of high intensity).

The initial shock wave must be considered "weak", i.e. to travel only slightly above acoustic speed. The initial wave leaving the burst site is unlikely to be steep because of the time taken to open the tube at the burst site.

We have been unable to identify mechanisms associated with tube burst which could produce large enough forces to cause rupture of a second pressure tube. The unsettled question is how such a second failure did occur in the Isles tests (admittedly with very high burst pressure and temperature). Computer simulation of this case should be done to relate how impulses of such magnitude developed and why the tube failed so far away from the burst site.

2.5.3 Possible Damage to Shut-off-rod Guide Tubes and Poison Injection System

There is no room for doubt that pressure impulses following tube burst can crush shut-off-rod guide tubes near the burst side. These perforated tubes are typically weaker than calandria tubes which have repeatedly been shown to crush easily under pressure pulse loading.

The question is not whether a single guide tube could be crushed, but whether of the typically 30 available for reactor shutdown, a large number could be sufficiently damaged to prevent shut-off rods dropping through. A pressure tube near the top of a horizontal axis calandria vessel could conceivably disable a number of shut-off rods (see Figures 1.1 and 1.4). The discharge from a propagating axial split could possibly damage all of the shut-off-rod guide tubes in an adjacent row.

Very little work has been done on the loading of shut-off-rod guide tubes from hot-water-filled pressure tube bursting in pools or calandria vessels. Limited information is available on the static strength of these tubes under two or three point loading (corresponding to the loading which might be imparted by relative deflections of adjacent pressure tubes large enough to pinch a shut-off-rod guide tube located between them).

Shut-of-rod guide tubes might be especially vulnerable to crushing under the impulse imparted by the initial shock wave. It appears that the initial shock wave impulses are small; yet we do not know how small they are relative to the crushing strength of the shut-off-rod guide tubes. Strengthening of these tubes, if necessary, may not be difficult.

Test data are unavailable on the strength of the poison injection pipes. Serious interference of this system would require crushing of two or more of the poison injection pipes near the points where these tubes enter the calandria vessel and in such a way as to reduce or prevent flow of liquid poison through the crushed section.

2.5.4 Possible Damage to Calandria Vessel

Test data indicate that pressure impulses imparted to calandria vessels are likely to cause tensile stresses well within the elastic limit, even when tube burst occurs near the vessel wall.

Complex pressure pulses including pressure waves generated by vapour collapse could conceivably cause local inward deformation of the wall (partial buckling) but this in itself would not be catastrophic.

The safety of the calandria vessel following bursting of a single pressure tube is not in serious doubt. If several tubes should fail simultaneously, or in very rapid sequence, say at the bottom of the calandria vessel, it is possible that the rutprue discs would not open soon enough to prevent substantial plastic deformation of the calandria vessel. Thus the key question is whether propagating pressure tube failure is a realistic possibility.

2.5.5 Questions Unanswered by Experiments to Date

In summary, certain questions not answered by available experimental results are:

(i) the vulnerability of Zircaloy or Zircaloy-2 tubes to failure under impulse loading if they are irradiated to a level which corresponds to reactor life;

(ii) the magnitudes of impulses which can be created in a horizontal axis calandria vessel (with no gas cap) due to collapse of vapour zones. It might be expected that, with no gas cap to provide spring-like storage of energy, these impulses would be small. However, no test data are available;

(iii) the magnitudes of the impulses which may be imparted to shut-off-rod guide tubes (following pressure tube burst) and the number of them which might be disabled by such a burst;

(iv) the speed with which an axial crack in an embrittled Zircaloy pressure tube could propagate and the magnitude of the resultant impulsive pressure loading of adjacent tubes; and

(v) the hydrodynamics in the tank which caused the propagating pressure tube failure in one of the Isles tests.

3.0 REVIEW OF ANALYTICAL WORK

3.1 INTRODUCTION

The complete pressure tube rupture problem, along with the multiplicity of succeeding events described by the experiments, is evidently too complex to be analyzed by a single, comprehensive model. Previous studies have therefore examined specific parts individually, or in some cases developed composite models by linking several separate mechanisms. Apart from the survey papers of Campbell, and Ross-Ross and Langford, this review considered previous works relating to pressure tube rupture models, bubble expansion and collapse, crack propagation and discharge flow models. In addition, basic physical phenomena such as shock waves and condensation effects were also reviewed.

As a very general division, analytical efforts can be broken into two categories: studies of simplified models representing portions of the physical events, sometimes leading to analytical relationships for pressures and flows; and studies in which point-by-point integration of the equations of motion is performed with a computer. The former types of study were found useful for obtaining a physical picture of the individual steps and their effect on overall results. In addition they involved relatively less cost and effort to conduct. The detailed point-by-point integration studies using large scale computation provide much more detailed information, without the limitation of simplifying assumptions. They are expensive however, and require careful formulation of boundary conditions before proceeding.

No complete model of the entire sequence of events important for the pressure tube rupture could be found; indeed, formulation of such a model may not be feasible. Similarly, large-scale computation of all events in a pressure tube rupture has yet to be performed

3.2 OVERALL PROBLEM: PRESSURE TUBE RUPTURE IN CLOSED VESSELS

At least three different analytical models have been developed for predicting pressure transients within closed vessels due to pressure tube rupture. Pendergast (1978) developed a model based on experimental data of Hareux and colleagues (1964) where N_2 gas was used to simulate the coolant. Kumar and colleagues (1975) analyzed the effects due to circumferential break on a pressure tube in a heavy water reactor. Both teams of investigators focused mainly on the loading of the calandria vessel. The study by Henry (1981) is the most comprehensive of the three. Henry developed models for the successive events following pressure tube rupture and computed the composite effects. This modular approach enables testing of the analytical solutions with data from many experiments having different boundary conditions. The solutions were used to predict loadings on adjacent tubes as well as those on the calandria vessel and will be reviewed separately in Section 3.4.

3.2.1 The Pendergast Model

In their experiments Hareux and colleagues (1964) observed that the nearly spherical gas bubble expanded until a maximum pressure was reached on the vessel wall, at which time flow from the relief pipe had barely started. They therefore assumed that the tank could be considered closed for modelling purposes. They further assumed the spherical gas bubble expands isentropically without mixing and that ideal gas relationships apply. They predicted maximum pressure loading on the vessel wall by equating the work done by the expanding bubble to the energy of deformation of the vessel and water surrounding this bubble. Their results have been described in Section 2.3.2 (p. 2-19).

Pendergast (1978) modified Hareux's solution and developed a model as shown in Figure 3.1, which allows prediction of pressure transients and effects of inflow and outflow from the vessel.

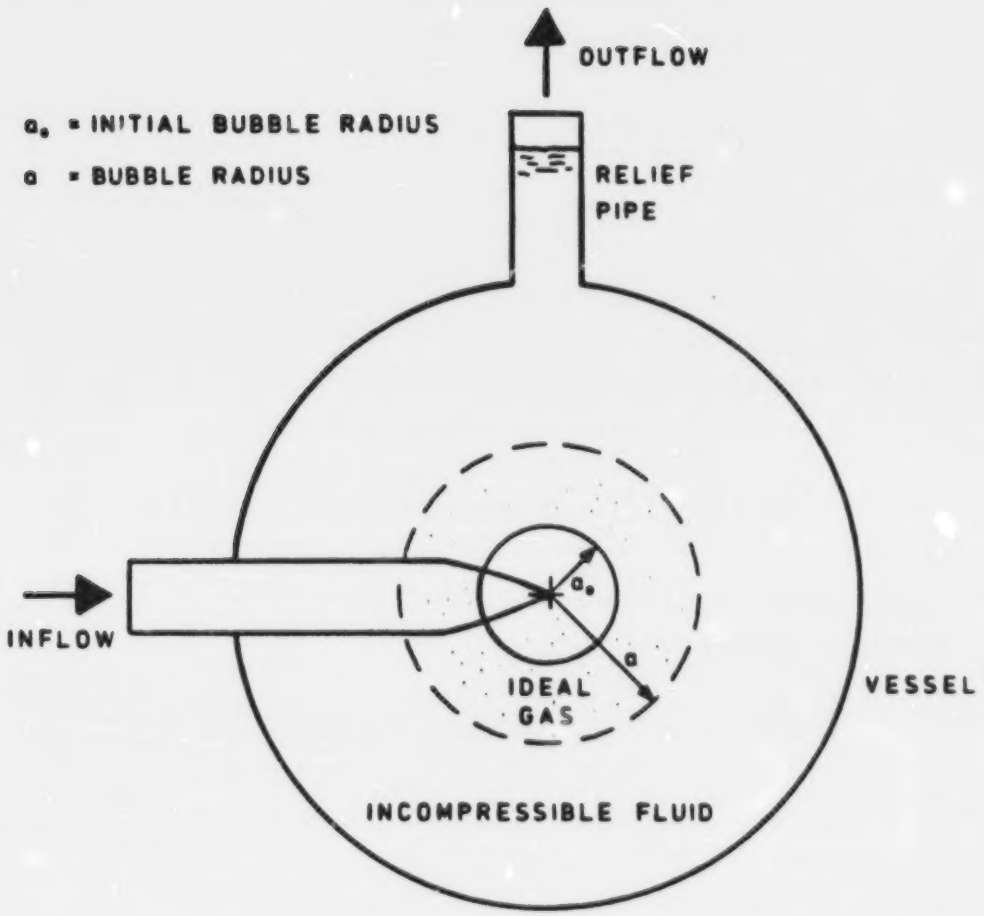

Figure 3.1 The Pendergast Model

Pendergast's model is described by six differential equations derived from the continuity and Navier-Stokes equations. An ideal gas, incompressible fluid and bubble symmetry were assumed. The solution is strongly dependent on initial bubble size; for large initial bubbles, variation of inflow area by a factor of 1000 produces little change in the peak pressure on the vessel wall. Figure 3.2 shows the measured and predicted vessel pressure and bubble radius.

3.2.2 The Kumar Model

Kumar (1975) and colleagues analyzed the pressure loading on calandria vessels due to circumferential breaks of a pressure tube in a heavy water reactor. They considered that the pressure loading is due to two components: shock waves from the coolant expansion; and net volume change within the vessel due to coolant inflow, moderator outflow through relief pipes and flashing and condensation of the coolant.

Considering the pressure tube rupture to correspond to the sudden rupture of a shock tube diaphragm, the investigators applied the continuity and momentum equations to the system and derived three first order differential equations for predicting the strength of a propagating spherical shock wave.

In considering the net volume change within the vessel, the investigators assumed that coolant flashes into perfectly spherical bubbles with an initial diameter equal to that of the pressure tube. The condensation of bubbles was calculated with a bubble-to-moderator heat transfer coefficient of 29.075 $kW/(cm^2\ ^oC)$.

Kumar and colleagues concluded that the pressure loading on the calandria vessel is dominantly governed by the relief pipe size and the initial amount of moderator in the relief pipes.

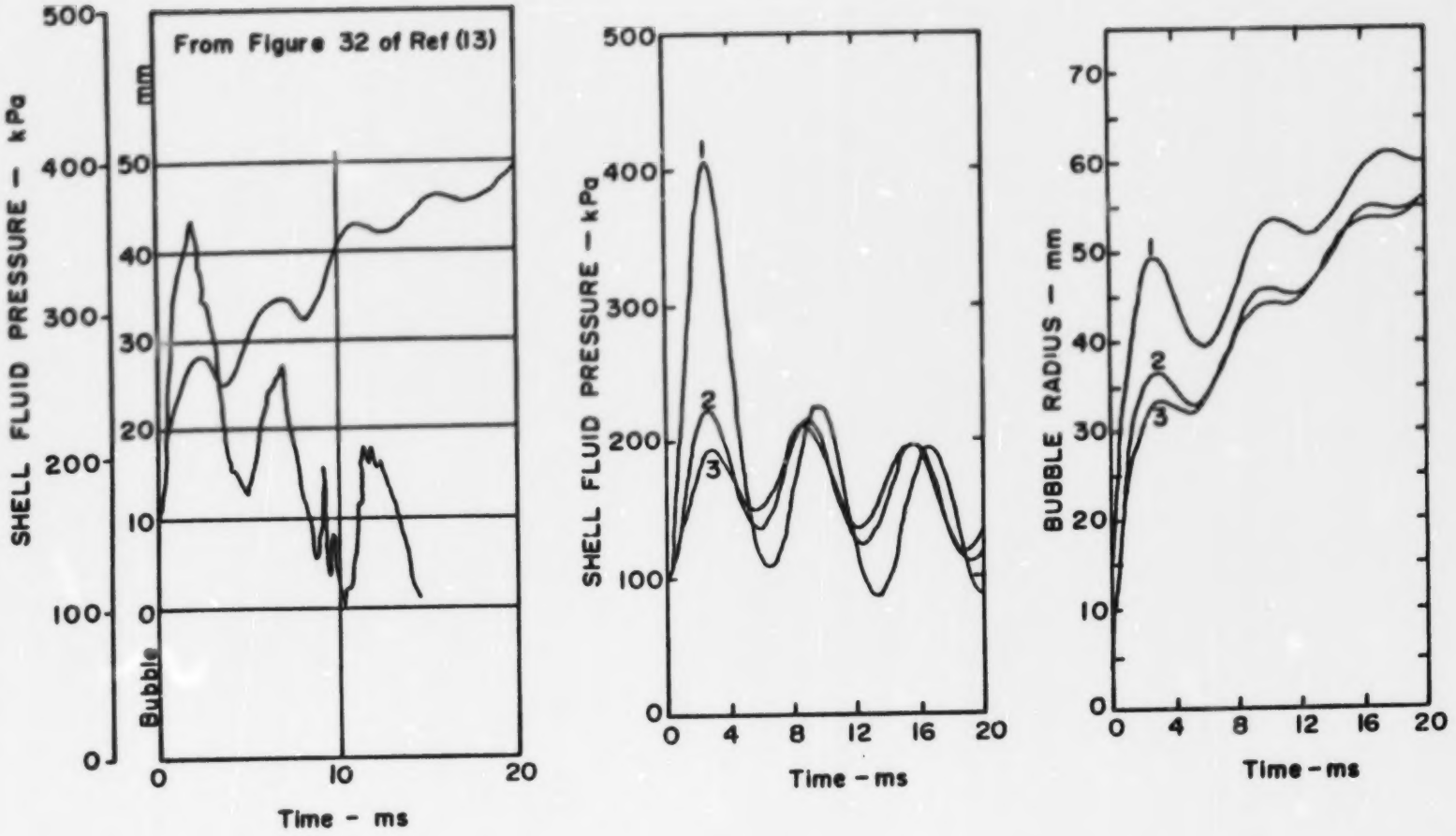
From Figure 32 of Ref (13)
SHELL FLUID PRESSURE - kPa
mm
Bubble
Time - ms
SHELL FLUID PRESSURE - kPa
Time - ms
BUBBLE RADIUS - mm
Time - ms
1 - Vao = 15·5 μm3 = Initial bubble volume
2 - Vao / 10
3 - Vao / 100

Figure 3.2 Measured and Predicted Vessel Pressure and Bubble Radius (Pendergast)

3.2.3 The Henry Models

The successive analytical models developed by Henry (1981) to describe the events following pressure tube rupture include:

1. bubble dynamics
2. discharge flow
3. slug inertial behavior
4. condensation
5. impulsive loading on adjacent tubes
6. dynamic stress behavior of the calandria vessel

By combining the individual effects of each of these models, an overall view of the pressure tube burst could be obtained. Since a review of Henry's work first requires an understanding of these individual models, a complete discussion of Henry's results is left to Section 3.4.

3.2.4 Computer Modelling

Considerable work has now been done by many investigators in developing computer models which treat transient hydrodynamic-structural interaction problems.. While these models or codes are flexible in the sense that they can be applied generally, greatest use has been made for studying the "hypothetical core disruptive accident" (HCDA) in breeder reactors. A historical perspective and review of the development of some of these codes has been given by Boudreau (1979). To the best of the author's knowledge, application of these types of computer codes has not been made for studying the overall presure tube rupture problem, although it appears possible that considerable information might be gained from such a study.

To gain some idea of the limitations of these codes as well as assess their usefulness for studying pressure tube rupture, two such codes, EURDYN and PISCES were reviewed more completely. These particular codes were chosen since they are typical of many of the other codes developed to date. In addition both of these codes have previously been used to study

transient hydrodynamic-structural interaction events in reactor situations not unlike those expected to occur in a pressure tube rupture problem.

Donea (1979) and co-workers have described the development of EURDYN. The code uses a finite-element Eulerian-Lagrangian method and can predict complete pressure and flow fields following a hypothetical release of a large amount of energy (or explosion) in an enclosed vessel having a liquid pool covered by a gas cap. Figure 3.3 shows a sequence of deformed computational meshes (displacement) following a finite energy release from a small initial volume. The bulk acceleration of the liquid, raising of the liquid level and impact with the roof, and subsequent non-linear distortion of the vessel walls can be seen clearly.

3.2.5 Summary

Analytical models have been developed to represent the initial shock wave propagation (for the case of instantaneous tube burst), bulk pressurization of the moderator due to coolant discharge, as well as the loading due to these pressure transients.

These models fall into two categories. The first class has been simplified by restriction to spherical symmetry and leads to fairly rapid calculation procedures. This class is not, in general, applicable to tube bursting near the calandria vessel wall. The second class involves two (or even three) dimensional finite-difference or finite-element methods applicable to very general geometrical configurations, but requires significant computer time.

All the simplified models fall short due to their inability to model the detailed nature of the tube rupture. Thus they all consider an initial bubble (however large or small) to exist at the initial moment. They proceed to calculate pressures on the vessel wall from this point onward. As such, the critical aspect of initial fluid-to-fluid communication across the crack is removed from consideration. The strength and directional property of the ensuing shock wave must critically depend on the breeching details; as such

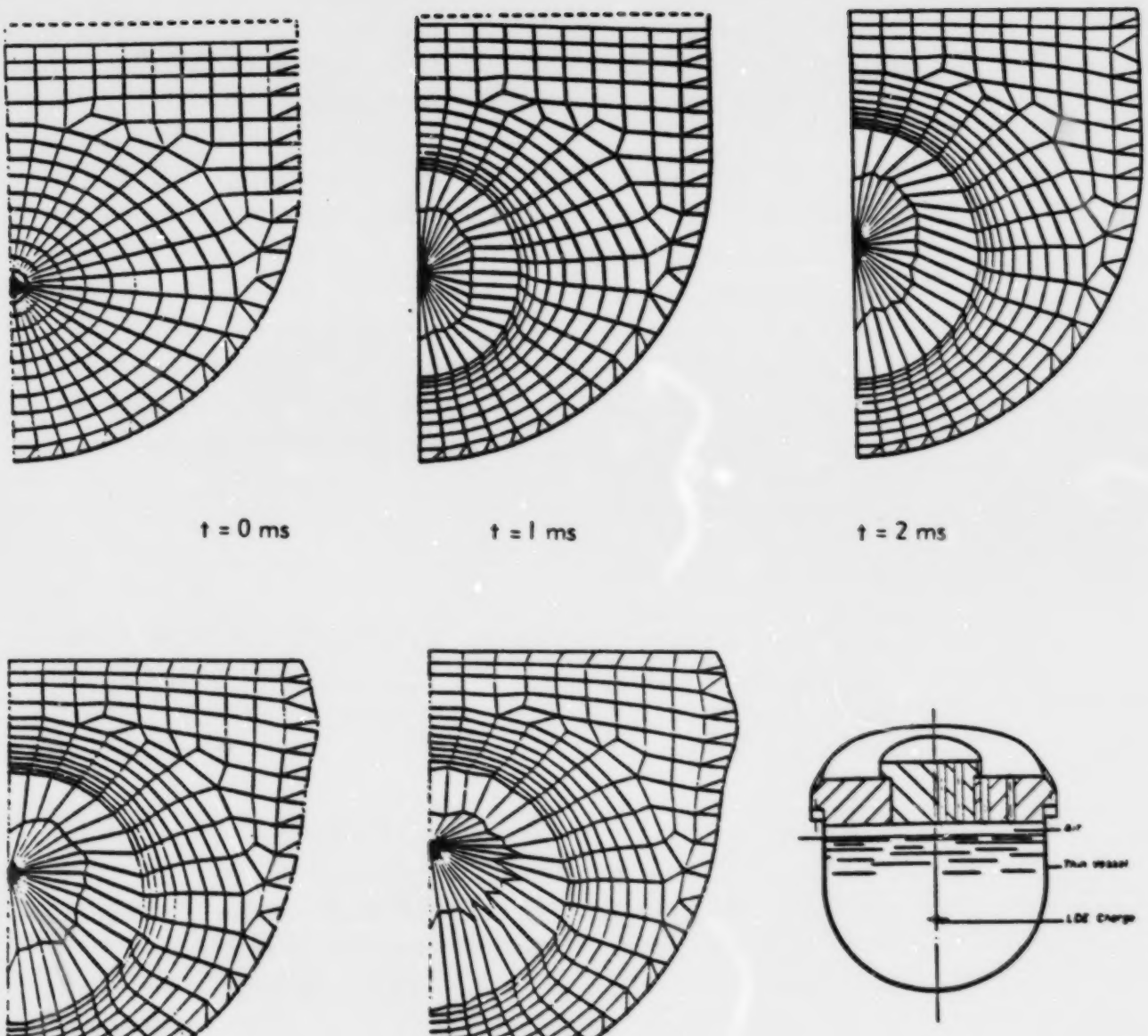

Figure 3.3 Application of EURDYN to Explosion in Enclosed Vessel

these models are inadequate for predicting the shock wave strength. It also appears from these models that opening size and rate of opening are unimportant; a not too surprising fact since their treatment is not initially included in the model. It should be pointed out that the experiments reviewed in Chapter 2 show considerable dependence on opening details.

The simplified models considered here also are restricted to spherical symmetry, and as such are incapable of predicting the local effects on a calandria wall due to a pressure tube rupture immediately adjacent to the wall.

The possible collapse of the vapour bubble is not treated in these models (except for Kumar) largely because the detailed way in which heat and mass transfer occurs at the bubble interface is not well understood.

The point-by-point numerical schemes (PISCES and EURDYN) are also inadequate for handling the opening details mentioned above. This is only because the actual opening mechanism must be specified as an initial condition for starting the computation. The opening rates however must depend on the way the hydro- and thermodynamic transient evolves; thus a "chicken-or-egg" circular argument ensues.

It should be noted that the point-by-point computer programs provide a wealth of information on pressure loadings on adjacent channels at any location in the vessel, for any location of break. This is a feature the simplified models cannot achieve.

3.3 MODELS OF SEPARATE MECHANISMS

3.3.1 Rupture Mechanisms

The entire sequence of events in a so-called "rupture" do not seem to have been developed into a single, comprehensive model suitable for thermo-hydraulic transient calculations. The most relevant work is that of Emery (1981) already discussed in Chapter 2. However, the detailed way in which crack propagation couples with plastic deformation of the tube wall away from the breech is not yet amenable to a model. The importance of the initial transient development on subsequent vessel and adjacent structure loading would suggest further study of this area. The detailed computer models may be able to partially generate rate of opening and depressurization information.

3.3.2 Shock Waves

The development of models for shock wave propagation in liquids follows directly from the case for shock waves in air or other gases. Kumar and colleagues (1975) considered the equation of state for water and combined that with well-known formulae from gas dynamics to obtain an equation for the pressure rise across a shock in heavy water. Their results indicate that at the pressures expected in a heavy-water reactor, the shock is considered "weak" in that it propagates at nearly acoustic velocity. On this basis, they concluded that calandria vessel loadings were quite moderate. No attempt was made to estimate the impulse on adjacent tubes due to passage of such a shock wave. It should be noted that this type of treatment of shock waves assumes spherical symmetry, which could only occur if the tube wall vanished instantaneously. There do not appear to be any models developed to account for shock waves generated from a non-symmetrical opening, nor for the subsequent and intricately complicated series of reflected shocks from the vessel walls and the pressure tube array.

An alternate theory of spherical shock wave propagation is that of Taylor (1950). No detailed opening mechanism is required; shock strength and speed is related to initial energy release in the explosion. Taylor's work does not appear to have been extended to liquids, but is is unlikely to produce significantly higher estimates of pressure loading than the conventional shock model since they are known to agree well for the case of air.

3.3.3 Bubble Dynamics

Consider a bubble as shown in Figure 3.4, with internal pressure Pi and initial radius Ro, expanding into an infinite pool of liquid with density ρ_ℓ and pressure P_ℓ. When the bubble expands to radius R with interface velocity U , the velocity of liquid away from interface μ may be expressed as

$$\mu = \left(\frac{R}{r}\right)^2 U \quad .$$

The kinetic energy of the liquid is

$$KE = \frac{1}{2} \rho_\ell \int_R^\infty \mu^2 \, 4\pi r^2 dr = 2\pi \rho_\ell U^2 R^3 \quad .$$

The work done is

$$\frac{4}{3} \pi (R^3 - R_o^3) (P_i - P_\ell) \quad .$$

Equating the kinetic energy and work done gives

$$U = \sqrt{\frac{2}{3} \frac{P_i - P_\ell}{\rho_\ell} \left[1 - \left(\frac{R_o}{R}\right)^3\right]} \quad .$$

If Ro/R is small

$$U \sim \sqrt{\frac{2}{3} \frac{P_i - P_\ell}{\rho_\ell}} \quad .$$

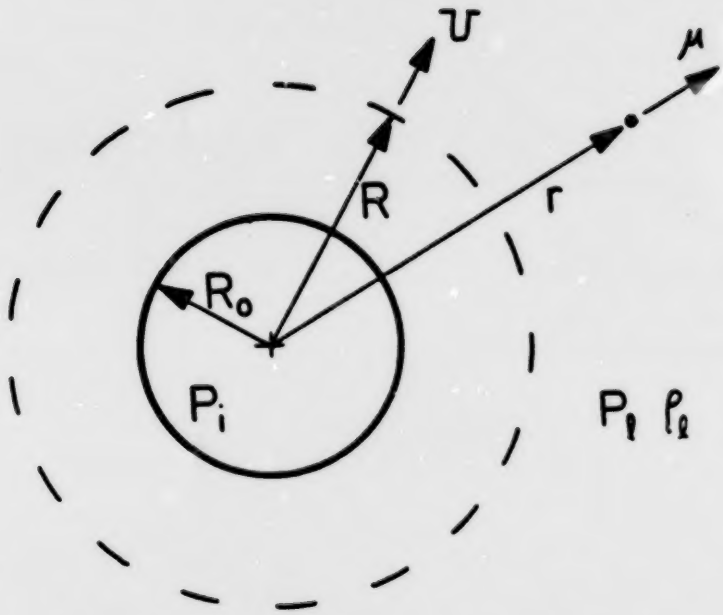

Figure 3.4 Bubble Expansion in an Infinite Pool

This equation is one solution to the Lord Rayleigh bubble equation (1917),

$$R\ddot{R} + \frac{3}{2}\dot{R}^2 = \frac{P_1 - P_\ell}{\rho_\ell} \quad ,$$

where $\dot{R} = U$, $\ddot{R} = \frac{dU}{dt}$.

The pressure in the liquid at the radial distance r is given by

$$P(r) = (P_1 - P_\ell)\left[\frac{4}{3}y - \frac{1}{3}y^4\right] + P_\ell \, ,$$

where $y = R/r$.

These relationships apply only to a very large body of incompressible liquid and where no heat transfer is involved. The Rayleigh bubble equation describes both bubble expansion and contraction. In the case of an underwater explosion, the inertia of the outward flowing water caused by the expanding bubble will eventually reduce bubble pressure below the equilibrium value and the motion of water will reverse, causing the bubble to contract until enough energy is built up in the gas to cause another bubble expansion. This oscillation may persist for many cycles with decaying amplitude. If the liquid is contained in a vessel, the oscillation of the bubble would be further influenced by the response of the vessel.

Depending on the boundary conditions at the vapour-liquid interface, a rapidly contracting bubble may produce very high internal pressures. In cases such as cavitation, the bubble may collapse and produce an outward-moving liquid shock wave. A review of this problem is given by Zel'dovich (1967).

It should be pointed out that bubble growth following a tube burst is subject to additional constraints which must be accounted for when using Rayleigh's model. The rate of discharge from the burst into the bubble is governed by the non-equilibrium decompression of the coolant, while the condensation

and mixing of the vapour at the moderator interface removes vapour from the bubble. The detailed jet mechanics can govern the directional properties of the bubble, while the energy absorption of the surrounding tube array arrests bubble growth. These are but a few of such constraints causing some researchers to maintain that only experimental investigations can yield realistic results.

3.3.4 Condensation and Collapse

Condensation is treated in Henry's model simply with the standard relationship

$$q = h_c A_{eff} (T_i - T_a).$$

In this expression, h_c is the condensation heat transfer coefficient, A_{eff} is the effective surface area assuming the bubble volume is spherical, T_i is the temperature inside the bubble and T_a is the average moderator temperature.

A value of 2500 $kW/m^2\,^oC$ was chosen by Henry for h_c, based on experimental results wherein direct steam condensation has been observed during discharge of supersonic saturated steam directly into large cold water pools.

3.3.5 Slug Inertia Behavior

This model simulates the vertical water slug movements (such as those in the Italian Tests) when a gas cap is present. The vertical acceleration of the slug is given by

$$\frac{d^2 z}{dt^2} = \frac{(P_m - P_g)}{\rho_m \ell_s} ,$$

where Pg is the pressure in gas plenum, Pm and ρ_m are the moderator pressure and density at rupture elevation, ℓ_s is the distance between the gas-moderator free surface and the rupture elevation.

This acceleration is assumed to remain constant over one time step (Δt) in the numerical calculation.

Velocity is calculated by

$$V = V_o + \left(\frac{d^2 z}{dt^2}\right) \Delta t,$$

where V_o is the velocity of the slug during the previous time step.

Displacement of the slug is calculated by

$$Z = Z_o + V_o \Delta t + \frac{1}{2} \left(\frac{d^2 z}{dt^2}\right) \Delta t,$$

where Z_o is the displacement at the beginning of the time step.

While this model is strictly one-dimensional and requires the presence of a gas plenum, Henry argued it could be used for a spherical bubble with no gas cap by simply equating the volume of one plenum to that of the growing bubble.

3.3.6 Impulsive Loading on Adjacent Structures

The impulse loading on an adjacent tube is calculated from the force history from the time of tube rupture and bubble formation until the moderator pressure equilibrates with the bubble pressure. The force is composed of the pressure difference across the tube and the local dynamic head,

$$\Delta F_f = D_{ct} \quad (0.05) \quad (P_{rl} - P_{sl} + \frac{\rho_\ell U_{rl}^2}{2} \cos \alpha) \quad ,$$

where P_{rl}, P_{sl}, and U_{rl} are local pressures and velocity at the target tube (see Figure 3.5).

This local force is assumed to act on a length of 0.05 m of the tube. The total force F_T is obtained by summing the local forces over the whole length of the tube,

$$F_T = \Sigma \Delta \ F_f \quad .$$

Impulse I is the integral of force with respect to time and is equal to the change in momentum,

$$I = \int_0^t F_T dt = mv,$$

where m and v are mass and velocity of the tube.

The impulse and kinetic energy KE are related by

$$KE = \frac{1}{2} mv^2 = \frac{I}{2m} \quad .$$

Considering the tube as a simply supported beam, the expression for beam displacement Y is

$$Y(x,t) = Y_{max} \sin \lambda x \sin C \lambda^2 t \ ,$$

where $\lambda = \frac{\pi}{L}$, L is the length of the beam and C is a constant. The kinetic energy is given by

$$KE = \tfrac{1}{2} \int_0^L \mu \dot{y}^2 dx = y_{max}^2 \ \frac{E I_x \lambda^4 L}{4} \ ,$$

where μ is mass per unit length of the tube, E is modulus of elasticity and I_x is the moment of inertia about the tube diameter.

From the two expressions for kinetic energy, maximum deflection may be calculated, once the impulse is obtained.

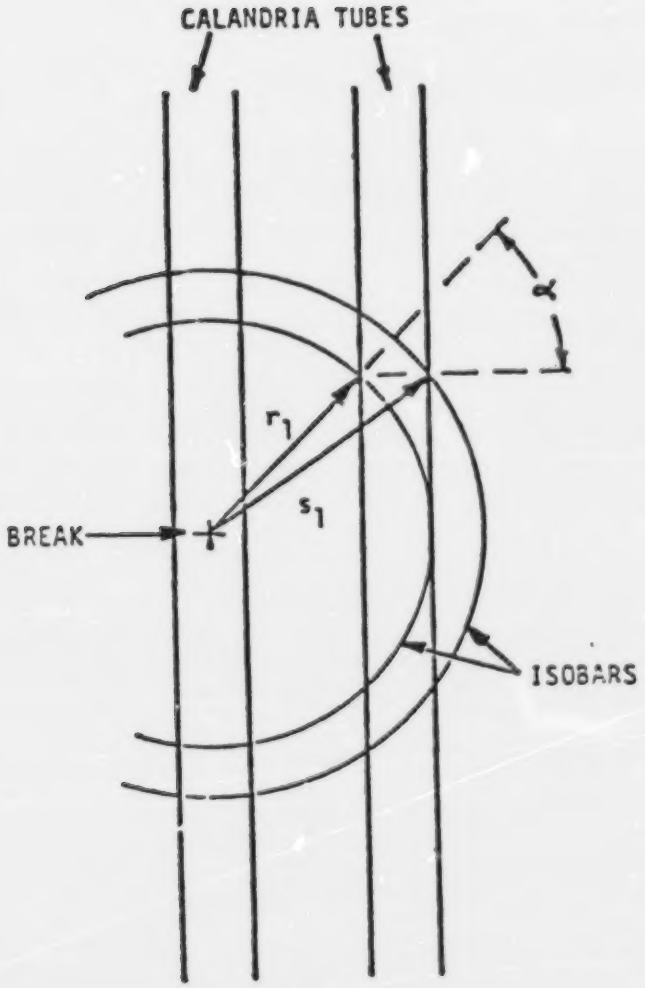

Figure 3.5 Loading on Adjacent Tube - from Henry

3.3.7 Calandria Stresses for the Calandria Vessel

When ΔP is the pressure difference across the calandria vessel wall at any instant, the force balance on the wall structure in radial direction may be expressed as

$$2r\ell\Delta P - 2\sigma_r b\ell = 2\pi r b\ell\rho_s \frac{d^2r}{dt^2},$$

where ρ_s is density of the vessel wall, σ_r is the hoop stress and other symbols are as illustrated in Figures 3.6 and 3.7 below.

The hoop stress is related to radial strain ε_r and axial stress σ_ℓ by

$$\sigma_r = E\varepsilon_r = E\left(\frac{r-r_o}{r_o}\right) + \mu\sigma_\ell,$$

where μ is Poisson's ratio and r_o is the original radius.

The radial wall acceleration then may be expressed as

$$\frac{d^2r}{dt^2} = \frac{\Delta P - \frac{b}{r}\left[E\left(\frac{r-r_o}{r_o}\right) + \mu\sigma_\ell\right]}{\rho_s \pi b}.$$

During the transient, the absolute magnitude of the radius does not change significantly. Given the pressure forcing function, the radial velocity of the wall V for each time interval Δt may be calculated by

$$V = V' + \left(\frac{d^2r}{dt^2}\right)\Delta t,$$

and the radial wall displacement given by

$$r = r' + V'\Delta t + \frac{1}{2}\left(\frac{d^2r}{dt^2}\right)\Delta t,$$

where the (') values are those at the beginning of a time step.

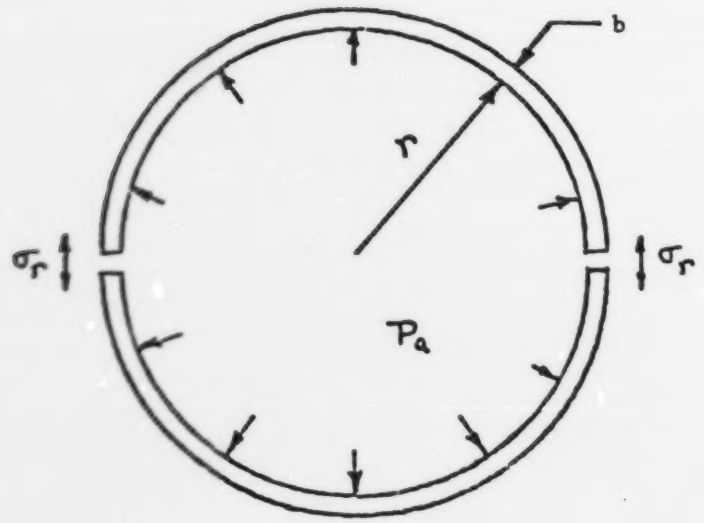

Figure 3.6 Hoop Stress in the Calandria Vessel - from Henry

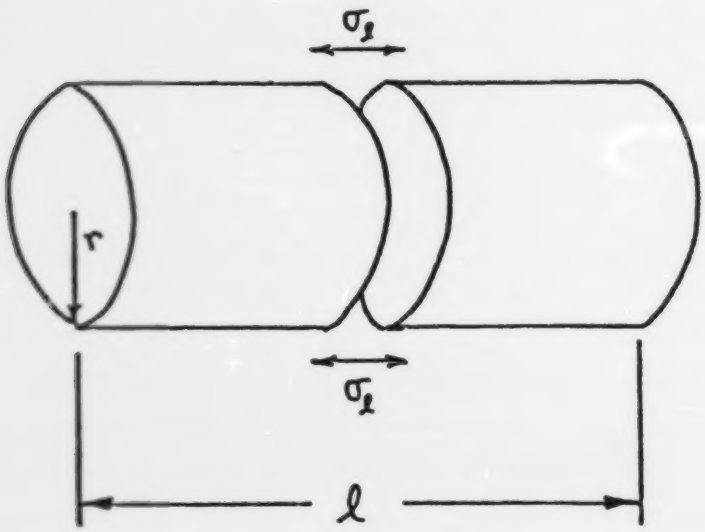

Figure 3.7 Longitudinal Stress in the Calandria Vessel - from Henry

Similarly, the axial wall acceleration is

$$\frac{d^2z}{dt^2} = \frac{r_o \Delta P - 2b\left[\varepsilon\left(\frac{\ell-\ell_o}{\ell_o}\right)+\mu\sigma_r\right]}{\rho_s b\,(2\ell_o + r_o)} \quad .$$

Axial velocity is

$$V_z = V_z' + \left(\frac{d^2z}{dt^2}\right)\Delta t \quad ,$$

and axial length is

$$z = z' + V_z' \Delta t + \tfrac{1}{2}\left(\frac{d^2z}{dt^2}\right)\Delta t \quad .$$

The combined membrane stress is calculated by

$$\sigma_c = \sqrt{\sigma_\ell^2 + \sigma_r^2} \quad .$$

3.3.8 Discharge Flow

Henry used an acoustic model and a two-phase critical flow model for discharge flow calculations. The acoustic model simulates systems with small coolant inventory, such as some of the Italian tests where the ends of the rupturing pressure tube were closed. The critical flow model was reasoned to be more appropriate for systems with large coolant inventory available or for steady discharge.

In the acoustic model, the flow rate is continually increased as a series of rarefaction waves propagate into the coolant source, driven by the pressure decrease inside the expanding bubble. This approximates an isentropic expansion of a one-component flashing system.

In the two-phase critical flow model, the flow rate is calculated from one of two models: the homogeneous-equilibrium model; and the Henry-Fauske model. These are but two of several discharge flow models now in use. A good review of these models was given by Hsu and Graham (1976), who also pointed out their limitations. A very important assumption in their derivation is steady flow, and serious discrepancy in flow rates may be expected particularly at the beginning of a tube burst.

3.4 APPLICATIONS OF HENRY'S MODELLING TO HORIZONTAL-AXIS PRESSURE TUBE REACTORS WITH NO GAS CAP

Henry performed calculations for loadings of the calandria vessel and in-core components in horizontal-axis pressure tube reactors due to pressure tube rupture. These calculations included the application of models for estimating load due to both short term and long term damage mechanisms. Short term mechanisms are mainly pressure loadings due to bulk pressurization from movement of the vapour bubble, whereas long term mechanisms refer to sustained jet discharge, missile impact and pipe whip.

3.4.1 Bulk Pressurization

Both axial split (fish mouth) and circumferential break (guillotine) of the pressure tube were considered in the calculation. The calandria vessel was assumed to have an outer diameter of 8.46 m and length of 5.03 m, with 0.0318 m stainless steel wall.

For the axial split, calculations were carried out for a rupture length of 1 m (8 L/D), with assumed coolant pressures of 10 MPa and opening times of 1 and 5 ms.

As shown in Figure 3.8 the calculations imply that the opening time does not have major influence on the dynamic loading on the calandria vessel. Opening times of 0.001 s and 0.005 s correspond to crack propagation speeds of 528 m/s and 106 m/s.

For the axial split of length 1 m and an opening time of 0.005 s, the maximum deflection of an adjacent pressure tube is calculated to be 0.02 m with a maximum bending stress of 17 MPa, producing no permanent distortion. An adjacent calandria tube would experience a maximum deflection of about 0.12 m and therefore would impact the pressure tube it enclosed. Henry concludes that shut-off-rod guide tubes in the same row as the rupture would not be excessively stressed if they are greater than 0.5 m

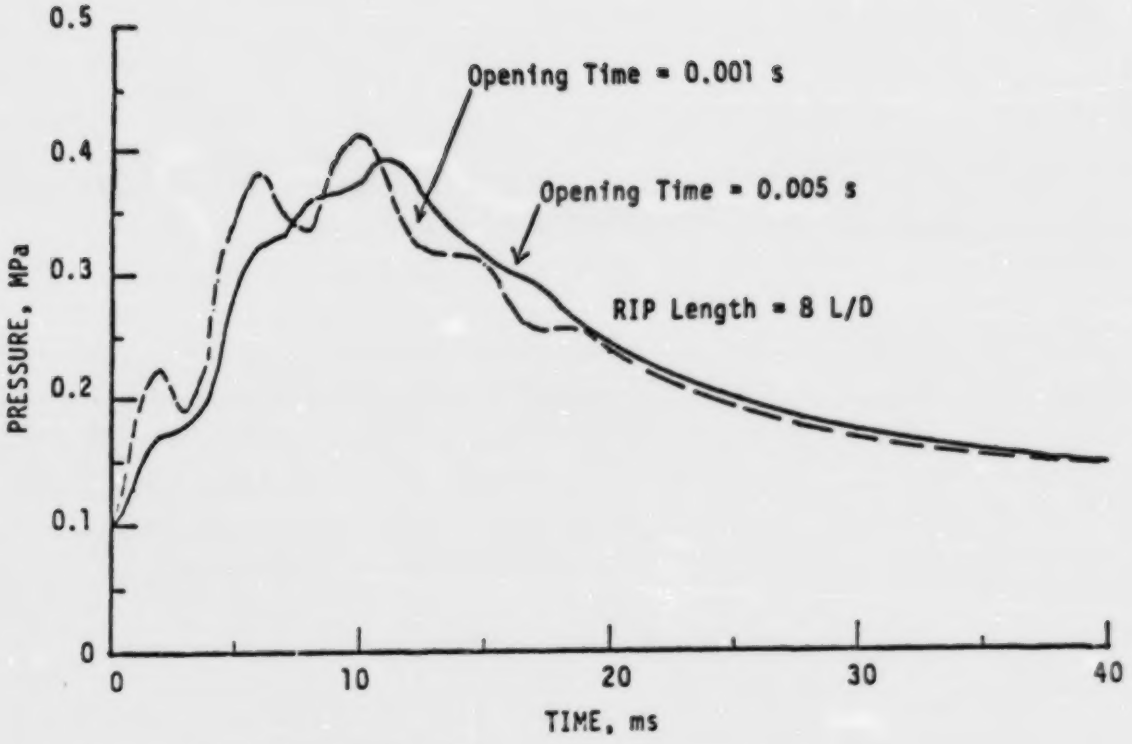

Figure 3.8 Effect of Break Opening Time - from Henry

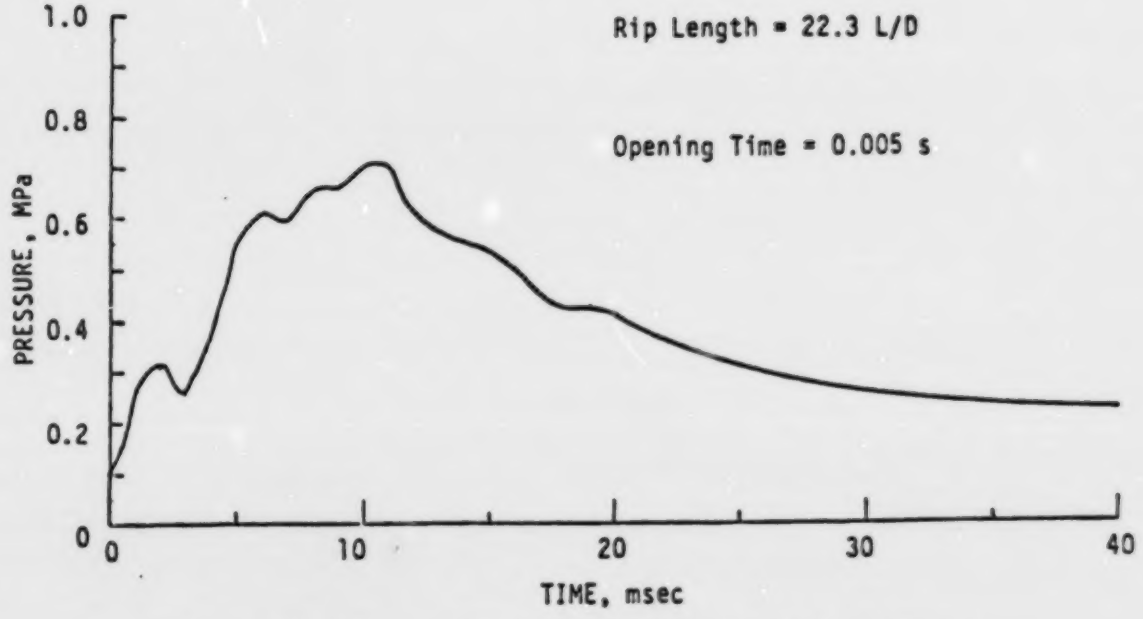

Figure 3.9 Pressure Transient within the Calandria Tank for a Very Long Rupture Length - from Henry

from the break location, and in other rows only those within 0.5 m are in jeopardy of denting by impact upon a calandria/pressure tube. Assuming the rupture occurs directly in front of a guide tube, he finds that only two additional tubes could potentially be jeopardized.

A second set of calculations was performed for a 3 m long axial rupture (22.8 L/D). The pressure transient on the calandria vessel is shown in Figure 3.9.

The maximum calandria vessel combined membrane stress is calculated to be 113 MPa, well within the elastic range of the stainless steel.

For a circumferential (or guillotine) break, the rupture was assumed to be spontaneous. The initial volume of the high-pressure expanding vapour bubble was assumed to be equal to a sphere having a diameter of the failed pressure tube. The rupture was assumed to occur in the middle of the calandria vessel. The calculated pressure transient is shown in Figure 3.10. It is seen that this results in a minimal pressurization of the calandria vessel, and the corresponding loading on adjacent pressure tubes is low.

These two sets of calculations were performed with the assumptions that the coolant is saturated at 10 MPa, no absorption of energy by the collapsing calandria tube and no fluid drag forces; therefore this represents a conservative approach. Saturated coolant at 10 MPa implies a coolant temperature of 310°C. Henry concluded that the maximum number of guide tubes that could be damaged is three. However, no figures were given for the deflection and maximum stress of an adjacent pressure tube for this case.

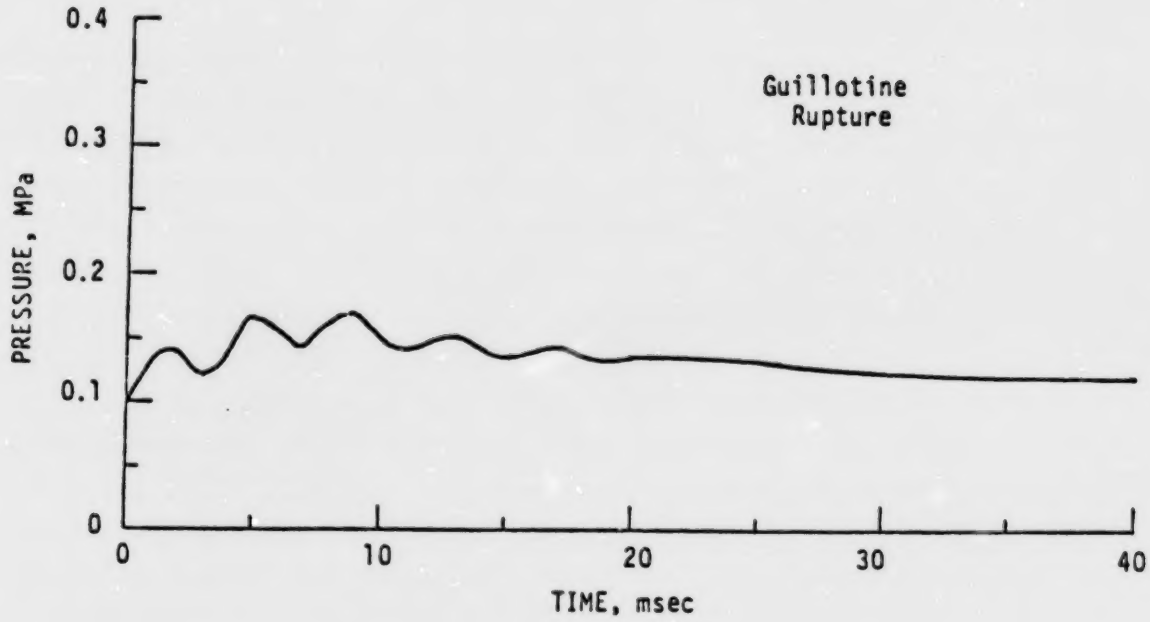

Figure 3.10 Pressure Transient within the Calandria Tank for a Postulated Guillotine Rupture of a Pressure Tube - from Henry

3.4.2 Jet Reaction and Impingement Forces on Adjacent Tubes with Sustained Discharge

In considering sustained discharge through a rupture opening in a pressure tube, Henry estimates that flow losses will reduce the pressure from about 10 MPa in the header to about 5 MPa ahead of the break, depending on whether the fuel bundles are retained or expelled through the break. He estimates lateral reaction forces in the range of 20,000 to 60,000 N. This calculated reactive force is taken up later in discussion of pipe whip.

Henry calculated that the maximum jet impingement force (assuming the jet discharges through air) on a adjacent tube occurs when the ruptured length on the explosion tube is 0.61 of the tube diameter. Under this condition, the maximum force on an adjacent channel is 10,400 N, causing a maximum stress of 257 MPa, while the yield stress of the Zircalloy pressure tube is 317 MPa. The calculated deflection of the channel is 0.066 m. The impact of the channel against two adjacent shut-off-rod guide tubes could load them beyond their elastic limit.

3.4.3 Pipe Whip Damage

The crushing strength of the shut-off-rod guide tube (under 2 or 3 point lateral loading corresponding to "pinching" between deflected pressure tubes) is small. Tests have shown it to be about 3,000 N total load when the tube is crushed to half its diameter. Such a load (as Henry calculates) could easily be applied by reactive forces, or even impingement forces for quasi-steady flow through a burst area. He speculates on whether a falling shut-off control rod would "straighten the dent". However, apart from this consideration it appears that crushing only one or two guide tubes would not disable the reactor shut-down system. The force required to sever a crushed guide tube (176,000 N) would substantially exceed the estimated maximum reaction forces.

3.4.4 Missile Damage

Henry calculates that acceleration of 6 fuel bundles (25 kg each) in a tube with unobstructed open end will produce ejection velocities of 13-15 m/s (corresponding kinetic energies 2-37 KJ). Allowing for fluid drag, he estimates a maximum impact velocity of 33 m/s and a maximum impact stress of 8 MPa (compared with an ultimate shear stress of the material of the tube sheet of around 500 MPa).

3.4.5 Summary

The use of a sequence of models for each event has allowed prediction of potential damage mechanisms following tube rupture. Using what he considered a conservative approach, Henry concluded

> "The resultant hydrodynamic transient would not endanger the shutdown of the reactor system...."

and further

> "The number of (shut-off-rod guide) tubes disabled by the initial hydrodynamic transient and these three additional long term damage mechanisms is between two and four depending on the specific nature and location of the break."

This has provided a useful first estimate of the hazard expected, but was not intended and indeed cannot represent the complete state of affairs following tube rupture. The effects of shock waves in particular are not considered, as well as the effects of non-central break location and real three-dimensional jet properties. Inclusion of such effects would complicate this type of analytical procedure immensely, while contributing marginally to the confidence of the results obtained.

3.5 COMPUTER MODELS

3.5.1 Computer Code EURDYN

This code was developed at the Joint Research Center, Commission of the European Communities, Ispra (Italy) by Donea, Fasoli-Stella and co-workers (1979). It is a finite element code for predicting non-linear dynamic response of reactor components following a "hypothetical energy excursion." The code is a two-dimensional fluid-structure code with capabilities for plane and axisymmetric configurations.

Computer codes for reactor safety evaluations should have the capability of computing fluid flows with wave propagation, momentum effects on highly distorted flows and structural effects with fluid-structure coupling. Donea and co-workers used the Arbitrary Lagrangian Eulerian (ALE) description first developed by Hirt (1974). This method includes both wave and momentum effects as well as fluid-structure coupling and does not need sophisticated logic to keep track of material interfaces as they move through a purely Eulerian mesh.

The finite element method was used as a basic discretization technique for both the fluid and the structure. This method is well established in structural mechanics and was adopted to provide a uniform numerical treatment.

Two applications of this code were described by Donea, each was compared with experimental results performed independently. One example is known as COVA/IT8 and consists of the vessel shown previously in Figure 3.3. It has a thin cylindrical shell with a spherical bottom. The vessel is nearly full of water and was loaded by detonation of a low density explosive charge located on the vessel axis. The deformations with time were discussed in Section 3.2.4.

Another example is that shown in Figure 3.11 (test series COVA-1T1). The experiment involved placing 29.3 gm of UK composition B explosive in the overstrong cylindrical vessel as shown. Pressure gauges were placed at selected locations of the wall, floor and roof of the vessel.

The model used a relatively coarse mesh (20 triangular elements for the explosive and 232 quadrilateral elements for the water), with the air space being considered as a void. The predicted impulse on the roof is compared with the measured values as also shown in Figure 3.11. The predicted values are in good agreement with, although consistently lower than, the experiments; this may have been due to the coarseness of a mesh.

While this code is extremely versatile and illuminating, it still requries the assumptions of two-dimensional geometry, instantaneous explosion, no continuous discharge and no phase change in the water.

3.5.2 Computer Code PISCES

The PISCES system of computer programs are available commercially from Physics International, San Leandro, California (the acronym PISCES stands for Physics International multi-Spatial Codes for Engineering and Science). The code has been described in a series of publications by Cowler and colleagues (1981, 1979). PISCES also uses a mixed Eulerian-Lagrangian scheme, however the cell or mesh size is a fixed Eulerian mesh (non-finite element).

An example of the two-dimensional version (PISCES 2DELK) is shown in Figure 3.12, as applied to a hypothetical core disruptive accident in a breeder reactor.

The numerically simulated accident begins with a hot sphere of high pressure sodium vapour in the core region. The successive plots show the acceleration of the surrounding fluid, closure of the cover void, impact on the cover plate and the response of the cover plate and core barrel.

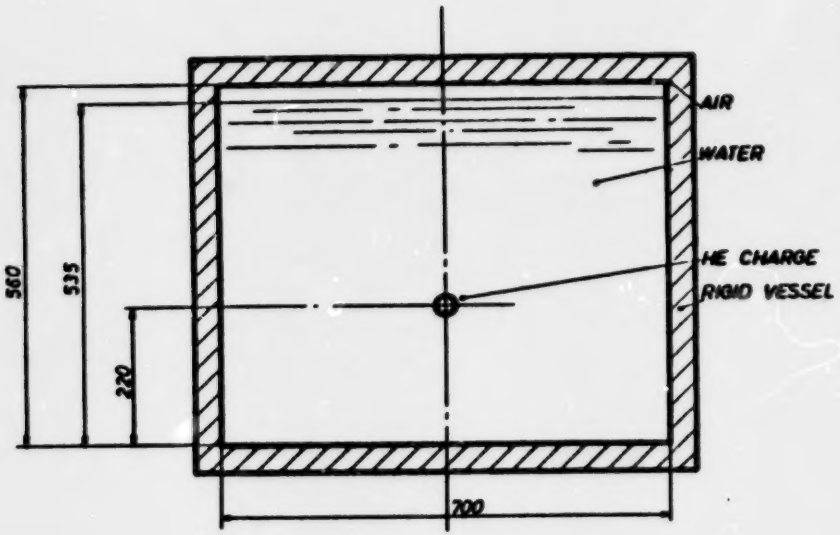

(a) Schematic of Test Configuration (COMA-1T1)

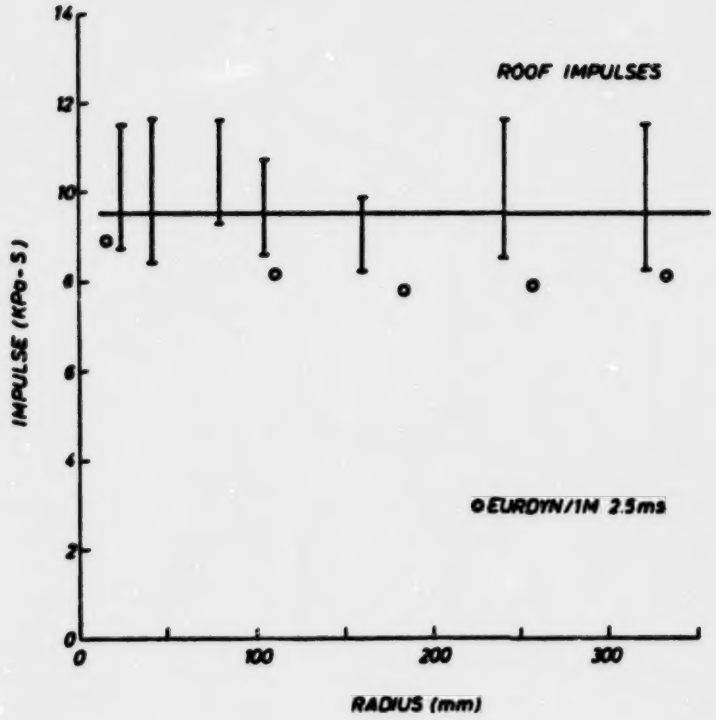

(b) Total Impulse on Roof of Containment at t = 2.5 ms

Figure 3.11 Total Impulse on Roof of Containment using EURDYN
(see also Figure 3.3)

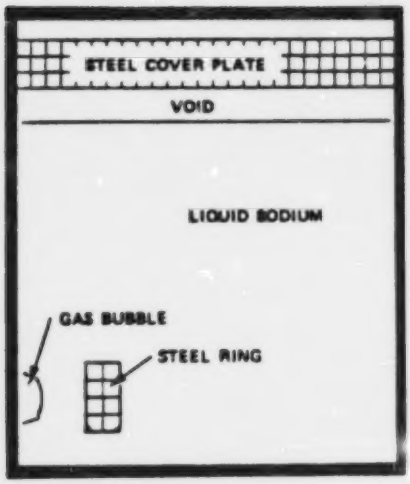

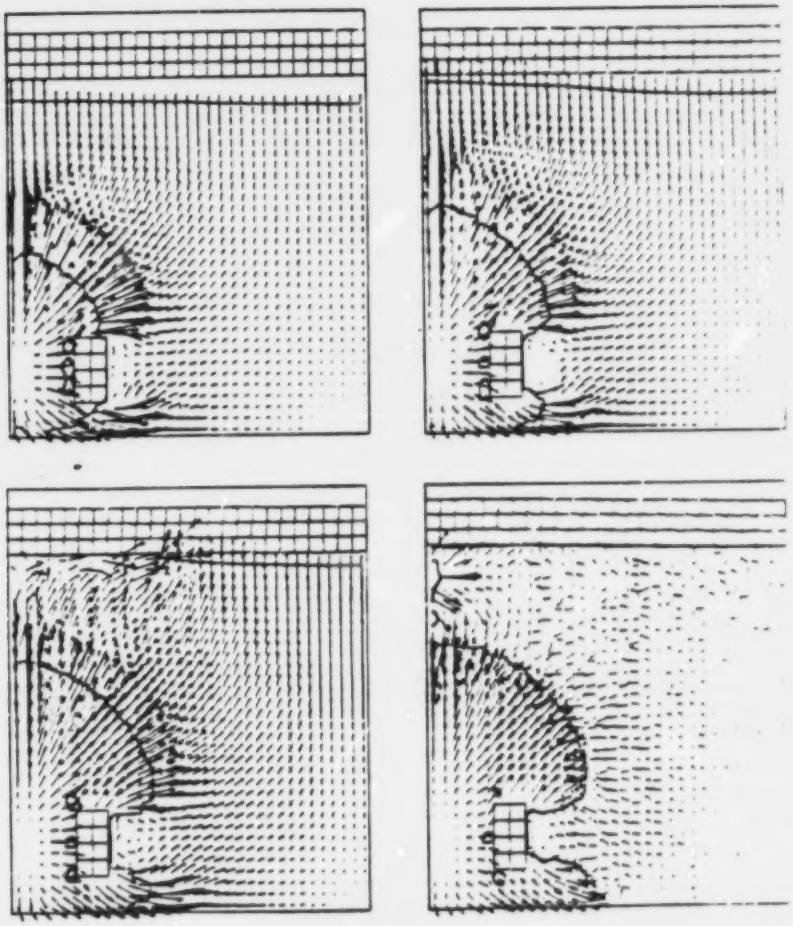

Figure 3.12 Simulated HCDA Transient Using PISCES

3.5.3 Summary

Computer models using point-by-point integration of the equations of motion for a fluid or solid can potentially provide a vast array of information about the events following pressure tube rupture. This is evidenced in the detailed velocity and deformations shown for example in Figures 3.11 and 3.12.

The limitations of these and other programs developed to date lie in their inability to handle realistic initial transients (except by incurring enormous costs), and in their inability to adequately handle the non-equilibrium aspect of decompression and phase change. While simple sub-routines can be added (such as the type used by Henry for condensation), no further confidence can really be attributed to the results. Further work on incorporating non-equilibrium two-phase effects with PISCES is currently underway, but awaits publication or commercial availability.

4.0 SUPPLEMENTARY INVESTIGATIONS

4.1 INTRODUCTION

In previously reported experimental investigations directly related to pressure tube rupture in pressure tube reactors, measurements were primarily concerned with pressure loading of the calandria vessel and adjacent tubes. Though some visualization data are available on crack propagation and decompression of pressurized hot water in tubes, these pertain to discharge into air; no experimental visualization data have been found on the bursting behavior of tubes submerged in water.

Directly related analytical investigations to date used simplified models exclusively. Due to the limitations of these models (such as assumptions of spherical symmetry and, in some cases absence of shock propagation), complete and detailed delineation of the complex pressure pulses resulting from the interacting physical processes is not feasible. To supplement previous investigations, exploratory experimental simulations and computer simulations of pressure tube rupture in both the central and peripheral positions of the calandria vessel were performed, with the objectives of gaining additional information on the dynamics of the processes.

The experimental simulation was carried out in the Department of Mechanical Engineering at the University of British Columbia. The computer simulations were performed by Physics International Scientific Codes and Engineering Services of California, using the computer code PISCES.

4.2 EXPERIMENTAL SIMULATION OF PRESSURE TUBE RUPTURE

To improve understanding of the physical processes which occur immediately after the initiation of an axial split, a simple visualization study using high speed photography was performed.

4.2.1 Experimental Set-up and Procedure

The explosion tube used was aluminum, 30.8 mm outside diameter and 1.25 mm wall thickness. A flat surface 360 mm long was milled by N/C machine to give a minimum wall thickness of 0.102 mm, which would allow the tube to burst at an internal pressure of 1.72 ± 0.14 MPa.

Figure 4.1 shows a schematic diagram of the experimental set-up. The explosion tube burst inside an open, transparent circular tank. At the start of the experiment, air in the loop was purged by repeated venting and filling with the coolant. After the coolant completely filled the system, it was heated to the desired temperature while being circulated and pressurized to slightly under the bursting pressure of the explosion tube. The explosion tube was then isolated from the rest of the loop by closing the inlet solenoid valve; then the coolant in the reservoir (accumulator) was overpressurized to produce a coolant pressure above 1.72 MPa at rupture. When the high speed movie camera accelerated the film to the selected speed, it triggered the inlet solenoid valve to open and initiate the rupture of the explosion tube. The film speed used was 3000-4000 frames/second.

4.2.2 Variation of Experimental Conditions

While keeping the moderator pressure, coolant pressure and defect thickness constant, selected experimental conditions were varied, as shown in Table 4.1, to test the difference with liquid or air outside the tube and liquid or gas as explosion fluid.

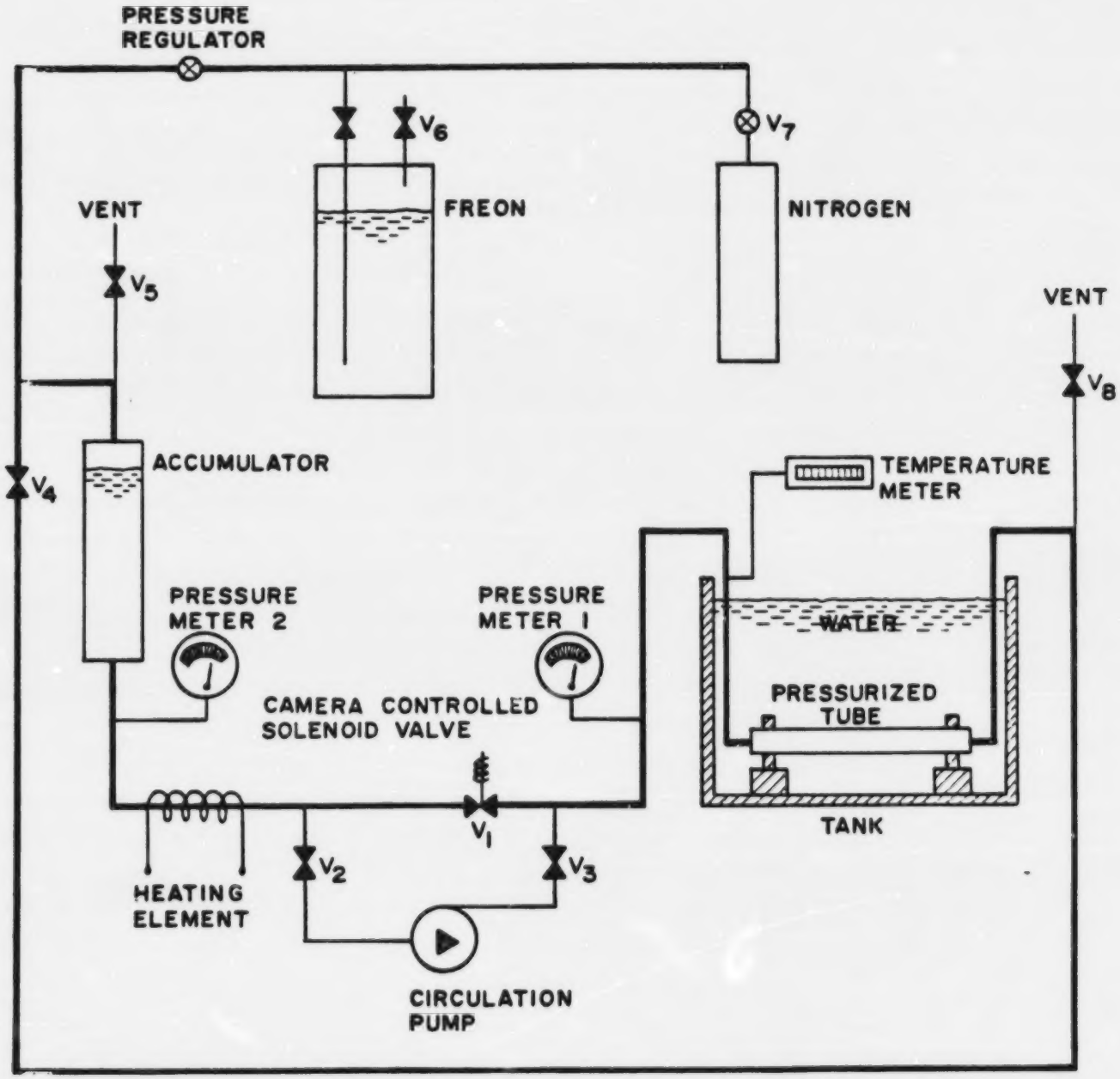

Figure 4.1 Simulation Loop Schematic

Table 4.1 Experimental Conditions

Run	Coolant	Temperature	Moderator	Temperature
1	N_2 Gas	21°C	Air	21°C
2	N_2 Gas	21°C	Water	21°C
3	Freon 114	57°C	Water	21°C
4	Freon 114	65°C	Water	40°C

These variations in experimental conditions permitted visualization of the effects of the moderator densities, phase change of Freon versus the single phase N_2 gas, and of increased coolant temperature. A silent colour movie was made from films recording the discharge patterns of the coolant under the four different sets of experimental conditions.

4.2.3 Results and Observations

In runs 1 and 2, where N_2 gas was used as coolant, explosions in water produced lower crack tip velocity and larger crack width than explosions in air; Freon at a higher temperature discharging into water in run 3 produced even lower crack velocity. An increase in Freon temperature in run 4 resulted in higher crack tip velocity and crack width, but still substantially below the values produced by N_2 gas explosions in runs 1 and 2. The final crack lengths in the four runs followed a similar trend; Table 4.2 gives the values of maximum crack width, crack lengths and average crack tip velocity for each run.

Table 4.2 Crack Opening and Crack Tip Velocity

Run	Maximum Crack Width, mm	Crack Length, mm	Average Crack Tip Velocity, m/s
1	60.0	360	300
2	12.0	360	240
3	0.2	215	53
4	1.0	360	115

Figure 4.2 shows the ruptured tubes from the four runs.

From the (slow-motion) movie, one can readily observe that the bubble formation and motion resulting from pressurization by N_2 gas are distinct from those produced by Freon. When N_2 gas was used, the bubble expanded and contracted repreatedly as it developed, whereas apparently continuous expansion was observed with Freon. Figure 4.3 shows traces of the bubble boundaries taken from selected frames of the films of runs 2 and 3; the time intervals from the initiation of rupture are the same in both runs.

As evidenced by the greater crack tip velocities, the bubble developments in N_2 gas explosions are faster than those in Freon explosions. Furthermore, the discharge patterns of the Freon in water was planar and mono-directional relative to the discharge patterns of N_2 gas, which were more globular.

Figure 4.4 shows photographs (taken with a strobe flash) of the vapour pockets in runs 2, 3 and 4. In the photo of N_2 gas discharging into water, the bright circular area over the centre portion of the explosion tube is not part of the vapour pocket, but reflection of lighting on the transparent tank wall.

RUN 1, NITROGEN INTO AIR

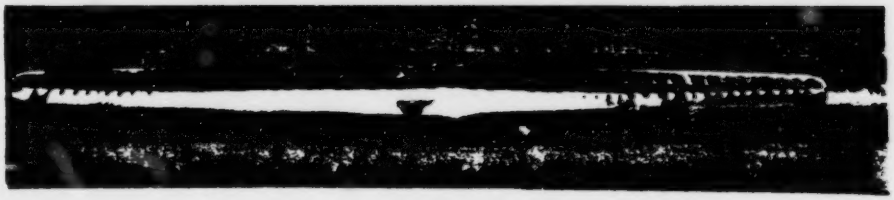

RUN 2, NITROGEN INTO WATER

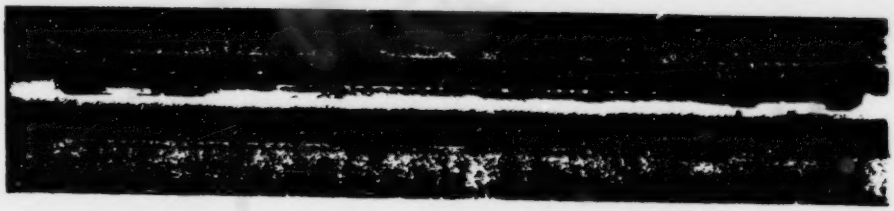

RUN 3, WARM FREON INTO WATER

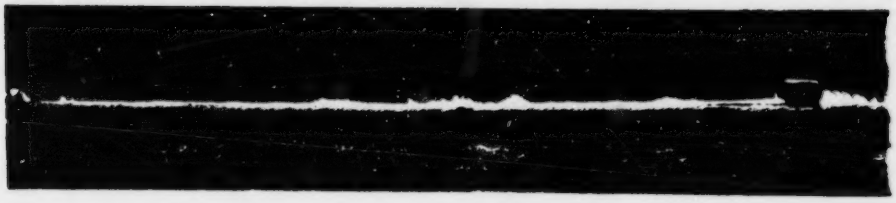

RUN 4, HOT FREON INTO WATER

Figure 4.2 Ruptured Tubes from Experimental Simulation

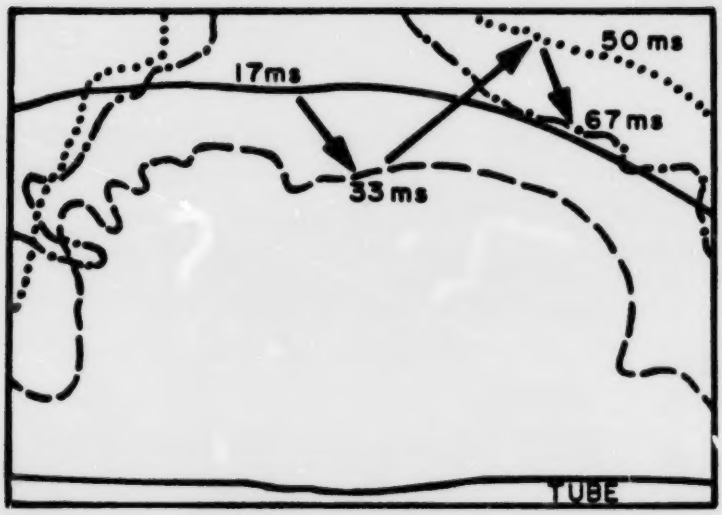

RUN 2 . NITROGEN
DISCHARGING INTO WATER

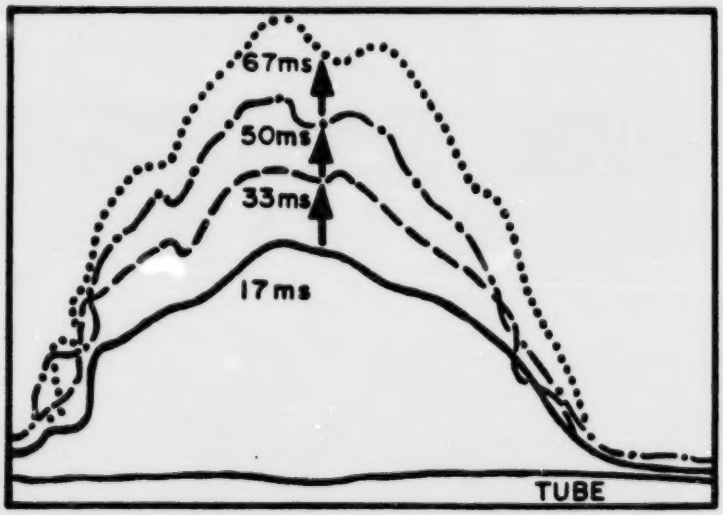

RUN 3 . WARM FREON
DISCHARGING INTO WATER

Figure 4.3 Bubble Boundary Motions from High-speed Movie

RUN 2,
NITROGEN INTO
WATER

RUN 3,
WARM FREON
INTO WATER

RUN 4,
HOT FREON INTO
WARM WATER

Figure 4.4 Snapshots of Vapour Pockets

4.2.4 Discussion

Surrounding Fluid

The different density of air and water when used as surrounding fluids caused lower crack tip velocity and smaller opening area in run 2 (water) than those in run 1, because more energy must be expended to overcome the inertia of the denser surrounding liquid as the lips of the fishmouth separated behind the crack tips. This reduction of explosive intensity illustrates the conservatism inherent in using results of measured crack propagation and burst opening measurements on tubes immersed in air rather than water.

Gas and Liquid Coolants

With the same initial conditions, gas coolant and subcooled liquid coolant explosions have very different characteristics, as shown by the results of run 2 and run 3. In the case of N_2 gas, the speed of sound (decompression wave) is close to that of the crack tip velocity and the crack tips are always driven by a volume of high pressure gas. In the case of liquid Freon the speed of sound is more than four times faster than that of N_2 gas, causing the driving pressure to drop to saturation pressure or lower and resulting in lower crack velocity, smaller opening area and planar discharge.

The expansions and contractions of the pulsating N_2 gas bubble have not been explained. They do not appear to be related to acoustic transmissions in the burst tube between the rupture site and the reservoir.

The observed differences in rupture process and bubble motion when comparing gas and liquid coolants as explosives suggest that pressure transients produced with such explosions in a closed vessel should not be identical (unless configurational factors dominate as in the Bettula tests, where the spring-like action of the gas plenums above the moderator and the vertical acceleration of the moderator slug determined the second pressure peak). In the case of horizontal pressure tube reactors which have no gas

caps, a simulation gas coolant would likely produce quite different bubble motion and pressure transients than a water coolant.

Liquid Coolant Temperature

The increase in explosive intensity of run 4 (compared with run 3) is mainly due to the initial Freon temperature increase from 57°C to 65°C. The 8°C increase corresponds to a 22% increase in saturation pressure. The effect of higher coolant temperature becomes more pronounced near the critical region, where the slope of the saturation line is much steeper. Figure 4.5 shows the regions of interest in pressure-temperature diagrams of Freon 114 and water. Also indicated are the decompressions to saturation pressure of the Freon coolant and water coolant in the experiments of Ross-Ross (1973) and Isles (1965).

The coolant discharge patterns are governed by the shape of the crack opening. The globular bubble from the N_2 gas explosion is the result of higher driving pressure and consequent wider crack width. For the subcooled Freon, a high coolant temperature would produce a more globular bubble; however, it is not likely that a symmetrical bubble centred at the original rupture site would be formed in an axial split. Since the side of the tube opposite to the split must accelerate the moderator next to it, it is conceivable that the pressure field is more spherical than the bubble, but this postulation awaits experimental confirmation.

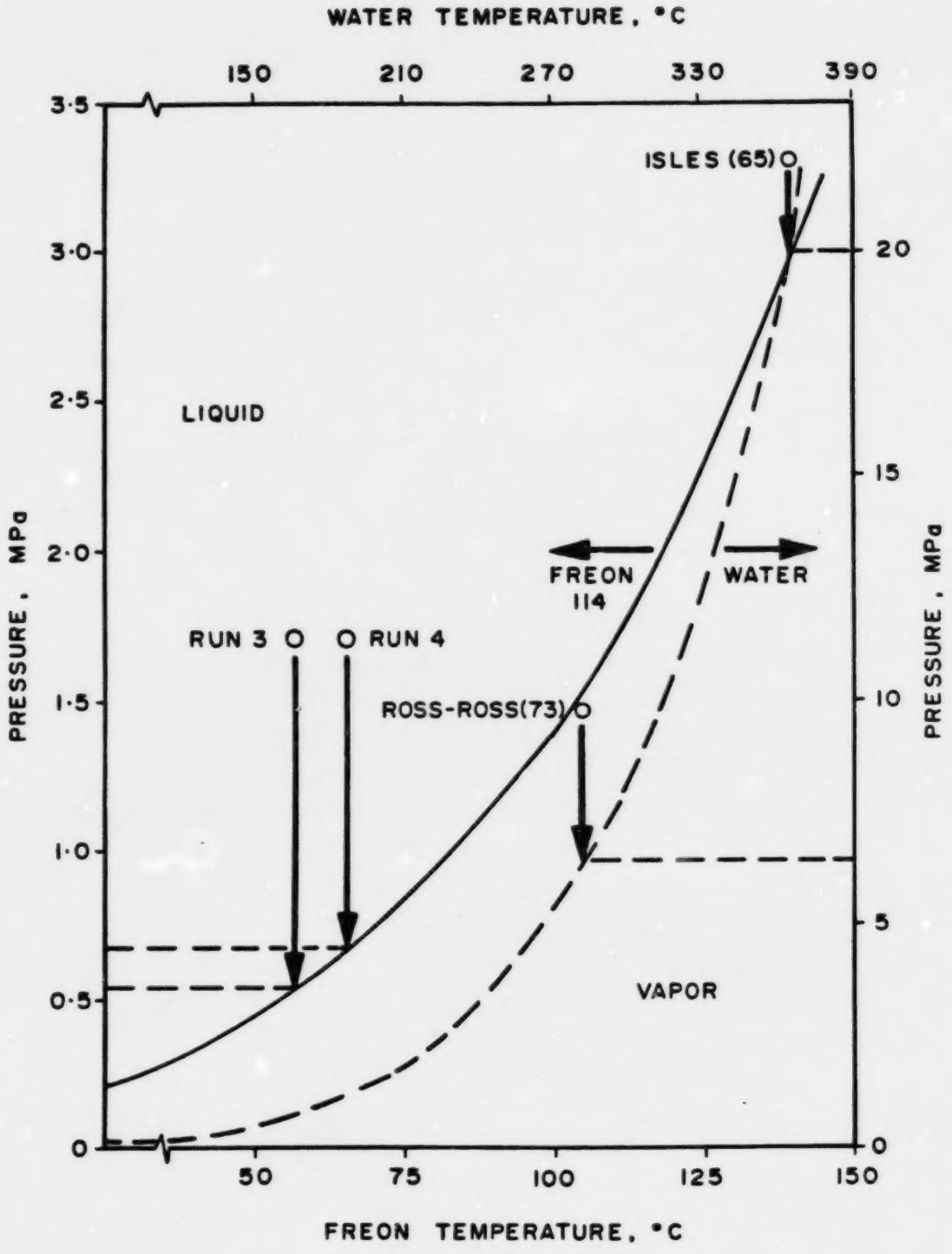

Figure 4.5 Saturation Pressures of Freon 114 and Water

4.3 COMPUTER SIMULATION OF PERIPHERAL PRESSURE TUBE RUPTURE

Previous analytical investigations have dealt exclusively with pressure tube rupture in the central position of the calandria vessel, while only one experimental investigation simulated peripheral pressure tube rupture. To examine the pressure transient resulting from a peripheral pressure tube rupture in a horizontal pressure tube reactor, a simple model (as shown in Figure 4.6) was constructed for computer simulation using PISCES.

4.3.1 Simulation Procedure and Boundary Conditions

The 20 x 50 grid was used to simulate half of the moderator as shown in Figure 4.7. Superimposed on its arc is the calandria vessel. Another 20 x 50 grid was used to represent the coolant and the moderator within 0.5 m radius around it. The states of the boundary nodes of this fine grid were mapped onto adjacent nodes of the coarser moderator grid during the computation by a procedure called rezoning. The fine grid enabled accurate simulation of the area around the decompressing coolant, while the coarser moderator grid allowed more economical computation.

The Lagrange Processor of the computer code PISCES was used to simulate the coolant and moderator and the SHELL Processor was used to simulate the calandria vessel. The two processors were coupled by the PISCES interface calculation technique called "blending" to simulate interactions between the moderator and vessel. A thermal equilibrium model was incorporated in calculation of the two-phase expansion of the coolant.

At time zero, the pressure tube was allowed to disappear and the coolant began to decompress. The length of the time steps were controlled by the computer program according to the magnitude of changes in the states of the variables. On the average, the time step was about 0.01 ms and the simulation proceeded for 10 ms.

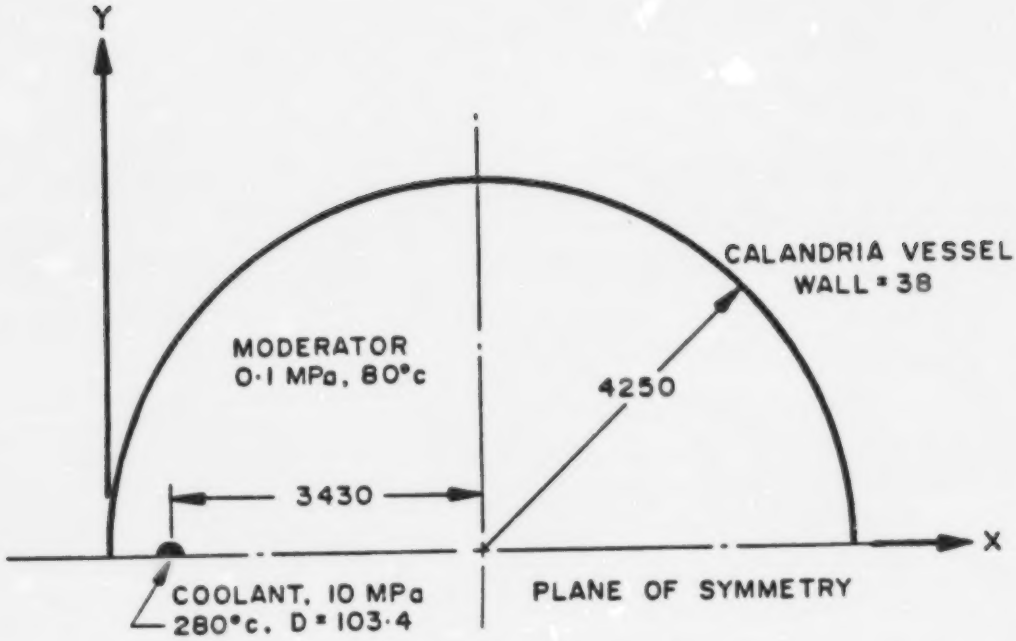

Figure 4.6 Peripheral Pressure Tube Rupture Model

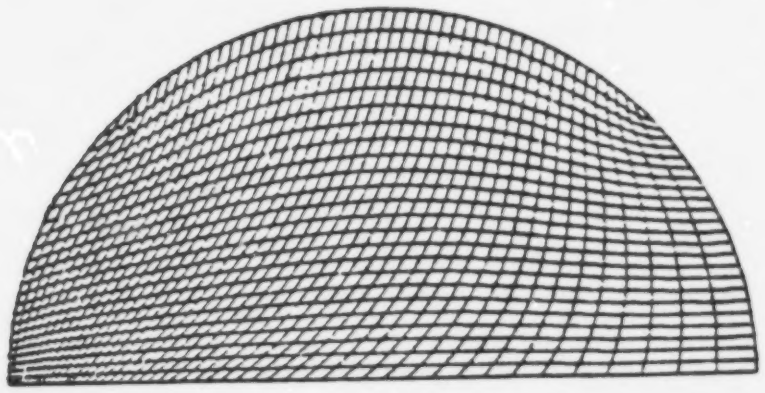

Figure 4.7 Moderator Grid for Peripheral Rupture

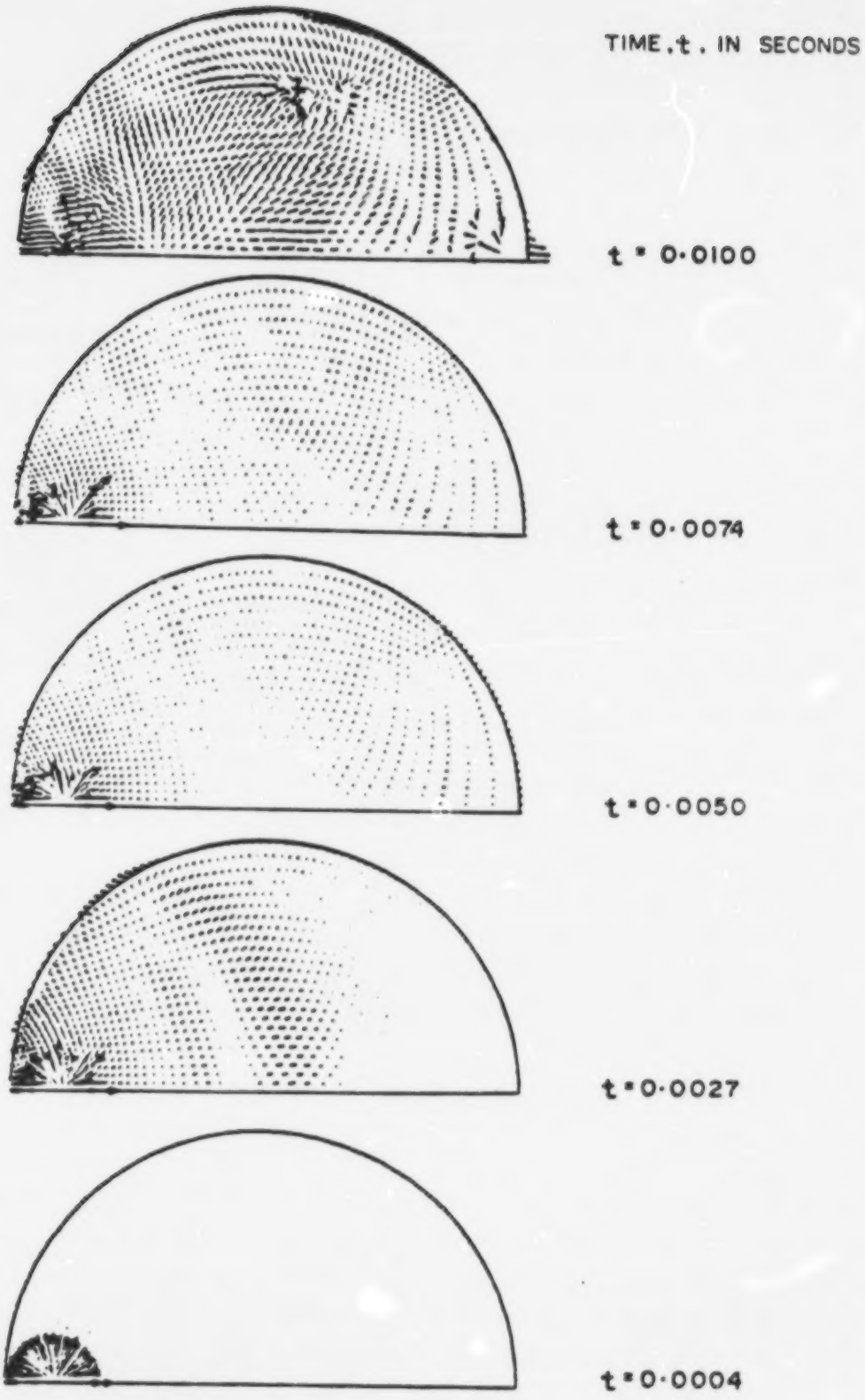

Figure 4.8 Velocity Vector Plots from Peripheral Rupture

The two-dimensional simulation implies finite coolant release, instantaneous rupture of pressure tube and infinitely long pressure tube and calandria vessel.

4.3.2 Hydrodynamic Transients Due to Peripheral Rupture

Figure 4.8 provides velocity vector plots at various time intervals. At 0.4 ms, the shock wave had already caused the moderator next to the boundary of the fine grid to start moving. At 2.7 ms, the original shock wave propagated almost half way across the vessel, while behind it a complex pattern was created by the reflections from the vessel and decompression of the coolant. The original shock wave reached the other end of the vessel at about 8 ms. As the process continued, the pattern became more and more complex as reflections from the entire vessel participated, creating patterns of substantial interference as illustrated by the velocity vector plot at 10 ms.

Figure 4.9 shows the pressure profile along the plane of symmetry at different times. The first profile at 0.4 ms shows two shocks travelling in opposite directions before either impacted the vessel. The next profile at 2.7 ms shows one of the shocks continuing its travel in its original direction, followed by the reflection of the other shock wave. At this stage, the peak shock strength decayed from 2.9 MPa to 0.64 MPa over a distance of 3.6 m. The pressurization due to vapour pocket expansion is evident in the profiles following.

Figure 4.10 shows the time histories of the pressure inside the pressure tube and at four other locations in the moderator where the pressure often drops below atmospheric. The coolant pressure dropped immediately to saturation pressure and was completely decompressed in 0.3 ms. At location B, which is a point on the vessel closest to the ruptured pressure pipe, the peak pressure due to the shock was about 2.6 MPa. The time histories at locations C, D and E show the successive arrivals of the original shock and its decay with distance. Following the shock is the vapour pocket bulk

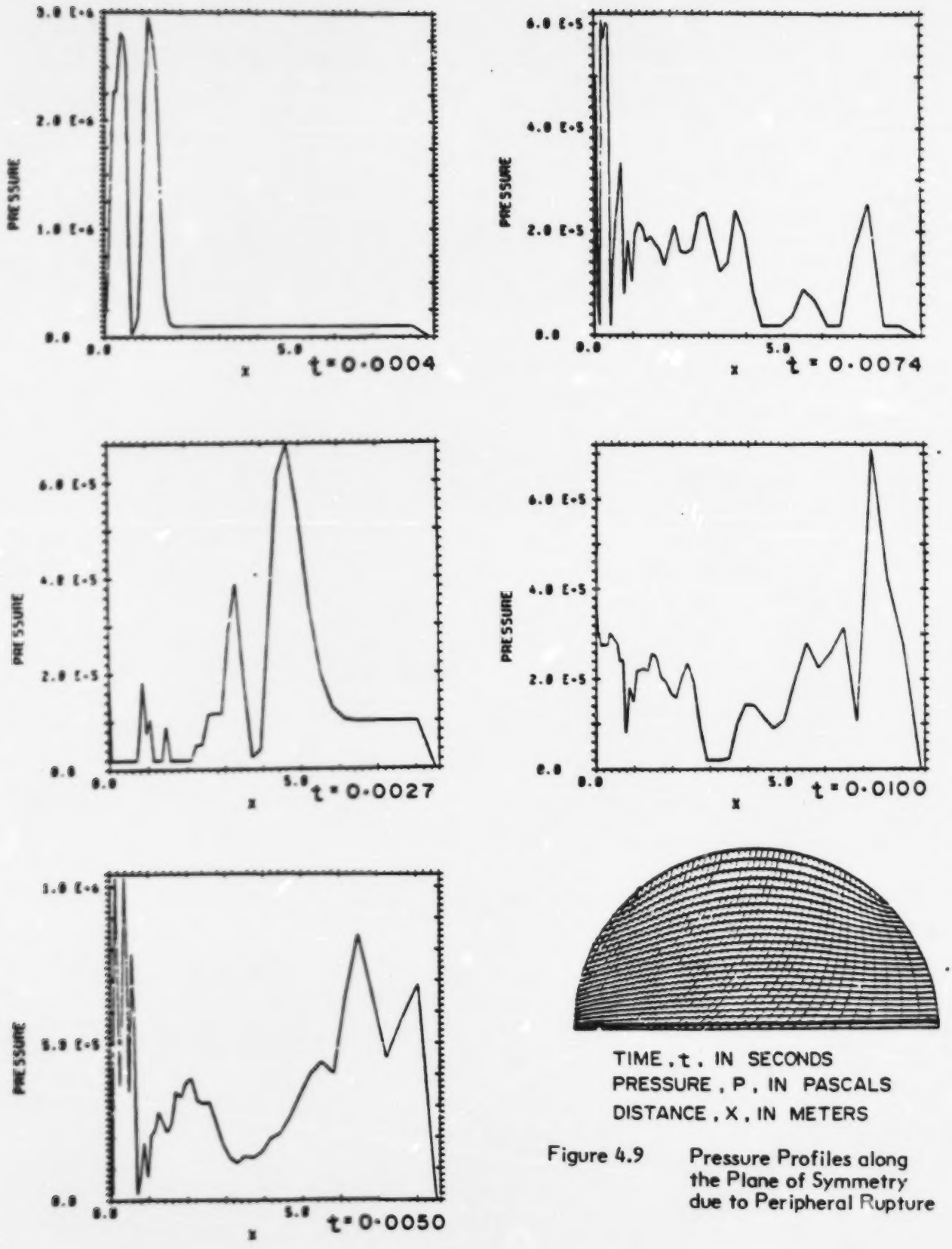

Figure 4.9 Pressure Profiles along the Plane of Symmetry due to Peripheral Rupture

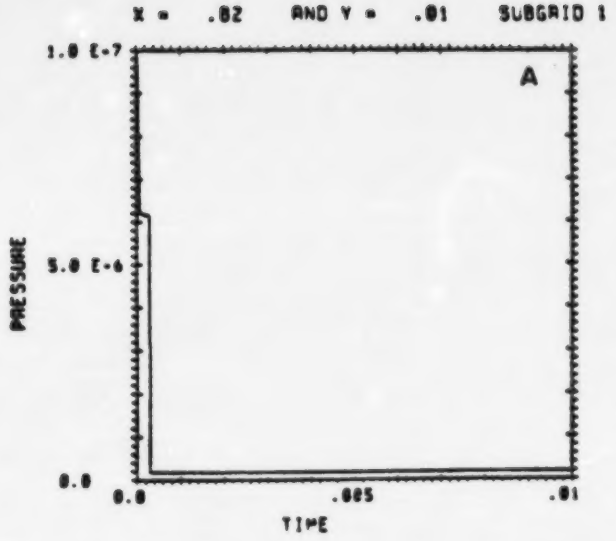

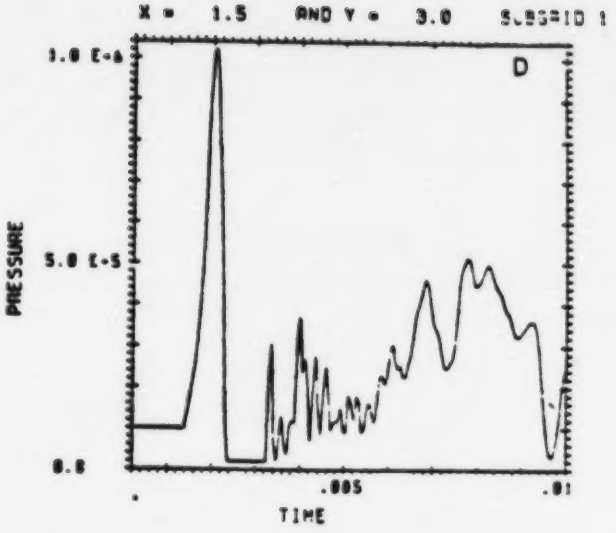

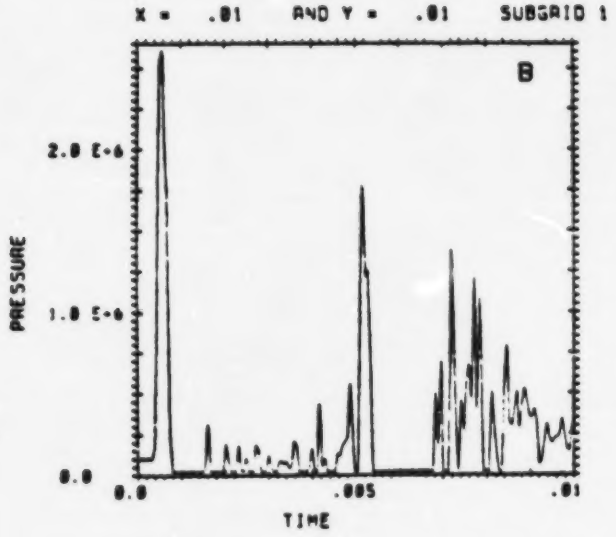

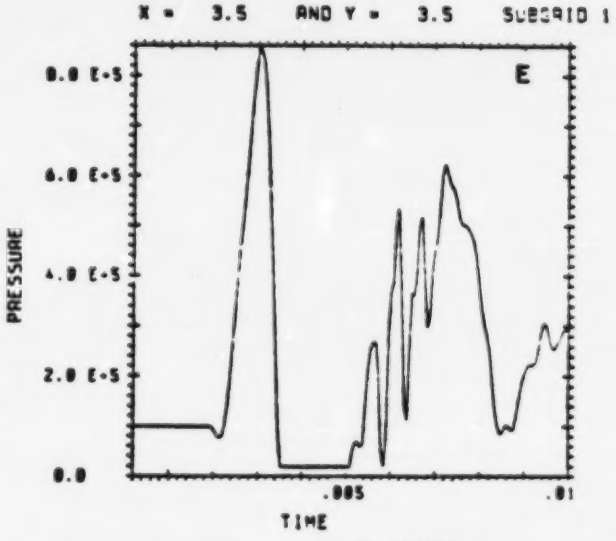

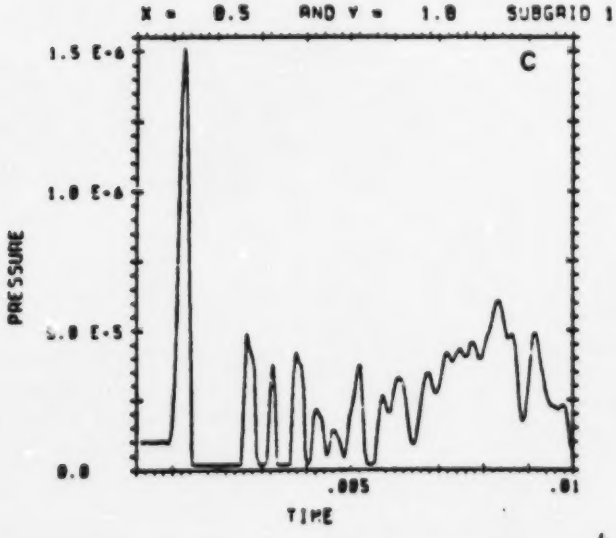

TIME, t, IN SECONDS
PRESSURE, P, IN PASCALS

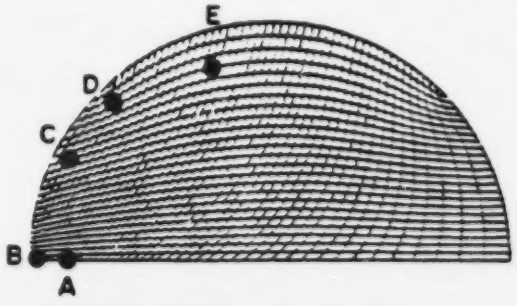

Figure 4.10 Pressure Histories due to Peripheral Rupture

pressu ation, with reflections superimposed. The time scales in this and other reduced computer plots are in seconds and pressure scales are in Pascals.

4.3.3 Loading of Calandria Vessel Due to Peripheral Rupture

Figure 4.11 shows the time histories of strain at four points on the calandria vessel. Despite the complex moderator motion, the responses of the vessel to shock and bulk pressurization are discernible. As evident in the pressure histories in Figure 4.10, the impulse due to the bulk pressurization is typically greater than that due to the shock. The strain histories reflect this difference in impulse. The maximum strain of 2.4×10^{-4} on the vessel occurred at about 8 ms after the rupture of the pressure tube at the point closest to the coolant. This maximum strain corresponds to a maximum stress of 46.8 MPa, a value well within the elastic range of stainless steel.

4.3.4 Loading of Adjacent Tube Due to Peripheral Rupture

The time histories of the force acting on 0.001 m length of two shut-off-rod guide tubes for the first 2 ms are shown in Figure 4.12. The force was computed by adding the presure differential across the tube and the dynamic head according to the equation below.

$$F = D_{tube}\ (0.001)\ (P_{front} - P_{back} + \tfrac{1}{2} \rho v_y^2),$$

where P_{front} and P_{back} are pressures at the front and back of the tube, ρ is density, D_{tube} is tube diameter, v_y is fluid velocity in the coolant discharge direction y.

These computations were based on pressure gradients from the present model, with no calandria tube array. For the shut-off-rod guide tube 0.143 m directly above the rupture, negative forces in the y direction were experienced due to the complex reflections of pressure pulses. The tube 0.286 m away experienced a peak force of about 240 N/mm due to the shock

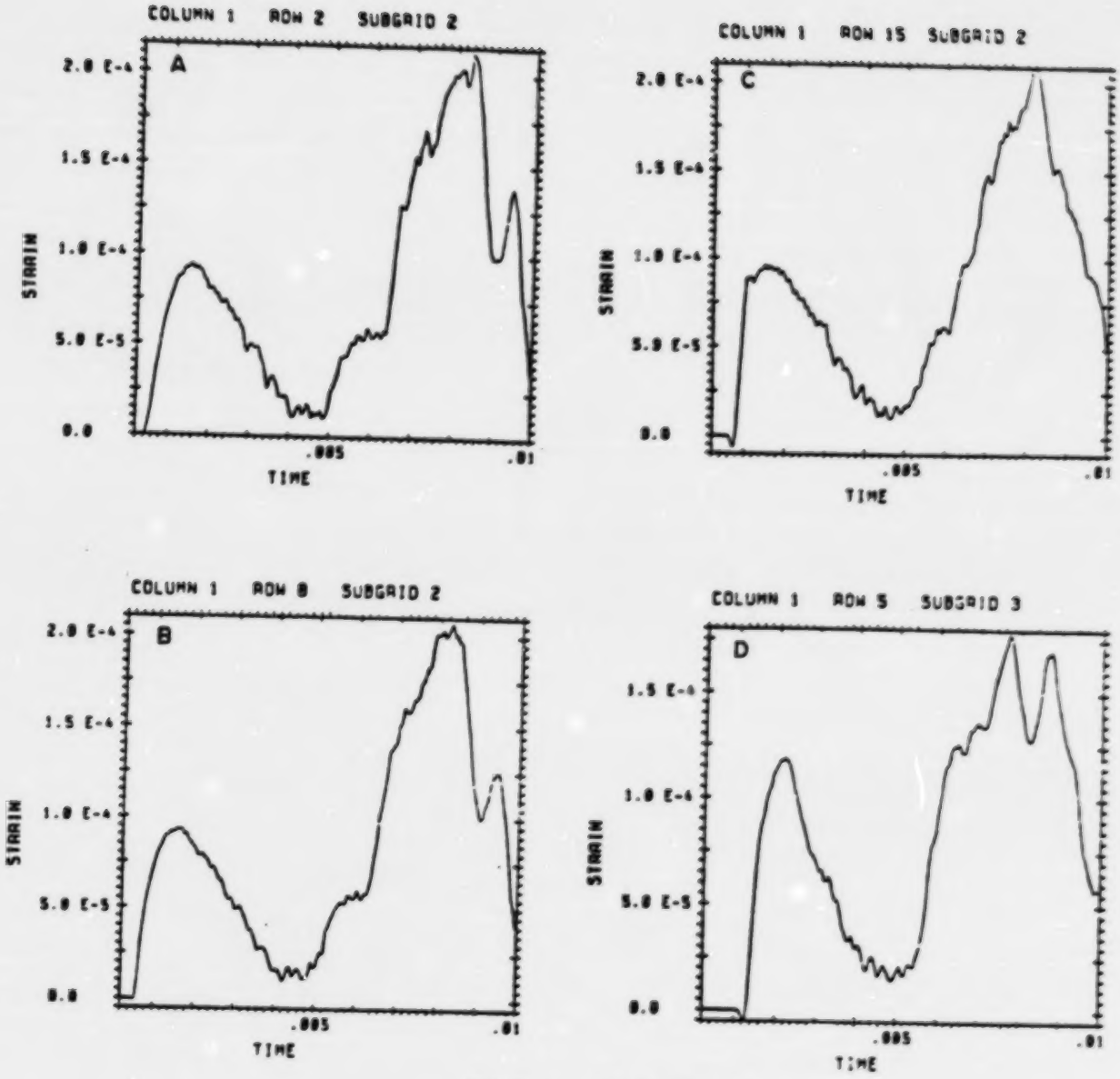

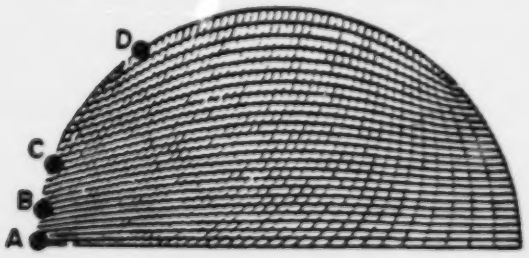

Figure 4.11 Vessel Strain Histories from Peripheral Rupture

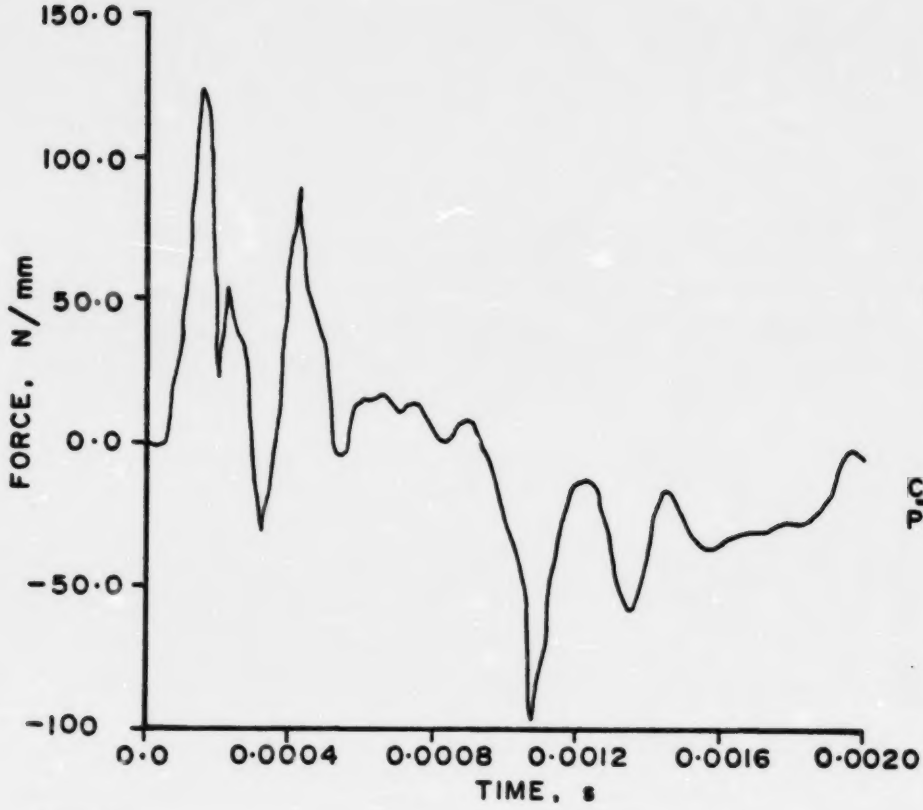

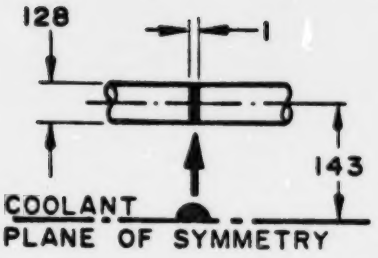

ALL DIMENSIONS IN mm

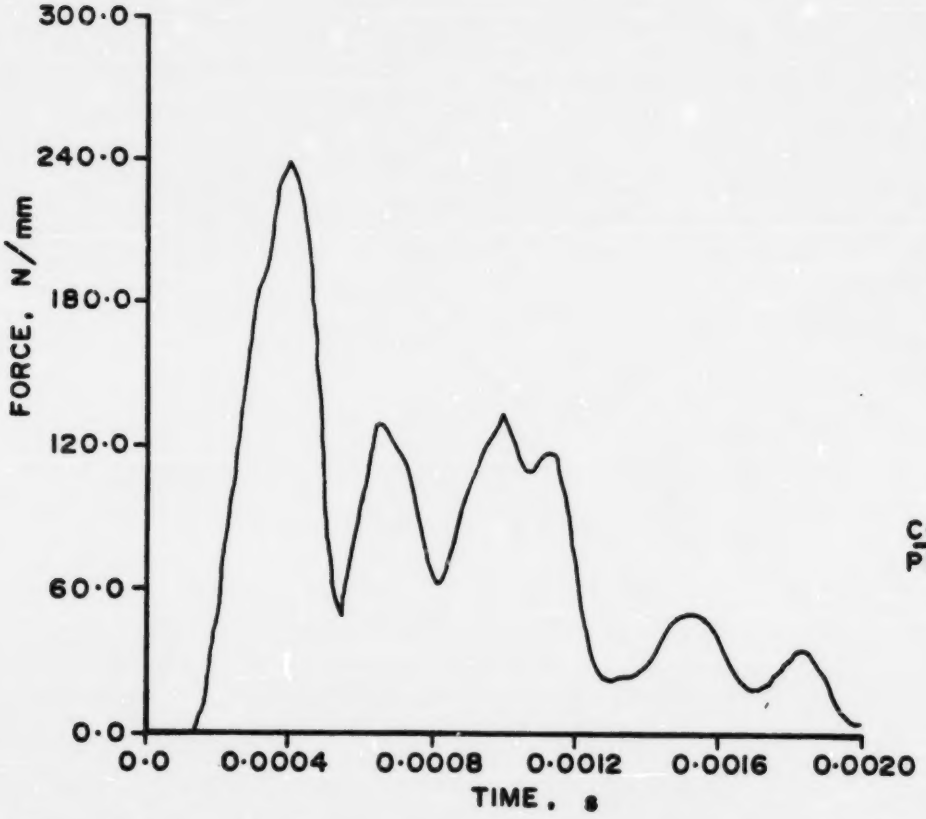

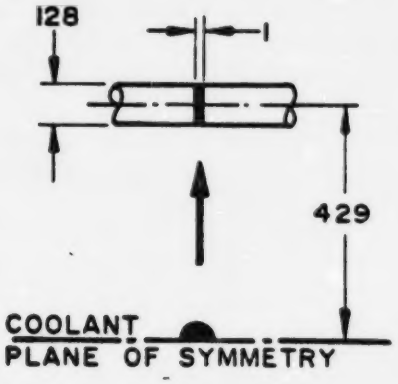

Figure 4.12 Forces on Adjacent Shut-off-Rod Guide Tubes due to Peripheral Rupture

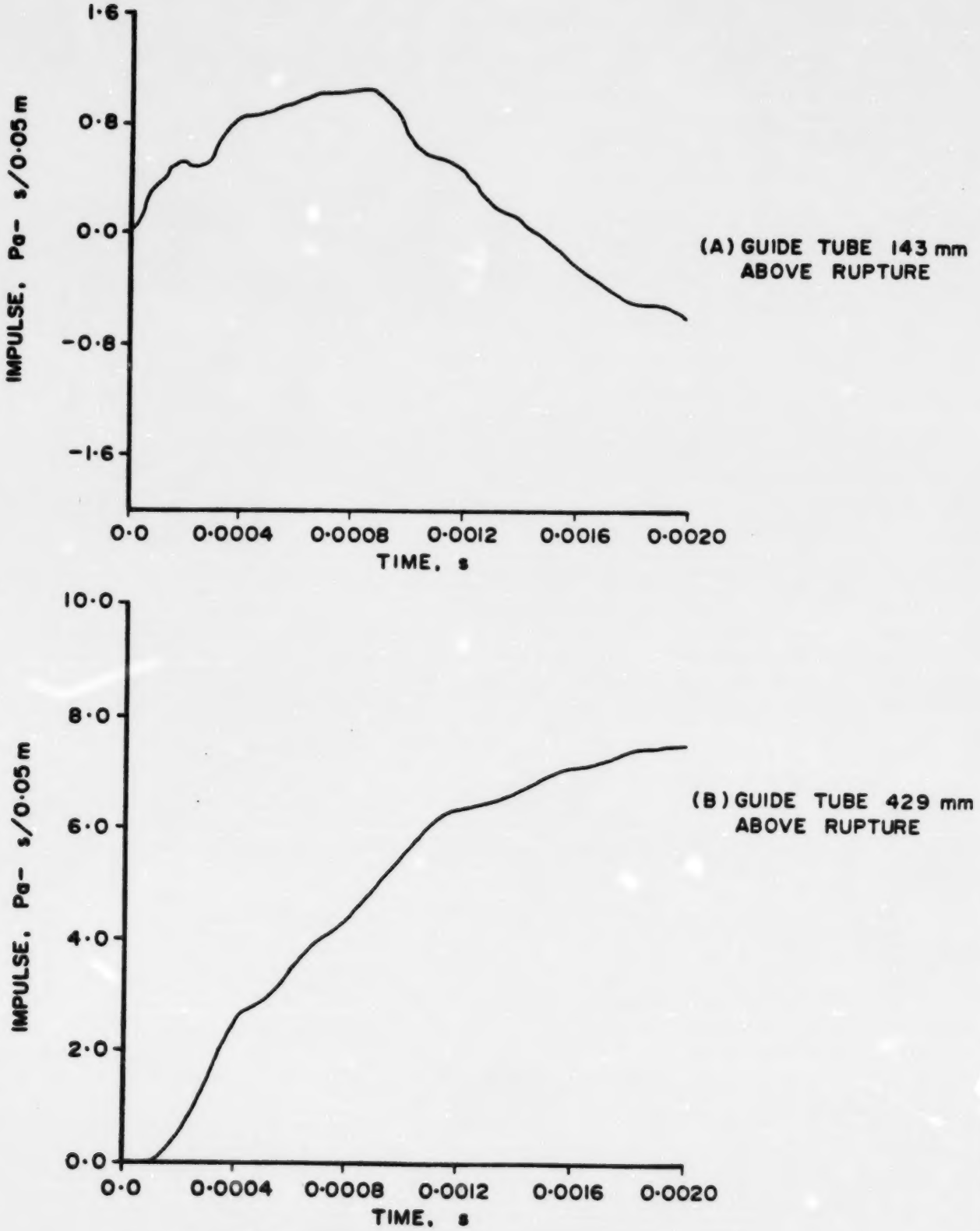

Figure 4.13 Impulses on Adjacent Shut-off-rod guide Tubes due to Peripheral Rupture

and a force of about 120 N/mm due to bulk pressurization. In both cases, the dominant contribution to loading is from the pressure differential which has a maximum value of 1.8 MPa, although the fluid velocity may reach 10 m/s at times. Figure 4.13 shows the corresponding impulses on a 0.05 m length of the adjacent shut-off-rod guide tubes as a function of time. As would be expected, the impulse due to the shock is small because of the short time interval during which it acted on the tube, although the back force is about twice as high as that due to bulk pressurization.

4.4 COMPUTER SIMULATION OF CENTRAL PRESSURE TUBE RUPTURE

The computation model used for simulation of a central rupture is shown in Figure 4.14. It represents one quadrant of the calandria vessel. The end shield is considered to be rigid, while the states of both the coolant and moderator are identical to those in the model for peripheral rupture. Only the central 3 m of the coolant inside the pressure tube was considered to participate in the instantaneous explosion corresponding to disappearance of the tube wall. The remaining portion of the central tube and the calandria tube array were not modelled.

The simulation procedure and boundary conditions were similar to those used in the case of peripheral rupture, except that the 40 x 49 grids were rectangular and that a cylindrical vessel of 6 m length was modelled.

4.4.1 Hydrodynamic Transients Due to Central Rupture

Figure 4.15 shows the rectangular grid used to model the moderator, and the velocity vector plots at various time intervals. Although the velocity fields are more orderly than those in the peripheral rupture case, the variation in velocity distribution next to calandria vessel wall (e.g. at 10 ms) indicates complex strain patterns.

Pressure histories of the coolant and of the moderator at four locations are shown in Figure 4.16. The distance from the axis of the vessel is the same for both location B and location C; the shock strengths experienced are 2.7 MPa and 1.66 MPa respectively. Comparison of pressure histories at locations D and E shows the complex superposition of reflections at the location E where the vessel joined the end shield. It is of interest to note that for a similar model, Henry calculated a peak pressure due to bulk pressurization of about 0.7 MPa on the calandria vessel at 10 ms after the rupture, whereas the pressure history at location D (the centre of the vessel in this simulation) has a corresponding peak pressure of about 0.5 MPa at about 8.5 ms. However, the pressure-time curves themselves differ significantly in shape due to the absence of shock waves and reflections in Henry's model.

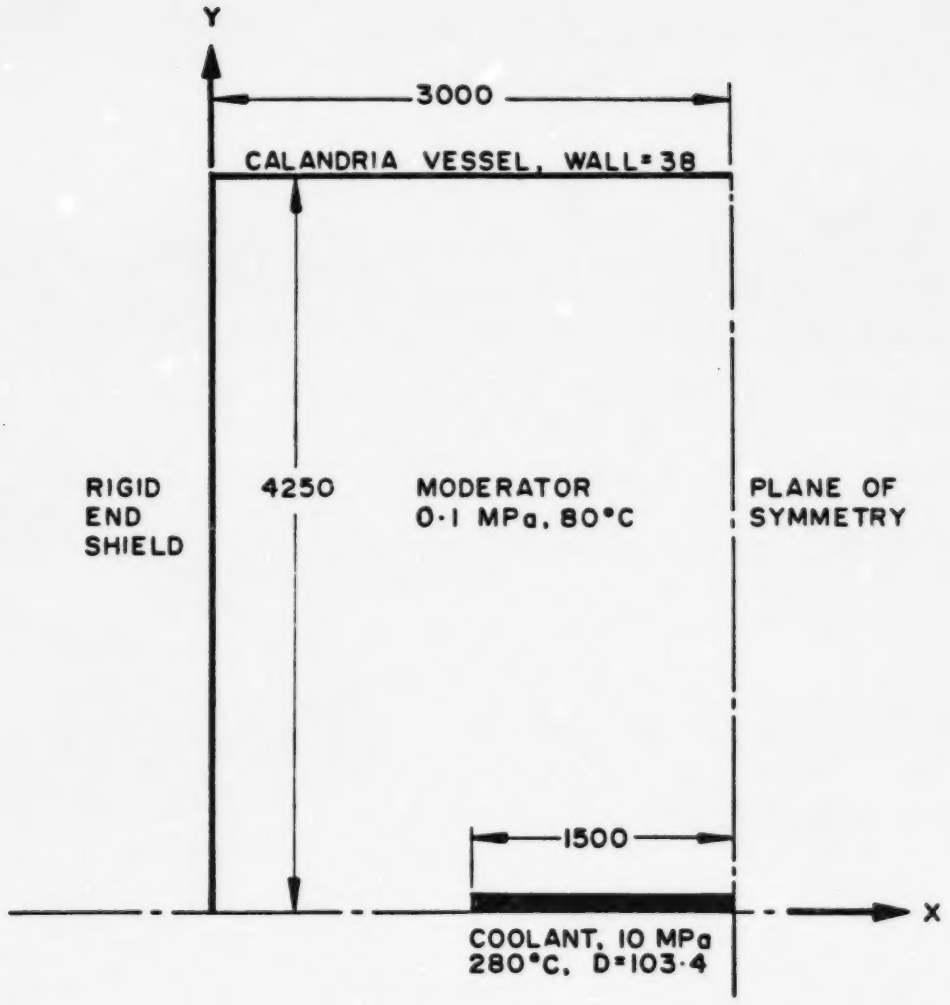

ALL DIMENSIONS IN mm

Figure 4.14 Central Pressure Tube Rupture Model

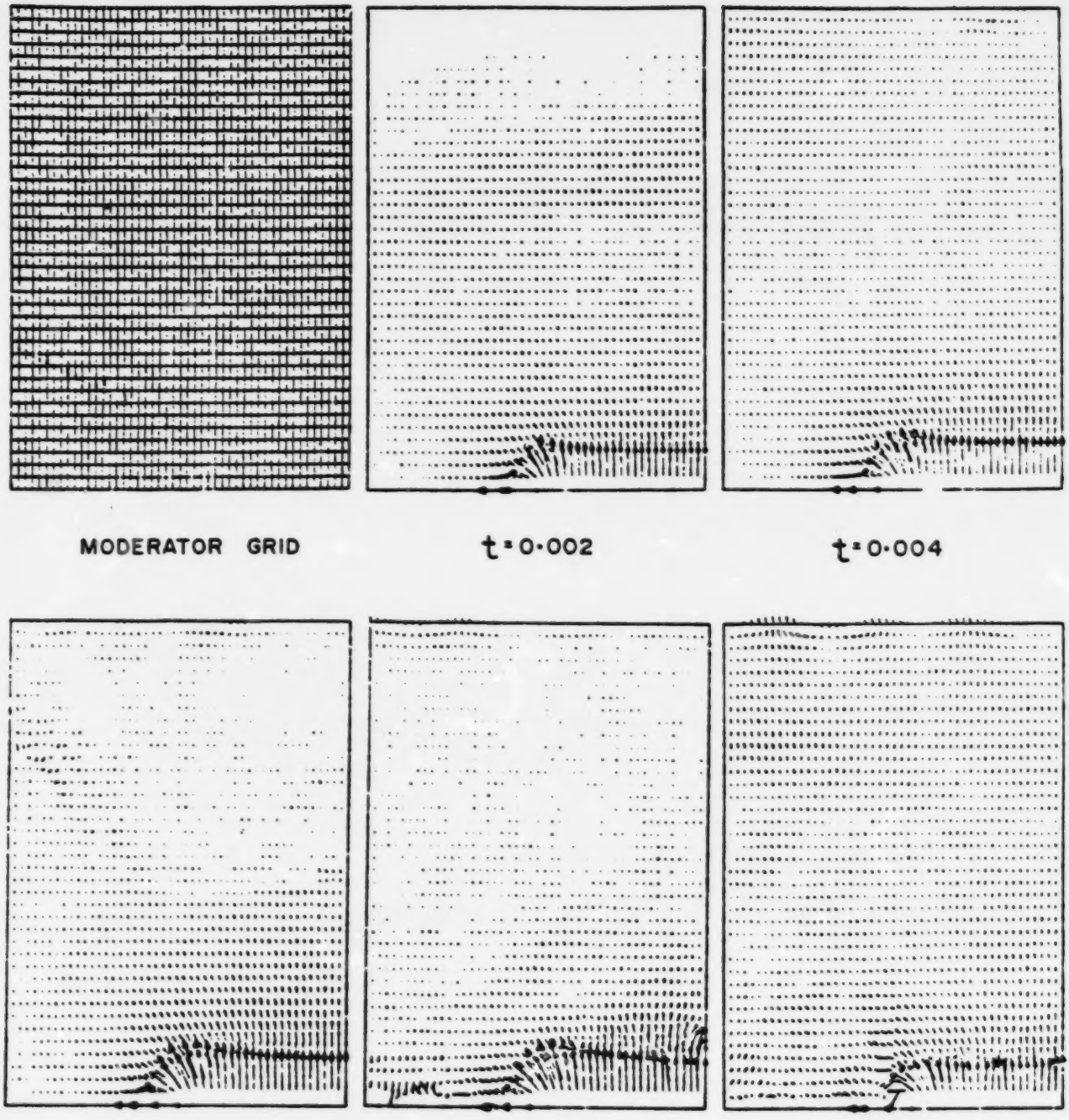

Figure 4.15 Velocity Vector Plots from Central Rupture

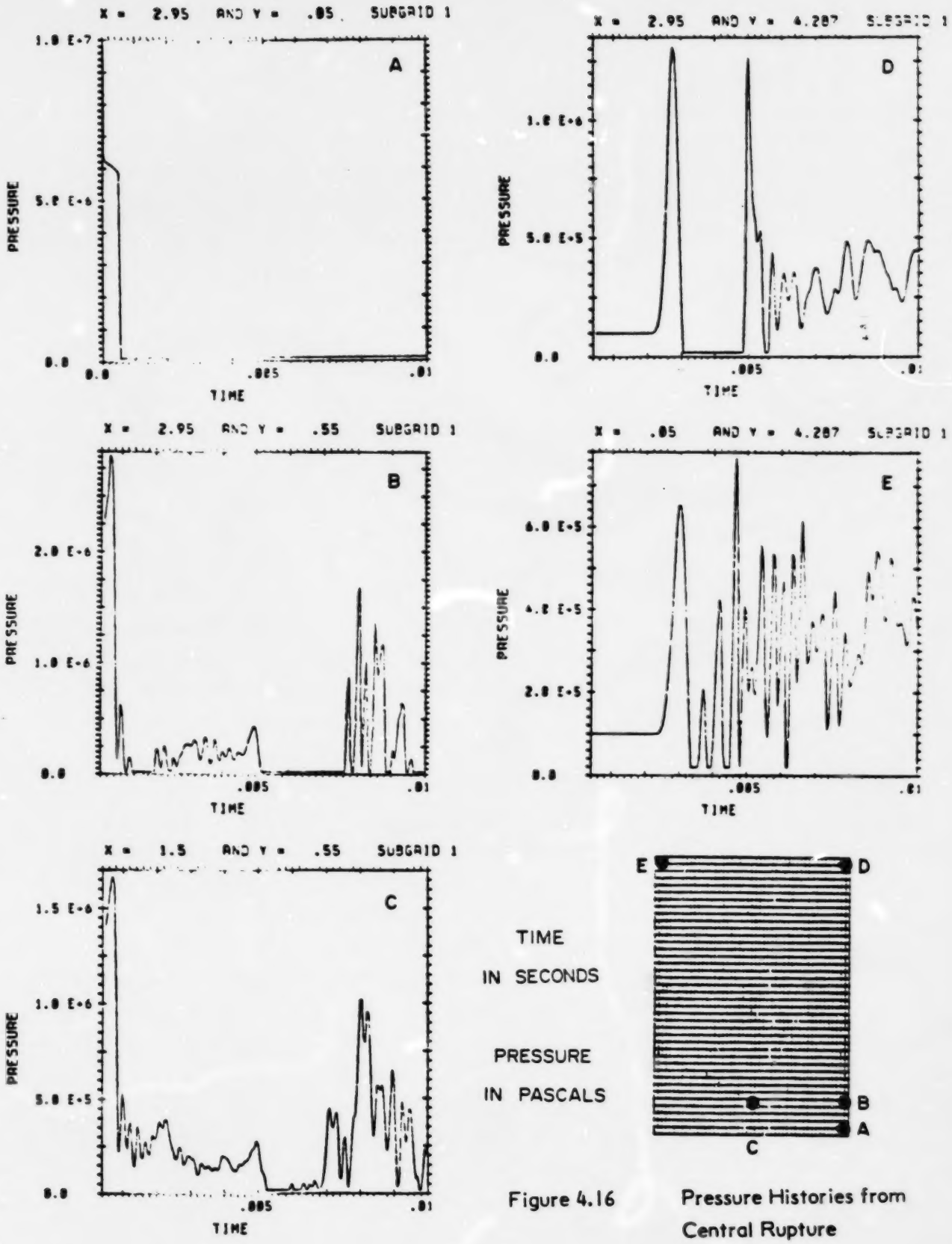

Figure 4.16 Pressure Histories from Central Rupture

4.4.2 Loading of Calandria Vessel Due to Central Rupture

Figure 4.17 shows the histories of longitudinal and tangential strains at the centre and the end of the calandria vessel. At the centre, the longitudinal strain is higher than the tangential strain and both strains are positive; whereas at the end of the vessel, the tangential strain is higher than the longitudinal strain, which is often negative. The maximum membrane strain of 1.9×10^{-4}, which occurred at the end of the calandria vessel, corresponds to a maximum membrane stress of 37 MPa. The maximum membrane stress is 46.8 MPa for the peripheral pressure tube rupture, 1.27 times that at the end of the vessel in the present model and 5.85 times that at the centre of the vessel.

4.4.3 Loading of Adjacent Tube Due to Central Rupture

The calculated force history for the first 2 ms on 1 mm of a pressure tube one lattice distance from the ruptured tube is shown in Figure 4.18. The peak force due to the shock is about 385 N/mm and that due to bulk pressurization is about 135 N/mm. Because the section of the pressure tube considered is almost at the centre of the calandria vessel, the force-time curve is quite orderly since reflections from the vessel wall had not arrived. The corresponding impulse history for the first 2 ms is shown in Figure 4.19.

The Betula II experiments indicated a peak force of about 100 N/mm and Henry predicted a peak force of 166 N/mm due to bulk pressurization for Betulla II operating conditions. The present simulation assumed a coolant pressure of 10 MPa and the Betulla II coolant was at about 6 MPa, but the size of the pressure tube, the lattice distance and coolant temperatures are almost identical. Since the 280°C coolant temperature in both cases determines the saturation pressure to which the coolant must compress, it is expected that the peak forces due to bulk pressurization will be in the same order of magnitude and indeed they are.

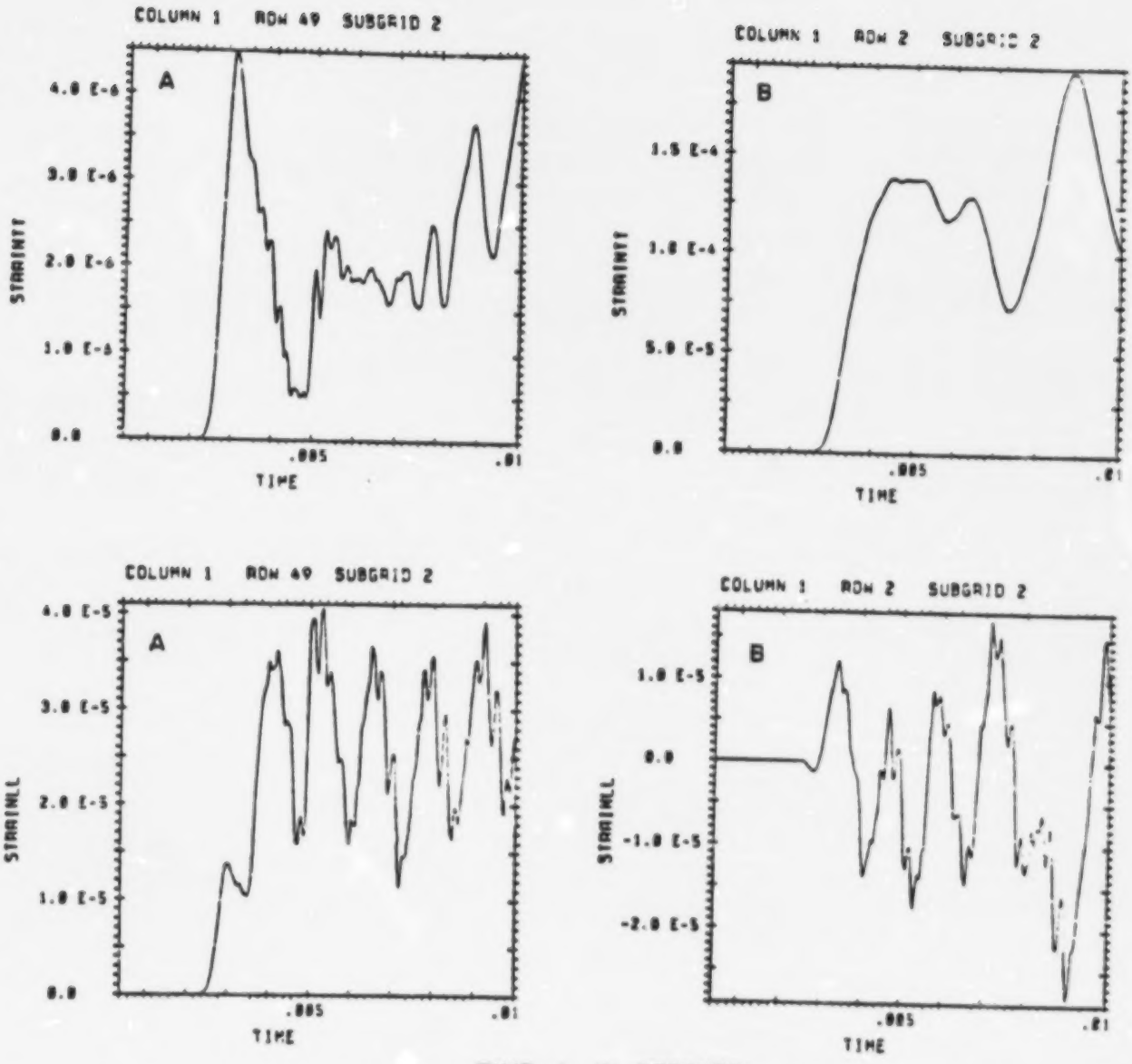

Figure 4.17 Vessel Strain Histories from Central Rupture

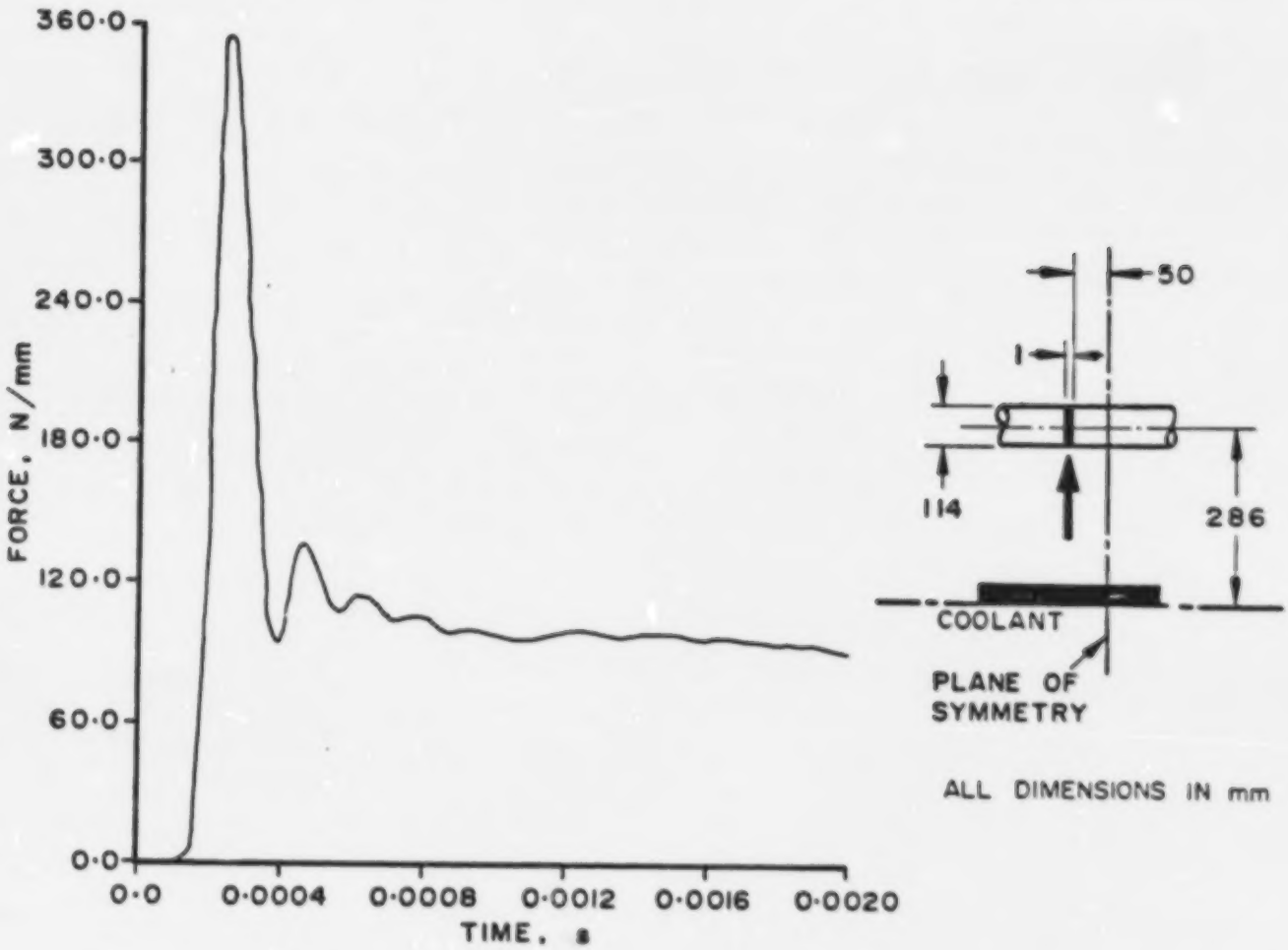

Figure 4.18 Force on Adjacent Pressure Tube due to Central Rupture

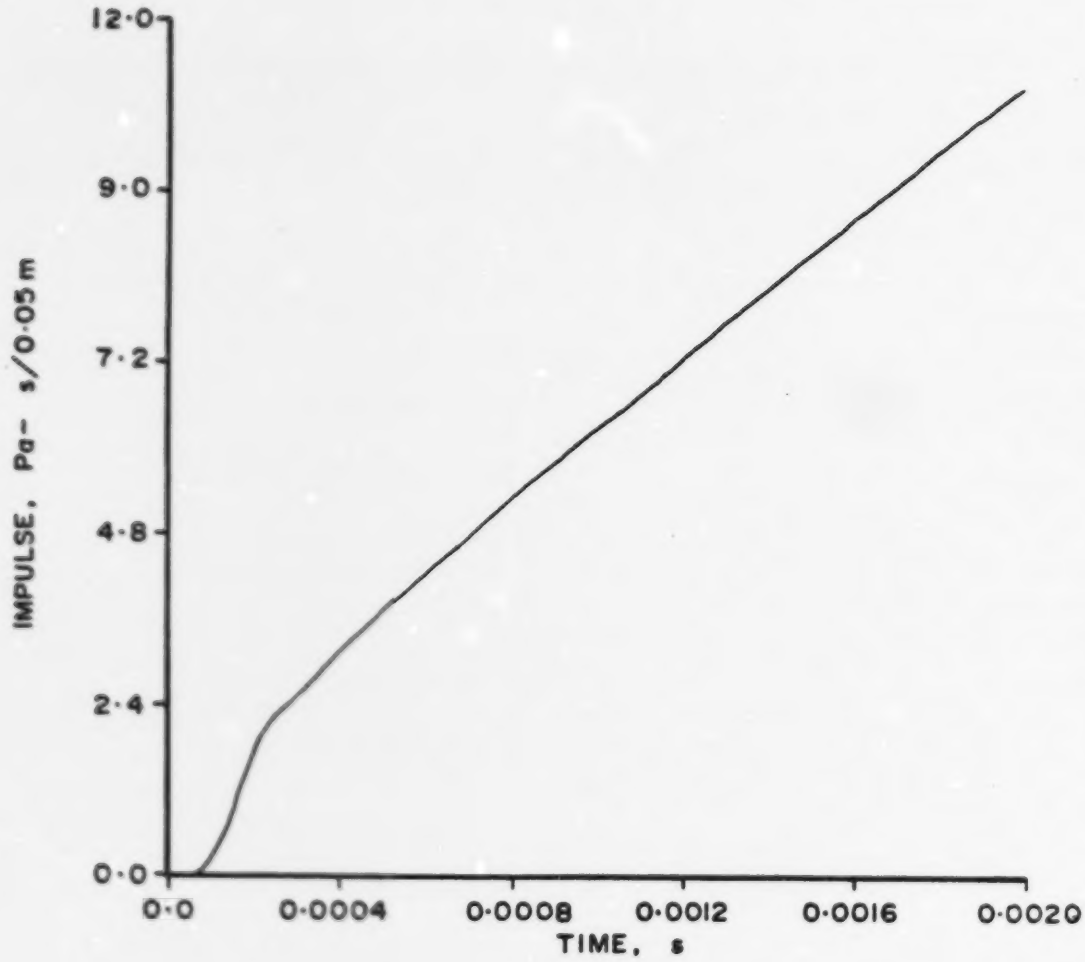

Figure 4.19 Impulse on Adjacent Pressure Tube due to Central Rupture

4.5 SUMMARY

4.5.1 Qualitative Conclusions from Experimental Simulations

Although the simple experimental simulations were not intended to yield definite quantitative results, some conclusions may be drawn concerning the effects of different coolants, moderators and coolant temperatures on axial crack propagation and discharge patterns.

(1) Dense surrounding fluids offer high resistance to the opening of the "fish mouth" of the crack and cause lower pressure transient intensity than moderators with lower density.

(2) The discharge pattern of the coolant into the moderator is determined by the width and length of the crack opening.

(3) Gaseous coolant produces faster crack propagation and a more globular bubble than liquid coolant at the same pressure and temperature; this may be explained by the higher speed of sound in liquid and its faster decompression to saturation pressure inside the tube.

(4) For sub-cooled liquid coolant. its temperature has a dominant influence on the intensity of the bulk pressurization of the moderator.

(5) A symmetrical bubble surrounding an axial rupture site is unlikely.

4.5.2 Results from Computer Simulations and Observations

Given the assumed configurations and boundary conditions in the models for computer simulations of peripheral and central pressure tube ruptures, the following observations may be made.

(1) Fluid-structure interactions such as shock and fluid particle reflections from surfaces and their superposition greatly influence the transient pressure distribution and fluid motion due to pressure tube rupture.

(2) The shock strength is dependent on the initial coolant pressure while the bulk pressurization intensity is dependent on the initial coolant temperature.

(3) Bulk pressurization contributes dominantly to the impulse on the calandria vessel, although the peak pressure due to the shock may be as high as 2.6 MPa, 3-4 times that due to bulk pressurization.

(4) The maximum membrane stress on the calandria vessel calculated by the simulation of peripheral rupture is 46.8 MPa and that for central rupture is 37 MPa, both well within the elastic range of the stainless steel.

(5) Different parts of the calandria vessel underwent different strain histories in both the central rupture and peripheral rupture simulations.

(6) The force on an adjacent tube is predominantly due to pressure differential across the tube, which reached 2.7 MPa across an adjacent pressure tube at one small section in the central rupture simulation, and that due to the impacting fluid reached only 0.1 MPa, though its velocity reached 14 m/s.

(7) For the central instantaneous rupture of 3000 mm of pressure tube with coolant at 280°C, the predicted peak forces on the adjacent pressure tube due to bulk pressurization from Henry's simplified models and the present simulation are 166 N/mm and 135 N/mm of tube length, respectively. These values are in general agreement with the 100 N/mm measured in the Bettula II experiments.

(8) Negative impulses experienced by an adjacent shut-off-rod guide tube in the peripheral rupture simulation indicate that over the time of the transient, reflection from surfaces strongly influences the loading distribution along the tube.

5.0 CONCLUSIONS

5.1 INTRODUCTION

The following conclusions relate to possible consequences of pressure tube failure in reactors designed and operated according to current best practice. No attempt is made to define causes or probabilities of failure; the focus is on possible consequences and particularly on those consequences which could lead to failure of other components, and thereby to catastrophic failure of the reactor.

The term "possible consequences" refers to those effects which can be understood quantitatively with existing knowledge of physical laws and the properties of materials. Some of these effects have been demonstrated experimentally; others may be estimated by numerical simulation. It is not enough to be able to conceive of the consequence in question - what is needed is a quantitative assessment of its magnitude. In many cases of course exact simulation (either experimentally or analytically) is not possible. The best that can be done is to provide a reasonable upper limit estimate of the magnitude.

The basic question underlying these conclusions is whether further work is needed. The general conclusion is that further work is needed, not because of potential danger in present pressure-tube reactors, but simply to improve understanding of possible consequences of pressure tube failure. The point where further understanding is particularly needed is on possible damage to shut-off-rod guide tubes.

5.2 MODES OF BURSTING

Since we have no experimental data on the spontaneous propagation of cracks in unweakened tubes (bursting in simulated calandria vessels) such failures are not subject to exact simulation.

We cannot be sure that artificially weakened tubes will open at the same rate or to the same width on bursting as tubes with natural flaws, or tubes overheated because of a flow blockage. We can, however, use numerical modelling of pressure tube bursting to test the importance of burst opening rate and extent. So far calculations have been done only for the limiting case of instantaneous opening.

There appear to be important physical reasons why the instantaneous opening assumptions will lead to a considerable over-estimate of the bursting pressure pulse. Calculations so far indicate that even this worst case provides impulsive loading of adjacent pressure tubes and the calandria vessel which is well within elastic stress limits.

We cannot say the same for the shut-off-rod guide tubes (see Section 5.5). The pressure pulses which would be generated by instantaneous tube burst could possibly crush several shut-off-rod guide tubes. For this reason more information is needed on actual burst opening rate, as well as extent.

Generally, long axial flaws or breaks are more dangerous than circumferential ones in that more fluid can be discharged in the first few milliseconds from the burst area. Experiments show that pulse amplitudes depend strongly on burst area. Circumferential breaks could conceivably cause serious damage due to expulsion of fuel bundles as missiles. Fuel bundle momentum could be much larger with rifling acceleration in the tube up to a circumferential (guillotine) break, with the open ends somewhat displaced from each other, than with lateral acceleration through a burst opening on one side of an unbroken tube.

Since, however, little experimental evidence has appeared on simulated reactor tests of serious damage of adjacent pressure tubes or tube sheets, due to missiles. The long axial break has been considered the most serious and received the most study.

Experimental studies of crack propagation in pressurized tubes (surrounded by air) show that typical crack speeds are lower than the speed of sound in pressurized hot water. This could mean sufficiently rapid depressurization ahead of the crack that the lateral pressure gradient necessary to continue the crack opening would almost disappear and the crack growth would be arrested. This behavior has been observed in pressure tube tests in one instance. However present evidence shows that the rate of crack growth and the burst area configuration depend strongly on the bursting medium (hot liquid, gas, or steam) and on whether the bursting tube is surrounded by liquid or gas as well as on the properties of the tube itself.

Further understanding of the tube bursting process requires detailed visual study of the first few milliseconds of the bursting process with full scale Zr-2 tubing and with realistic coolant and moderator conditions, as well as with a variety of burst inducement mechanisms.

In summary, the results of numerical simulation of the tube bursting may considerably overestimate the magnitude of the subsequent pressure pulse. This is not of serious concern in considering the effect of the pulse on an adjacent pressure tube or on the calandria vessel, but it may be quite important in considering the ability of a number of shut-off-rod guide tubes to resist the crushing effect of the pressure pulse. More, therefore, needs to be known about the manner, the rate and the extent of tubing opening with actual coolant and moderator conditions.

5.3 PRESSURE PULSE DEVELOPMENT

The initial shock wave must necessarily be considered weak, i.e. one which propagates at very nearly the acoustic speed of the moderator liquid. The magnitude of the peak pressure due to the wave and the impulse imparted by it to tubes adjacent to the burst appear to be small, but this may be in part because in experiments conducted to date the instrumentation did not respond quickly enough to register a sharp spike in pressure. The question of how large the maximum pressure and the impulse are cannot be fully answered until the details of the burst opening transient (see Section 5.2) are clarified by adequate experimental or numerical studies.

For the type of reactor with a large gas plenum on top, there is abundant evidence of the pressure pulse associated with pressurization of moderator by forcing high pressure coolant into it. The magnitude of this pulse has been shown to be strongly dependent on vessel flexibility (since the cool moderator liquid is not very elastic) and thus on whether a gas cap is or is not present. Data are not available on pressure pulses resulting from tube burst in modern horizontal axis pressure tube reactors with no gas cap. For this we are dependent on the results of numerical simulation. Results to date show that even with no calandria tube array present and with the assumption of instantaneous tube burst, the pressurization pulses are complex and show strong effects of the wall when the tube is near the wall.

As indicated earlier, the magnitude of the peak pressures and impulses due to bulk pressurization calculated so far with the PISCES code are consistent with the results of the simpler calculations where spherical symmetry is a reasonable approximation. This indicates that the merchanism is fairly well understood and that the order of magnitude of the results has been established.

Two effects need further exploration:

(i) the possible reinforcement of interacting pressure pulses resulting from a tube burst near a wall. One indication of such a reinforcement point is shown in Figure 4.8 showing the PISCES calculation of velocity vectors in the moderator and an instantaneous stagnation point quite far removed from the burst tube. This effect could increase the local loading of a pressure tube or shut-off-rod guide tube.

(ii) the effects of the calandria-tube/pressure-tube array. Experimental evidence indicates that the crushing of calandria tubes (without damage to their pressure tubes) can significantly attenuate the magnitude of the pressure pulse. There is no evidence that crushing of the calandria tube in itself is catastrophic; it has the merit of absorbing part of the impulse. Whether this absorption can be relied on to prevent a pressure tube burst from damaging a large number of shut-off-rod guide tubes is not certain.

Accurate prediction of transient pressures in calandria vessels following tube burst requires not only knowledge of vessel and tube lattice compliance, and the dynamics of tube opening, but also a knowledge of the non-equilibrium flashing and condensation of vapour as it drops in pressure, and then is cooled near the burst site. Experimental observations of non-equilibrium behavior are virtually unavailable. The PISCES code at present assumes equilibrium two-phase conditions. It is known that in some circumstances (e.g. boiling water reactors downcomers) rapid large scale condensation can cause pressure forces damaging to structures. Large pressure pulses associated with recondensation have been measured in the Bettula experiments where the large gas cap clearly had a strong effect on liquid motion. With no gas cap the rate of vapour formation as the burst proceeds, and the subsequent collapse of such vapour would be expected to be much less in extent.

In summary, the magnitudes of pressure pulses in calandria vessels following a tube burst cannot be said to be well understood without further information on the effects of calandria tube collapse and non-equilibrium vapour evolution and collapse.

5.4 LOADING OF CALANDRIA-TUBE/PRESSURE-TUBE ASSEMBLIES

Present calculations, which appear to overestimate the impulse arising from tube burst, indicate that an adjacent pressure tube (considered as an impulsively loaded-beam) will be strained to much less than its elastic limit.

The failure of a pressure tube in one of the Isles tests (with substantial over-pressure and over-temperature of the coolant) is still unexplained. A puzzling feature of the failure is its distance from the burst site. The PISCES simulation model should be used for the coolant pressure and temperature of the Isles tests to estimate the impulsive loading which may be possible, at least in the absence of the calandria tube bundle.

PISCES calculations are expensive and time consuming but potentially useful in clarifying possible loadings of pressure-tube/calandria-tube assemblies under simplified (conservative upper limit) conditions.

5.5 LOADING OF CALANDRIA VESSELS

Recent experimental and analytical results indicate that bursting of a single tube, and near the calandria vessel will produce stresses in the calandria vessel wall which will not exceed the elastic limit.

Even if tube bursting led to missile impact on the vessel wall of sufficient force to cause penetration, that failure of the wall would not in itself be catastrophic, because of the presence of the shield tank.

5.6 LOADING OF SHUT-OFF-ROD GUIDE TUBES

The basic concern is whether a large number of these tubes would be crushed by a single tube burst, say near the top of the calandria vessel, and prevent dropping of the shut-off rods under emergency shutdown.

Limited experimental data has been available to us on the static strength of these perforated guide tubes under two- or three point lateral loading. The crushing strength under pressure transients with sharp spatial gradients does not appear to have been tested. No definite evidence of serious vulnerability has been found but further study is appropriate.

5.7 POISON INJECTION PIPES

No experimental tests or numerical simulations have been made on the vulnerability of the poison injection pipes to damage from pressure pulses or missiles. To prevent the possibility of rapid poison injection, however, 2-3 of the poison injection pipes would have to be crushed near their point of entry into the calandria vessel in such a way as to prevent flow.

The missile impact and crushing pressure impulses necessary to cause this improbable result have not been estimated.

5.8 SUMMARY

5.8.1 Propagating Pressure Tube Failure

We have been unable to identify a mechanism of strength sufficient to lead to propagating failure as a possible consequence of failure of one pressure tube.

However, since the analytical tools are available, we believe they should be used for further examination of this problem under conditions not yet considered (e.g. non-equilibrium flashing and condensation, finite tube bursting time, a range of geometrical conditions).

The one experimental case of propagating failure which occurred with extra high bursting pressure and temperature should be studied with the benefit of modern computational methods.

5.8.2 Calandria Vessel Failure

We have been unable to find a mechanism which would lead to failure of the vessel following one tube burst. In such a case the pressure loads applied to the vessel wall will not lead to stresses above the elastic limit of the vessel material.

With propagating tube failure it is conceivable that damaging loads could be applied to the wall before opening of the rupture discs. This case has not been considered because of the unavailability of a mechanism for propagating failure.

5.8.3 Shut-down System Failure

More work should be done to establish the circumstances under which a number of shut-off-rod guide tubes could be crushed following one tube burst.

Experimental data are needed both on crushing strength of these tubes under impulsive pressure loading and on pressure transients in a calandria vessel. Modern numerical simulation methods can throw helpful light on these pressure transients.

Failure of the poison injection system is considered much less likely than the rendering inoperative of several shut-off-rod guide tubes.

6.0 RECOMMENDATIONS FOR FURTHER EXPERIMENTAL AND ANALYTICAL INVESTIGATIONS

6.1 INTRODUCTION

Previous experimental and analytical investigations have concentrated on the larger effects of pressure tube rupture such as loadings on the calandria vessel and adjacent tubes, while little has been done on the detailed crack propagation mechanism of submerged tube rupture. The crack tip velocity and crack opening area development determine all the ensuing transient events of shock propagation, discharge pattern, pressure transient and fluid-structure interaction. Experimental investigations on loading of adjacent tubes have been limited and lacking in detailed measurements, while analytical investigations contain simple physical and geometric assumptions which disallow accurate pressure wave forms and fluid-structural interactions. Although crack propagation in a gas-pressurized tube discharging into air has been investigated recently, details of crack propagation for submerged liquid-pressurized pipe burst, which has fundamentally different characteristics in decompression and crack propagation, have yet to be obtained.

The long term damage mechanisms such as missile and pipe whip impacts require further examination. Experimental investigations in this category have been mainly carried out in air; the effects of fluid drag and the complex pressure gradients in the moderator due to reflection and interference of the pressure waves on the moving objects have to be considered when impacts of these mechanisms are being evaluated in a submerged environment. Analytical investigations to date circumvented the above complexity by conservatively neglecting the influence of the moderator, or by assigning a drag coefficient in calculating the velocities of the moving objects.

Previous experimental and analytical results have indicated that damage to the calandria vessel due to the pressure transient of a single pressure tube

rupture is unlikely. It is recommended that parallel experimental and analytical investigations of submerged tube rupture be carried out, with the main objectives of acquiring experimental measurement and analytical evaluation of the pressure loadings on adjacent pressure tubes and shut-off-rod guide tubes at the operating conditions of typical pressure tube reactors. The analytical investigations are to be carried out using advance 3-dimensional computer simulations with realistic inputs, including crack tip velocity, obtained in the experimental investigations. Following are some concepts for and remarks on the investigations.

6.2 EXPERIMENTAL INVESTIGATIONS

6.2.1 Explosion Chamber

Central to the experiment is a closed cylindrical vessel, within which all tests are to be conducted. Because the focus of the investigation is on loadings on nearby tubes, the length of the vessel should be equal to the length of the calandria vessel of a pressure tube reactor, to allow for the flexibility of the adjacent pressure tube which serves as the target tube. The chamber diameter could be smaller, since the shut-off-rod guide tube is orthogonal to the bursting tube and the load on it is concentrated during the initial phase, although a full size diameter is desirable. A proposed cylindrical explosion chamber is shown in Figure 6.1. Energy absorbent material is to line the inside of the chamber to reduce loading and reflections of shock waves and pressure wave, but if a full size diameter is used this precaution is not necessary. A high speed camera will record the displacement history of the target tubes and the crack propagation pattern on the explosion tube.

6.2.2 Explosion Tube

The explosion tube should be a full size pressure tube with insulation on the outside to prevent boiling of the surrounding moderator. The machined defect could be an axially milled slit instead of the usual flat to reduce the amount of material removed, since there is experimental evidence that the opening rate of the lips of the "fish mouth" is inertia dominated.

For tests where crack propagation is to be studied, the machined section of the pipe could be enclosed with a glass tube and nitrogen gas circulated in the annulus to prevent condensation for visualization of the motion of the "fish mouth".

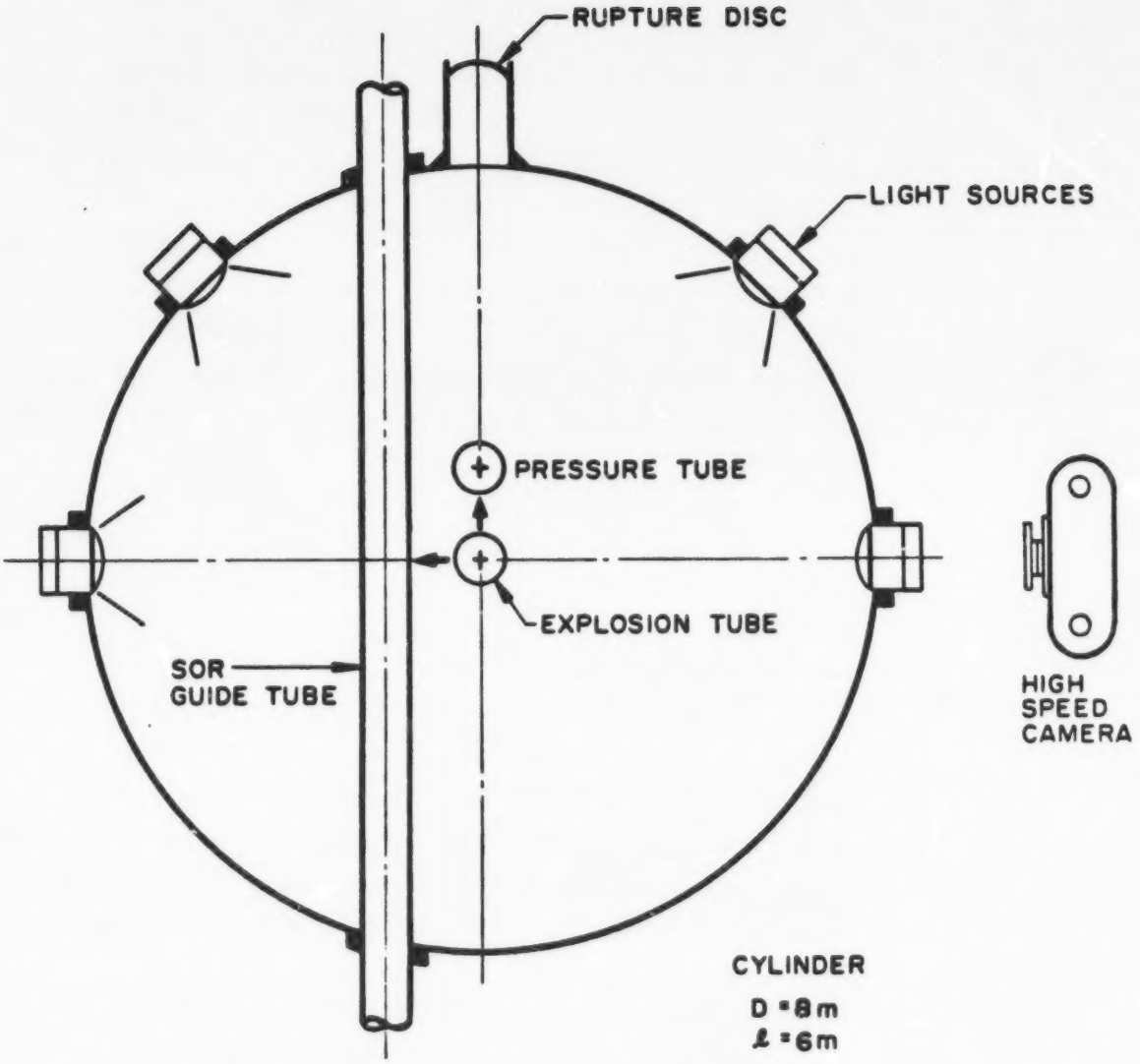

Figure 6.1 Explosion Chamber

To measure the pressure adjacent to the crack tip as it advances and the propagation of the decompression wave, fast response pressure transducers mounted inside the explosion tube are required. Some tests should be performed with dummy fuel bundles to investigate their effects. Furthermore, electrical heating to produce axial temperature gradients should be employed in some tests. In an operating system there is typically a temperature increase of 50°C in the coolant from the inlet to the outlet of the pressure tube and this increase corresponds to a substantial increase in saturation pressure.

6.2.3 Pressure Tube and Shut-off-rod Guide Tube at Target

Since the force experienced by a particular segment of the target tube at a particular instant in time is dependent mainly on the pressure differential across the tube and the impact velocity of the fluid, pressure transducers placed axially to measure both the dynamic and static pressures should yield data for the calculation of impulse integrated over time and the whole length of the tube. Strain gauges on the target tube should also be used to record the deformation history. Additional pressure transducers placed orthogonally to the explosion tube would yield information on the spatial distribution of pressure transiences. (Figure 6.2)

When the shut-off-rod guide tube is the target tube, it should be similarly instrumented.

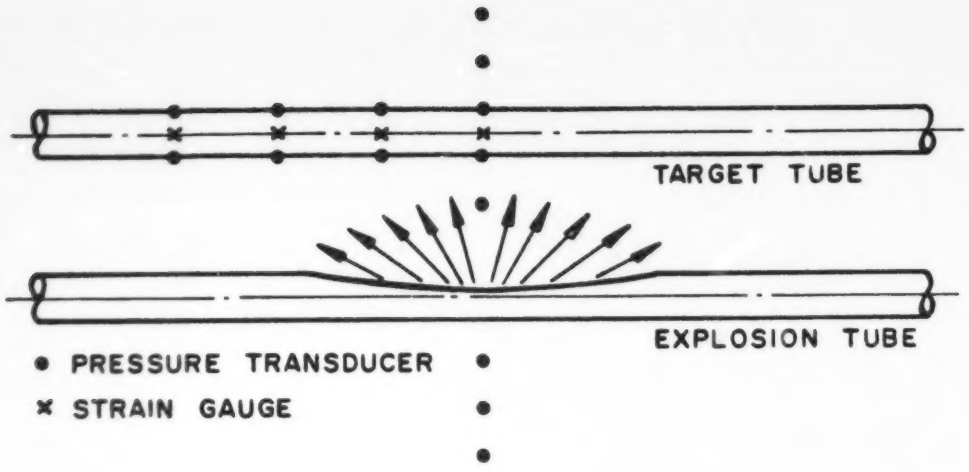

Figure 6.2 Pressure Tube as Target

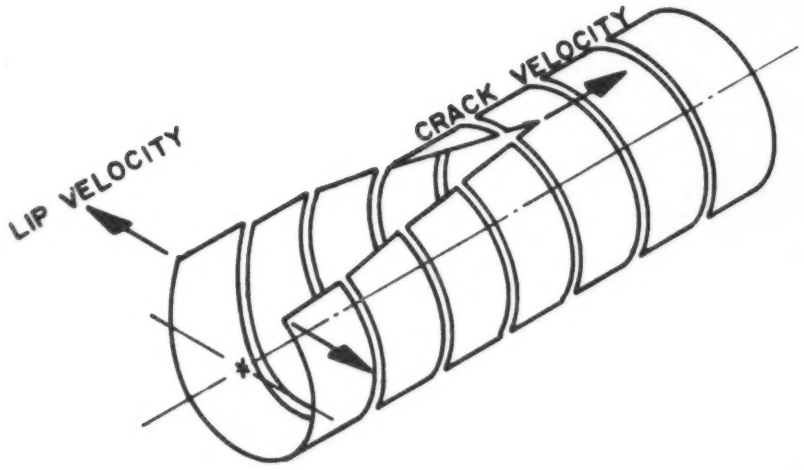

Figure 6.3 Split Ring Model for Computer Simulation

6.2.4 Instrumentation and Data Acquisition

Since the crack propagation phase of the pressure transient lasts a very short time, the transducers used must have very fast response. The triggering and synchronization of devices in the experiments, such as the initiation of rupture and the acceleration of the film to desired speed, have to be well controlled. A small computer would enable recording of the large amount of data in short time and proper initiation of the sequential triggering required.

6.3 PARALLEL ANALYTICAL INVESTIGATIONS

Both experimental and detailed computer simulation have individual merits and limitations and they are complementary to each other. In the PISCES simulations in Section 4, for example, the physical processes of shock propagation, the pressure transients due to vapour pocket expansion, the responses of the calandria vessel and the complex interactions among them are delineated in totality, but the resultant patterns are critically dependent on inputs of the boundary conditions to the computer program. On the other hand, experimental results may be apparatus dependent, such as tube ruptures in open tanks, and lacks the generality for broad application. However, once a simulation technique has been developed and verified by experimental results, it may be employed for prediction of results produced by changes in system parameters. It is desirable to consolidate the experimental knowledge by performing detailed computer simulations of the pressure tube loading and shut-off-rod guide tube loading, which have been experimentally investigated.

6.3.1 3-D Simulations

Because of the asymmetric configurations of the proposed investigations, computer simulations need to be three-dimensional (3-D). 3-D simulation of the whole reactor core would require very large computer memory capacity and long computation time, thus would be very costly; however, 3-D simulation of limited region and simple configuration such as the proposed investigations are quite feasible.

The PISCES code is capable of 3-D simulation, but at present it employes an equilibrium model for phase change of the liquid. It is desirable to use a non-equilibrium model so that the vapour pocket may be well defined and modelling of vapour pocket collapse be possible. The authors of PISCES code mentioned that a non-equilibrium model was developed for a European client but permission must be obtained before use. Regardless of the availability of the non-equilibrium model in PISCES, a broad search for

appropriate 3-D codes should be carried out to ensure efficient computation and accurate modelling.

6.3.2 Modelling of Tube Ruptures

The modelling of axial split of the explosion tube in the cases of pressure tube and shut-off-rod guide tube loadings is complex. Although it may be possible to model the crack propagation by introducing a through wall crack with length equal to or greater than the critical crack length at the start and let the specified energy potentials and material properties drive and determine the ensuing propagation. Very fine grids (hence high costs) would be required to represent the explosion tube, the coolant and moderator next to it. An alternative would be to let small sections of the explosion tube split open sequentially in short time steps as small rings, using the crack tip velocity and lip velocity of the "fish mouth" measured experimentally as inputs. (Figure 6.3)

6.3.3 Computation Costs

Because of the high cost of retaining a code application specialist for program preparation (which is greater than two-thirds of the total costs), it would be more cost efficient for the investigator to acquire the skills to run the code if he has sufficient background in computer programming. The investigator's familiarity of the physical processes would aid him in selection of inputs for definition of the problems and desirable outputs. Furthermore, he would then be able to extract from the large amount of output data on tape files as required for examinations of specific aspects of the process at any given instant of time. After experimental verification of the code application, he could perform parametric variations to study the responses of the system to different boundary conditions.

6.4 CONCLUDING REMARKS

The proposed experimental program involve large equipment, with the greatest capital expenditure being the construction of the explosion chamber. However, once the chamber is available, many submerged experiments relevant to pressure tube reactor design and safety may be conducted; for example, the attenuation and interference of pressure wave due to power channel arrays. Experimental results obtained from tests using the core of a HDR reactor in Karlstein/Main, Germany had given impetus to numerous code developments and applications to study HCDA and other safety issues in PWR with very successful results. It is highly desirable that such a facility be constructed for experimental investigations specifically related to pressure tube reactors.

Bibliography

Alamgir, Md., Kan, C.Y. and Lienhard, J.H.
"An Experimental Study of the Rapid Depressurization of Hot Water"
Journal of Heat Transfer, Vol 102, Aug 1980

Alamgir, Md., and Lienhard, J.H.
"Correlation of Pressure Undershoot during Hot-water Depressurization"
Journal of Heat Transfer, Vol 102, Nov 1980

Ayres, D.J.
"Determination of the Largest Stable Suddenly Appearing Axial and Circumferential through Cracks in Ductile Pressurized Pipes"
SMIRT, 1977

Baum, M.R.
"The Relationship between Breach Development and the Depressurization Transient during Axial Rupture of a Gas-pressurized Steel Pipe"
Journal of Pressure Vessel Technology, Vol 104, Feb 1982

Bell, C.R. and Bohl, W.R.
"Estimation of LWR Vessel Loads from Postulated In-vessel Steam Explosion"
SMIRT, 1981

Belytschko, T. and Tsay, C.S.
"WHAMSE: A Program for Three-dimensional Non-linear Structural Dynamics"
EPRI NP-2250, Feb 1982

Boudreau, J.E.
"The Mechanistic Analysis of LMFBR Accident Energetics"
Nuclear Safety, Vol 20, No 4, Jul-Aug 1979

Brimley, W.J.G.
"Steam Jet Mixing in Water"
AECL Report TDVI-362, Sheridon Park, 1979

Campbell, F.R.
"An Examination of the Consequences of Pressure Tube Failure in a CANDU Reactor" (draft)
AECB

Couquelin, C., Caumette, P., Garcia, J.L. and Sermet, E.
"Experimental Studies of PWR Primary Piping under LOCA Conditions"
CEA, France, SMIRT 1977

Cave, L.
"Licensability of CANDU-Type Reactor in the U.S. - A Preliminary Assessment of the R and D Requirements"
University of California, Los Angeles, U.S.A., Sep 1979

Centi, R., Faravelli, M., Gaspari, G.P. and Lo Nigro, F.
"Experimental Jet Impingement Loads in Steam Blowdown from 2" Pipes"
SMIRT, 1981

Chang, F.H., Brockett, G.F., Mortensen, G.A. and Santee, G.E.
"LOCA Hydroloads Calculations with Multi-dimensional Non-linear Fluid/Structure Interaction Methodology"
SMIRT, 1981

Chevallard, G., Famiglietti, M. and Possa, G.
"Simulation of the Dynamic Loads and Stresses due to Explosive Rupture of a Pressure Tube in a Scaled-down Model of the CIRENE Reactor Structure"
SMIRT, 1979

Cohen, L.M. and Gross, M.B.
"STEALTH Modelling of Time-dependent flows in Piping"
EPRI NP-1441, Dec 1980

Cologne, S.E.M.
"Physical Interpretation of Dynamic Fluid-structure Effects for HDR Blowdown Calculations with DAISY"
SMIRT, 1981

Cole, R.H.
"Underwater Explosions"
Princeton University Press, 1948

"Containment Integrity Following Multiple Channel Failures"
AECL, Jul 1976 (Commercial in Confidence)

Cowler, M.S. and Hancock, S.L.
"Dynamic Fluid-Structure Analysis of Shells Using PISCES 2 DELK Computer Code"
Physics International Co., Calif., U.S.A., SMIRT 1979

Cowler, M.S., Hancock, S.L. and Trigg, M.
"PISCES 3DE - A Computer Code for Analyzing Dynamic Fluid Structure Interactions in Three Dimensions"
SMIRT, 1981

Dallavalle, F., Hotz, W. and Possa, G.
"Explosive Rupture of a Power Channel Pressure Tube in a D_2O Moderated Reactor"
SMIRT, 1977

Daly, T.A., Duncan, R.M. and Rogers, J.T.
"Pressure Transient Following Coolant Tube Rupture inside the WR-1 Calandria"
CGE, CAP 57-2, 1965 (Commercial)

D'Arcy, D.
"Shocks in Gentilly Calandria Following Runaway"
CRNL (unpublished)

Donea, J., Stella, P.F., Giulani, S., Halleux, J.P., Jones, A.V.
"An Arbitrary Lagrangian-Eulerian Finite Element Procedure for Transient Dynamic Fluid-structure Interaction Problems"
SMIRT, 1979

Edwards, A.R. and O'brian, T.P.
"Studies of Phenomena Connected with the Depressurization of Water Reactors"
Journal of British Nuclear Energy Society, Vol 9, 1970

Emery, A.F., Love, W.J. and Kobayashi, A.S.
"Crack Openings and Fluid Pressure Profiles for Axial and Circumferential Cracks in Pipes"
SMIRT, 1979

Emery, A.F., Perl, M., Love, W.J. and Kobayashi, A.S.
"On the Motion of an Axial Through-crack in a Pipe"
Journal of Pressure Vessel Technology, Vol 103, Aug 1981

Famiglietti, M., Parmeggiani, A., Possa, G., and Galbiati, L.
"Pressure Bursts due to Power Channel Explosion in a Pressure Tube Reactor"
Energia Nucleare, Vol 23, No 2, Feb 1976

Florschuetz, L.W. and Chao, B.T.
"On Mechanisms of Vapor Bubble Collapse"
Journal of Heat Transfer, Vol 87, No 2, 1965

Frescura, G.M. and Brown, R.A.
"An Assessment of the Adequacy of SDSI Reactivity Depth"
Ontario Hydro, Dec 1981

Fritzsche, A.F.
"Accident at the Experimental Nuclear Power Station in Lucens"
Nuclear Safety, Vol 22, No 1, Jan-Feb 1981

Garcia, J.L., Caumette, P. and Huet, J.L.
"Study of Pipe Whip and Impact"
SMIRT, 1981

Giencke, E.
"Pressure Distribution due to Steam Bubble Collapse in a BWR Suppression Chamber"
SMIRT, 1979

Hareux, F., Roche, R. and Vrillon, B.
"Study of Consequences of the Rupture of a Pressure Tube in the Vessel of a Gas Cooled, Heavy Water Moderated Reactor"
CEA-R2459, 1964

Hayamizu, Y., Tokumitsu, M. and Hayashi, T.
"Experimental Studies of Dynamic Forces Caused by Pipe Rupture"
JUICE, Toronto, Nov 1977

Henry, E.R.
"An Assessment of a Pressure Tube Rupture within a Calandria Tank"
Fauske and Associates, Inc Ill., U.S.A., Apr 1981

Henry, E.R.
"Mechanical Damage Resulting from a Hypothetical Pressure Tube Rupture"
Fauske and Associates, Inc. Ill., U.S.A. Dec. 1981

Hirt, C.W., Amsden, A.A., and Cook, J.L.
J. Comp. Physics, Vol. 14, p. 227, 1974

Hirt, C.W. and Nichols, B.D.
"A Computational Method for Free Surface Hydrodynamics"
Pressure Vessel and Piping Conference, San Francisco, Calif., U.S.A.. Aug 1980

Hirt, C.W., Rivard, W.C. and Torrey, M.D.
"Post Test Evaluation of K-FIX Computations for a Full Scale HDR Blowdown Test"
SMIRT, 1981

Holtbecker, A., Montagnani, M. and Verzeletti, B.
"Consequences of the Rupture of a Pressure Tube or of a Complete Channel in an ORGEL-type Reactor"
EUR-4493e (ISPRA), 1970

Hsu, Y.Y. and Graham, R.W.
"Transport Processes in Boiling and Two-Phase Systems"
McGraw-Hill, New York, 1976

Isles, R.
"Lattice Site Shock Tests"
AECL (OVO) TDVI-95, Dec 1965

Kitade, K., Nakatogawa, T., Nishikawa, H., Kawanishi, K. and Tsuruto C.
"Experimental Study of Pipe Reaction Force and Jet Impingement Load at the Pipe Break"
SMIRT, 1977

Kitade, K., Nakatogawa. T., Nishikawa, H., Kawanishi, K. and Tsurutu. C.
"Experimental Study of Pipe Reaction Force and Jet Impingement Load at the Pipe Break"
SMIRT, 1979

Krishnan, L.V. and Garg, D.D.
"Scaling Laws for Contained Explosion"
Nuclear Engineering and Design, Vol 56, 1980

Kumar, S.N., Dixit, K.B. and Ghosh, A.K.
"Calandria Vessel Loading due to a Pressure Tube Rupture in Heavy-water Reactor"
SMIRT, 1975

Langford, W.J.
"Metallurgical Properties of Cold-worked Zircaloy 2 Pressure Tubes Irradiated under CANDU-PHW Power Reactor Conditions"
American Society for Testing and Materials, 1970

Leigh, K.M. and Lawton, W.T.
"Consequences of Pressure Tube Failure in the S.G.H.W. 100 MW(E) Prototype"
UK, 1963 (Commercial)

Lienhard, J.H., Alamgir, Md. and Trela. M.
"Early Response of Hot Water to Sudden Release of High Pressure"
Journal of Heat Transfer, Vol 100, Aug 1978

Marks, J.S. and Andeen, G.B.
"Chugging and Condensation Oscillation Tests"
EPRI NP-1167, Project 1067-2, Sep 1979

Masuda, F. and Nakatogawa, T.
"Experimental Study and Design Evaluation of Impingement Steam Jet"
SMIRT, 1981

Ohte, H., Yoshizawa, H., Chiba, N. and Shida, S.
"The Strength of Steel Plate Subjected to Missile Impact"
SMIRT, 1981

Pendergast, D.R.
"Pressure Transient Following Fluid Discharge into a Liquid-filled Vessel"
AECL, Mar 1978

Pickles, B.W.
"Pressure Tube - Calandria Tube Interaction Tests at Foulness"
Foulnes, UK, 1975 (Commercial)

Pressure Vessel Study Group
"Review of the Preliminary SGHWR Pressure Tube Safety Case"
Nuclear Installation Inspectorate, UK, Apr 1976 (Commercial in Confidence)

Rayleigh, Lord
"On the Pressure Developed in a Liquid during the Collapse of a Spherical Cavity"
Philosophical Magazine, Vol 34, 1917

Ross-Ross, P.A.
"Experiments on the Consequences of Bursting Pressure Tubes in a Simulated NPD Reactor Alignment"
AECL, 1963

Ross-Ross, P.A.
"Burst Testing of NPD Calandria Tube by the Decompression of Hot Pressurized Water"
AECL, Jun 1965

Ross-Ross, P.A.
"Experiments on the Consequences of Bursting Pressure Tubes in a Simulated Power Reactor Arrangement"
SMIRT, 1973

Ross-Ross, P.A., Duncan, J.T., Mitchell, A.B., Towgood, G.R. and Hunten, T.A.
"Some Engineering Aspects of the Investigation into the Cracking of Pressure Tubes in the Pickering Reactors"
AECL-5261, 1976

Ross-Ross P.A. and Langford, W.J.
"A Review of Experiments Relevant to the Possible Causes and Consequences of Pressure Tube Rupture in a CANDU Reactor" (draft)
AECL

Sargis, D.A., Masiello, P.G., Stuhmiller, J.H. and Wang, S.S.
"Analysis of Steam Chugging Phenomena"
EPRI, NP-1305, Jan 1981

Schükamp, H. and Pohl, W.
"Behavior of Presure and Fragments after Vessel Rupture with PISCES TM-2 DELK-CODE"
SMIRT, 1979

Swinhoe, R. and Roberts, W.H.
"Bursting Tube Experiments for the Steam-generating Heavy-water Reactor"
UKAEA, 1960

Romander, C.M. and Cagliostro, D.J.
"Structural Response of a 1/20 Scale Model of the SRBR to Simulated HCDA"
SMIRT, 1979

Taylor, G.I.
"The Formation of a Blast Wave by a Very Intense Explosion"
Proc. Roy. Soc., Ser. A., 201, 175-186, 1950

Tobin, R.J. and Cagliostro, D.J.
"Energetics of Simulated HCDA Expansions: Some Potential Attenuation Mechanisms"
Nuclear Engienering and Design, Vol 58, 1980

Ueda, S., Kurihara, R., Isozaki, T., Miyazaki. N., Kato, R. and Miyazono, S.
Experimental and Analytical Results of 4-inch Pipe Whip Tests under BWR Conditions"
SMIRT, 1981

Wang, S.S. and Stuhmiller, J.H.
"SAMPAC Hydrodynamic Pool Response Code"
EPRI NI-1067-1, Jan 1981

Zel'dovich, Y.B. and Raizer, Y.P.
"Physics of Shock Waves and High-temperature Hydrodynamic Phenomena"
Academic Press, New York. 1967